

HETERONUCLEAR GOLD CLUSTER COMPOUNDS

D. MICHAEL P. MINGOS and MICHAEL J. WATSON

Department of Chemistry, Imperial College of Science, Technology, and Medicine,
South Kensington, London SW7 2AY, England

- I. Introduction
- II. Synthesis and Reactivity
 - A. Synthesis from Homonuclear Compounds
 - B. Reactions of Heteronuclear Gold Cluster Compounds
- III. Characterization of Heteronuclear Gold Cluster Compounds
 - A. Fast Atom Bombardment Mass Spectrometry
 - B. Mössbauer Spectroscopic Studies
 - C. NMR Spectroscopy Studies
 - D. X-Ray Crystallographic Studies
- IV. Structure and Bonding in Heteronuclear Gold Cluster Compounds
 - A. Isolobal Analogies
 - B. Supplementary Au...Au Interactions
 - C. Tensor Surface Harmonic Theory
- V. Applications of Heteronuclear Gold Cluster Compounds
- References

I. Introduction

Since the first examples of transition metal cluster compounds were characterized and reported in the 1950s, this field of chemistry has expanded at a very rapid rate, aided primarily by advances in X-ray crystallographic techniques and NMR spectroscopy instrumentation. This growth has been stimulated by a desire to understand the unusual reactivities and structures of these compounds. As the electronic and steric factors responsible for influencing the stoichiometries, geometries, and reactivities of metal cluster compounds have become better understood, more emphasis has been placed on finding potential applications for these compounds. Of particular note are the efforts directed toward catalytical applications, in particular the synthesis of highly selective cluster derived catalysts, and toward understanding at a molecular level the catalytic processes that occur on metal surfaces by

means of the metal cluster-metal surface analogy. A great deal of interest in this area has been directed toward heteronuclear cluster compounds, as the selectivity of a catalytic metal center can often be enhanced by bonding to a heterometallic fragment.

The development of the area of heteronuclear gold cluster chemistry can be traced to the pioneering work of Lewis and Nyholm, who reported the first syntheses and crystallographic determinations of compounds containing gold-metal bonds in a series of articles from 1964 onward. Since then, over 200 examples of crystallographically characterized heteronuclear gold cluster compounds have appeared in the literature, ranging in complexity from simple binuclear systems to the gold-silver cluster compounds of Teo, containing 38 or more metal atoms. Table I summarizes the examples of these compounds that have been structurally characterized by X-ray methods and are considered to exhibit gold-heterometal bonding interactions.

TABLE I
STRUCTURALLY CHARACTERIZED EXAMPLES OF
HETERONUCLEAR GOLD CLUSTER COMPOUNDS

Heterometal	Reference
Ag	1-10
Co	11-28
Cr	29-32
Cu	33
Fe	11, 25, 34-56
Hg	57-61
Ir	52, 62-77
Mn	78-83
Mo	13, 19, 84, 85
Ni	86
Nb	87, 88
Os	89-114
Pb	115
Pd	116, 117
Pt	3, 57, 58, 118-144
Re	145-153
Rh	24, 148, 154-161
Ru	17, 18, 25, 40, 63, 89, 162-193
Sn	194-196
Tl	115, 197
V	198, 199
W	19, 121, 130, 156, 200-209

In this chapter, a review of the current literature relevant to heteronuclear cluster compounds containing gold-metal bonds is given, with particular emphasis being placed on those clusters that contain a high proportion of gold in the metal framework. This will neglect the homonuclear cluster chemistry of gold, which has recently been reviewed by Hall and Mingos (210), and compounds such as $[\text{Pt}_2\text{Au}(\mu_3\text{-S})(\text{CO})(\text{PPh}_3)_4]$ (211), in which the gold-metal interactions are considered to be negligible. The reader is also directed toward recent reviews on gold cluster chemistry by Braunstein (212), Pignolet (213), Salter (214), and the series of articles by Jones dealing with the structural aspects of gold chemistry (215–217).

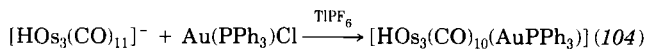
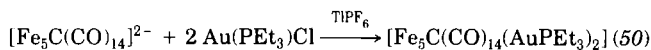
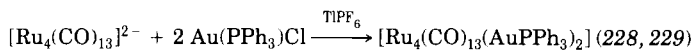
II. Synthesis and Reactivity

A. SYNTHESIS FROM HOMONUCLEAR COMPOUNDS

1. Addition of the $\text{Au}(\text{PR}_3)$ Fragment

The most widely exploited synthetic route used in the formation of gold-metal bonds involves addition of the gold center as the gold phosphine fragment AuPR_3 . The use of this procedure can be traced to the original work of Nyholm and Lewis, who recognized the bonding similarities between the AuPR_3 fragment and the H and CH_3 ligands, and used this to synthesize heterometallic gold cluster compounds by the addition of $\text{Au}(\text{PPh}_3)\text{Cl}$ to mononuclear metal carbonyl anions (21, 218–221). In modern terminology, this analogy is described as *isolobal*. This synthetic route has since been extended to include reactions of anions derived from other ligands (222–225), polynuclear metal carbonyl anions (104, 106, 226), and gold phosphine fragments based on chelating phosphine ligands (38, 227). A number of examples illustrating the generality of this synthetic procedure are given in Fig. 1.

The yields of these reactions are often improved by the addition of thallium(I) or silver(I) salts to act as halide scavengers and so generate the gold phosphine fragment *in situ*. This modification has been most extensively utilized in the addition of $\text{Au}(\text{PR}_3)^+$ to anionic and neutral cluster compounds, and a number of examples are given below:



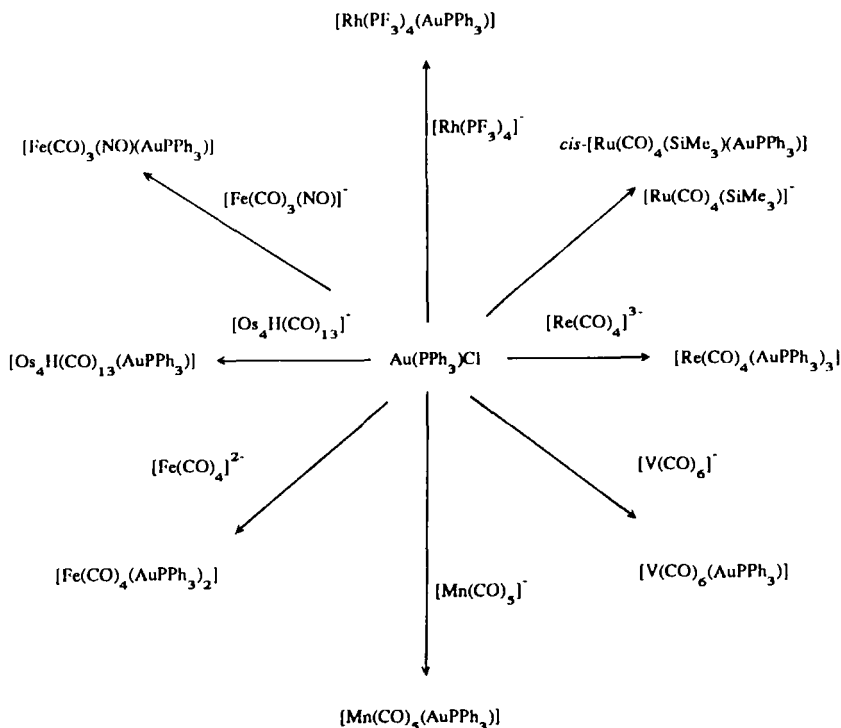
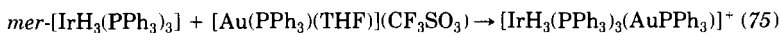
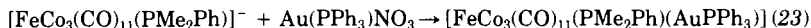
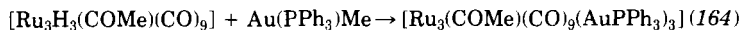
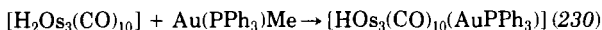
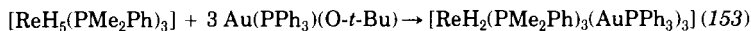


FIG. 1. Examples of the synthesis of heteronuclear gold cluster complexes by the reaction of $\text{Au}(\text{PPh}_3)\text{Cl}$ with transition metal anions.

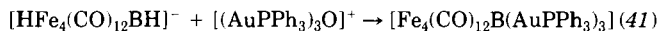
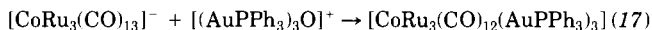
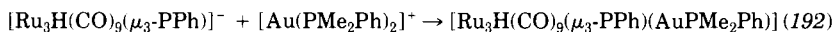
Alternatively, the $\text{Au}(\text{PR}_3)^+$ cation may be prepared as the nitrate or trifluorosulfonate salt and will add directly



For reactions that involve transition metal hydride compounds, the gold(I) compounds $\text{Au}(\text{PR}_3)\text{Me}$ and $\text{Au}(\text{PR}_3)(\text{OR}')$ have been shown to act as precursors to AuPR_3 , with the driving force for these reactions being provided by the elimination of methane or an alcohol, as in the following examples:

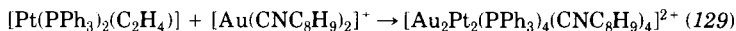
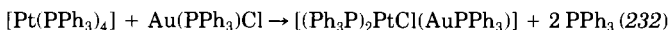
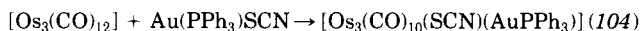


Other reagents that have been used as sources of the gold phosphine fragment include $[\text{Au}(\text{PMe}_2\text{Ph})_2]^+$ (79,192) and $[(\text{AuPPh}_3)_3\text{O}]^+$:



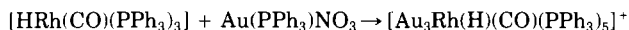
The oxonium reagent $[(\text{AuPPh}_3)_3\text{O}]^+$ has been found to be particularly useful in the synthesis of higher nuclearity mixed-metal clusters, as its reaction with cluster substrates can result in the addition of up to three gold phosphine groups. In contrast, the number of gold atoms introduced into a cluster by reactions involving $\text{Au}(\text{PR}_3)\text{Cl}$ is limited by the charge on the anionic precursor.

In the reactions described above, only the AuPR_3 fragment of the gold phosphine precursor has added to the cluster. Oxidative addition of $\text{Au}(\text{PR}_3)\text{X}$ [where $\text{X} = \text{Cl}$ (90, 188, 191), Br (90, 188), I (179), SCN (104), NCO (231), C_2R (92, 97), etc.] has also been observed to occur, yielding clusters in which the transition metal is in a higher oxidation state. This type of reaction was first investigated by Nyholm and co-workers (90, 232), and some examples are given below:



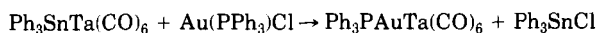
In the latter example the gold isocyanide cation $[\text{Au}(\text{CNC}_8\text{H}_9)_2]^+$ has been used as a source of the AuPPh_3^+ fragment, the gold-platinum cluster $[\text{Au}_2\text{Pt}_2(\text{PPh}_3)_4(\text{CNC}_8\text{H}_9)_4]^{2+}$ resulting from a combination of ligand exchange and oxidative-addition reactions.

Addition of $\text{Au}(\text{PR}_3)\text{NO}_3$ to metal hydrido species can result in simple addition of the gold fragment or substitution of the isolobal H by AuPR_3 . Pignolet has also reported the reaction of $[\text{HRh}(\text{CO})(\text{PPh}_3)_3]$ with $\text{Au}(\text{PPh}_3)\text{NO}_3$, which results in the formation of a heteronuclear cluster compound containing a high proportion of gold in the metal framework (148):



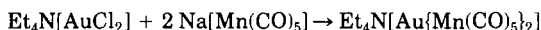
The formation of this gold-rhodium cluster compound has been attributed to a mechanism involving partial reduction of the $\text{Au}(\text{PPh}_3)\text{NO}_3$ species by the metal hydrido complex.

Metal exchange reactions have also been utilized to synthesize gold-transition metal bonds (233):

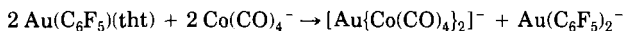


2. Addition of Gold Atoms

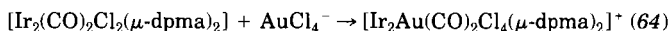
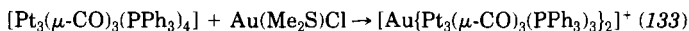
Replacement of the $\text{Au}(\text{PR}_3)\text{Cl}$ molecule by the AuCl_2^- anion in reactions with transition metal anions gives rise to linear trinuclear Au-M-Au heterometallic complexes, as in the reactions (234)



This type of compound has also been obtained from $\text{Au}(\text{C}_6\text{F}_5)(\text{tht})$, (tht = tetrahydrothiophene) according to the equation (26)



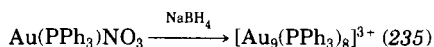
Other synthetic strategies that have been utilized to introduce bare gold atoms into cluster compounds include the addition of AuXCl , where X is a labile group such as Me_2S or CO, in the presence of TlPF_6 and oxidative addition of AuCl_4^- , as the following examples illustrate:

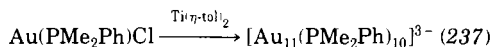
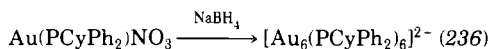


The same result has been achieved, somewhat unexpectedly, by addition of a mixture of $\text{Au}(\text{PR}_3)\text{Cl}$ (where $\text{PR}_3 = \text{PPhMe}_2, \text{PPh}_2\text{Me}, \text{PMe}_3$, or PEt_3) and TlPF_6 to $[\text{HFe}_4(\text{CO})_{12}\text{BH}]^-$, to yield $[\text{Au}\{\text{HFe}_4(\text{CO})_{12}\text{BH}\}_2]^-$ in 20% yield (46). In contrast, when this reaction is carried out with $\text{PR}_3 = \text{PPh}_3, \text{P}(p\text{-MeC}_6\text{H}_4)_3$, or PCy_3 , straightforward addition of the gold phosphine fragment results.

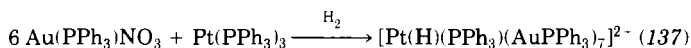
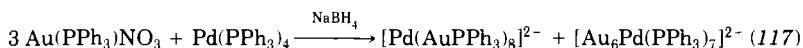
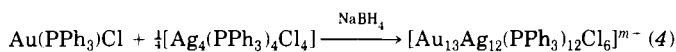
3. Coreduction

The first examples of homonuclear gold cluster compounds were obtained by the reduction of gold(I) phosphine complexes using solutions of borohydride. Subsequent work has shown the generality of this method, and the syntheses of gold clusters of varying nuclearity have been completed by altering the steric requirements of the phosphine ligands and the nature of the reductant, as the following examples illustrate:





An interesting recent development in the synthesis of heteronuclear cluster compounds has been the extension of this approach to include reductions of intimate mixtures of gold and transition metal complexes. This approach has been utilized effectively by a number of workers to yield clusters that are rich in gold and offer interesting analogies with homonuclear gold cluster compounds. A number of examples illustrating the use of this synthetic procedure are given below:



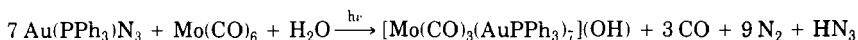
If the reduction of a mixture of $\text{Pt}(\text{PPh}_3)_3$ and $\text{Au}(\text{PPh}_3)\text{NO}_3$ is performed with carbon monoxide in place of H_2 , $[\text{Pt}_3\text{Au}(\text{CO})_3(\text{PPh}_3)_5]^+$ is obtained as the main product, together with a small amount of $[\text{Au}_6\text{Pt}(\text{PPh}_3)_7]^{2+}$ (122).

4. Reactions of Preformed Gold Cluster Compounds

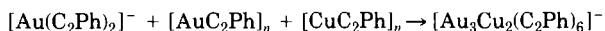
Only two examples of the synthesis of heterometallic gold cluster compounds from homonuclear gold cluster precursors have been described. The reaction between $[\text{Au}_8(\text{PPh}_3)_7]^{2+}$ and two molar equivalents of $\text{Li}[\text{Co}(\text{CO})_4]$ results in cluster degradation to give $[\text{Au}_6(\text{PPh}_3)_4\text{Co}_2(\text{CO})_8]$ in low yield (27, 28). The gold-tin cluster compound $[\text{Au}_8(\text{PPh}_3)_7(\text{SnCl}_3)]^+$ has also been synthesized, by the reaction of $[\text{Au}_9(\text{PPh}_3)_8]^{3+}$ or $[\text{Au}_8(\text{PPh}_3)_7]^{2+}$ with SnCl_2 and by reaction of $[\text{Au}_8(\text{PPh}_3)_8]^{2+}$ with SnCl_3^- (194).

5. Miscellaneous Reactions

A number of heteronuclear gold cluster compounds have been prepared using methods that are not readily classified in the above categories, and a number of examples are given here. $[\text{Mo}(\text{CO})_3(\text{AuPPh}_3)_7](\text{OH})$ has been synthesized by the photochemical degradation of $\text{Au}(\text{PPh}_3)\text{N}_3$ in the presence of $\text{Mo}(\text{CO})_6$ (84), in a reaction believed to proceed via the formation of AuPPh_3 radicals:

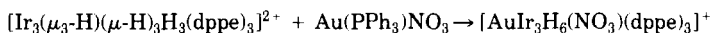


The reaction between $\text{Bu}_4\text{N}[\text{Au}(\text{C}_6\text{F}_5)_2]$ and AgClO_4 in dichloromethane, followed by addition of tetrahydrothiophene to the solution, has led to the isolation of the polymeric compound $[\text{AuAg}(\text{C}_6\text{F}_5)_2(\text{SC}_4\text{H}_8)]_n$ (9). The gold–silver complex $[\text{Au}_2\text{Ag}_2(\text{C}_2\text{Ph})_4(\text{PPh}_3)_2]$ has also been reported (1), obtained by the reaction of $\text{Au}(\text{PPh}_3)\text{C}_2\text{Ph}$ with AgC_2Ph and by the reaction of triphenylphosphine with polymeric $[\text{AuAg}(\text{C}_2\text{Ph})_2]_n$. A related gold–copper cluster, $[\text{Au}_3\text{Cu}_2(\text{C}_2\text{Ph})_6]^-$, has been prepared from the reaction (33)



and is based on a trigonal bipyramidal arrangement of metal atoms.

A number of examples of gold heteronuclear cluster compounds containing AuX fragments, where X is a ligand other than phosphine, have also been synthesized. An interesting example is provided by the compound $[\text{AuIr}_3\text{H}_6(\text{NO}_3)(\text{dppe})_3]^+$ (71), prepared by the reaction

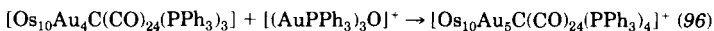
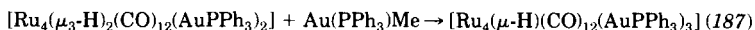
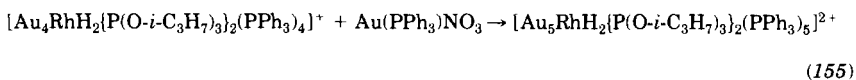


Cleavage of the strong Au–P bond occurs in the above reaction and results in the formation of a gold–iridium cluster containing a μ_3 -bridging AuNO_3 entity. Puddephatt has also described the synthesis of a number of gold–platinum clusters based on the reactions of the gold acetylide compound $[\text{AuCC-}t\text{-Bu}]$. Whereas addition of this gold fragment is observed to occur on reaction with $[\text{Pt}_2(\mu\text{-dppm})_3]$ (139), the reaction of $[\text{AuCC-}t\text{-Bu}]$ with $[\text{Pt}(\text{PPh}_3)_3]$ results in cleavage of the robust Au–C bond to give the cationic cluster compound $[\text{Pt}(\text{PPh}_3)(\text{CC-}t\text{-Bu})(\text{AuPPh}_3)_6]^+$ (144).

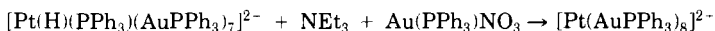
B. REACTIONS OF HETERONUCLEAR GOLD CLUSTER COMPOUNDS

1. Aggregation Reactions

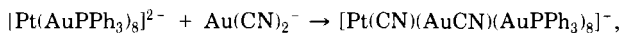
The addition of gold phosphine fragments to transition metal compounds is readily extended to include reactions of heteronuclear gold cluster compounds and has been used to build up clusters of increasing nuclearity, as the following examples illustrate:



An interesting application of this synthetic strategy that invokes the isolobal analogy is the base-induced substitution of the hydrido ligand in $[\text{Pt}(\text{H})(\text{PPh}_3)(\text{AuPPh}_3)_7]^{2+}$ by $\text{Au}(\text{PPh}_3)^+$ (123). The reaction is accompanied by a change in the metal cage geometry from a platinum-centered distorted cube to a platinum-centered toroidal ring in $[\text{Pt}(\text{AuPPh}_3)_8]^{2+}$ and is entirely analogous to the conversion of $[\text{Au}_8(\text{PPh}_3)_8]^{2+}$ to $[\text{Au}_9(\text{PPh}_3)_8]^{3+}$ by reaction with $\text{Au}(\text{PPh}_3)\text{NO}_3$:



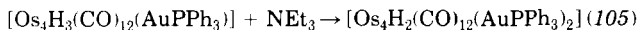
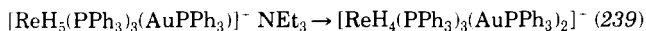
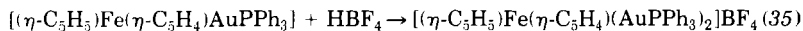
Oxidative addition of the AuCN fragment has also been reported (125),



as has the photochemically induced synthesis of $[(\text{AuPPh}_3)_6\text{AuCo}_2(\text{CO})_6](\text{NO}_3)$ from $[\text{Co}(\text{CO})_4(\text{AuPPh}_3)]$ and $\text{Au}(\text{PPh}_3)\text{N}_3$ (13).

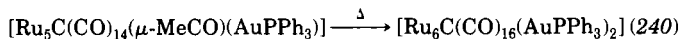
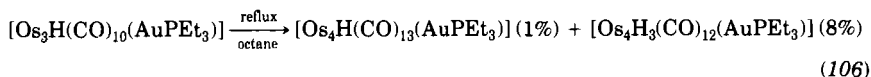
Fewer examples of the addition of transition metal species to heteronuclear gold cluster compounds have been described, although the gold-platinum clusters $[\text{Pt}(\text{AuPPh}_3)_8](\text{NO}_3)_2$ and $[\text{Pt}(\text{CO})(\text{AuPPh}_3)_8](\text{NO}_3)_2$ have been shown to undergo electrophilic addition reactions with AgNO_3 and $[\text{Hg}_2(\text{H}_2\text{O})_2](\text{NO}_3)_2$ to generate the trimetallic cluster compounds $[\text{Pt}(\text{AgNO}_3)(\text{AuPPh}_3)_8](\text{NO}_3)_2$, $[\text{Pt}(\text{HgNO}_3)_2(\text{AuNO}_3)(\text{AuPPh}_3)_7](\text{NO}_3)$, and $[\text{Pt}(\text{CO})(\text{AgNO}_3)(\text{AuPPh}_3)_8](\text{NO}_3)_2$, respectively (3, 238). Ito *et al.* have also reported the unusual oxidative addition reaction of $[\text{Hg}_2(\text{H}_2\text{O})_2](\text{NO}_3)_2$ to $[\text{Pt}(\text{PPh}_3)(\text{AuPPh}_3)_6]^{2+}$, which is accompanied by elimination of a gold phosphine group to yield the platinum-centered cluster $[\text{Pt}(\text{PPh}_3)(\text{AuPPh}_3)_5(\text{HgNO}_3)_2]^+$ (58).

Changes in cluster nuclearity have also been observed to accompany the addition of acid or base to heteronuclear gold cluster compounds and may result in aggregation, as in the reactions

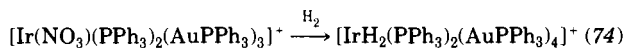
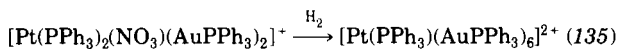


In theory, pyrolysis of carbonyl-based heteronuclear cluster compounds should, by analogy with homonuclear carbonyl cluster chemistry, cause elimination of carbon monoxide followed by cluster aggregation. In practice it is difficult to predict the course of these reactions, which can involve simple loss of ligand, cluster aggregation, or degradation, and reactions are often complex and result in low yields. A few

examples of pyrolysis leading to higher nuclearity clusters are given below:



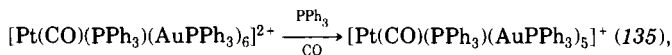
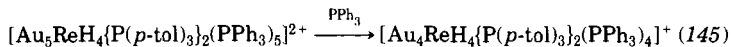
Two examples of cluster growth reactions resulting from the action of H_2 on heteronuclear gold cluster compounds exist in the literature, $[\text{Pt}(\text{PPh}_3)(\text{AuPPh}_3)_6]^{2+}$ and $[\text{Ir}(\mu\text{-H})_2(\text{PPh}_3)_2(\text{AuPPh}_3)_4]^+$ having been synthesized by the reactions



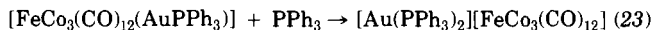
The anion $[\text{Os}_6\text{Au}(\text{CO})_{20}\text{H}_2]^-$ has also been prepared by the reaction of $[\text{Os}_3(\text{CO})_{10}\text{H}(\text{AuPR}_3)]$ (where $\text{R} = \text{Ph}$ or Et) with chloride ion and provides a rare example of cleavage of an Au-P bond (103).

2. Degradation Reactions

In contrast to the above reactions, a gold phosphine fragment can often be readily removed from a heterometallic cluster by the addition of free phosphine. This can result in degradation to novel heterometallic clusters containing fewer gold atoms,



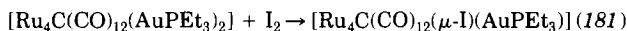
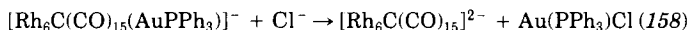
or complete removal of gold from the cluster,



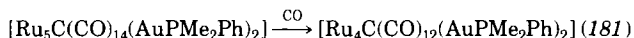
The apparent driving force for the elimination of $\text{Au}(\text{PPh}_3)^+$ in the above reactions is the formation of $[\text{Au}(\text{PPh}_3)_2]^+$. Comparable reactions have been observed in gold cluster chemistry. This reaction does not always proceed as, for example, when excess PPh_3 is added to $[\text{Au}_3\text{Rh}(\text{H})(\text{CO})(\text{PPh}_3)_5]^+$ (145).

The gold phosphine fragment has also been abstracted from heteronuclear cluster compounds as $\text{Au}(\text{PR}_3)\text{X}$ by reaction with halide ions

X^- or halogens X_2 as the following examples illustrate:

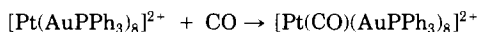


Degradation has been observed to occur on reaction of $[\text{Ru}_5\text{C}(\text{CO})_{14}(\text{AuPMe}_2\text{Ph})_2]$ with carbon monoxide:



3. Ligand Addition, Elimination, and Substitution Reactions

The cluster compound $[\text{Pt}(\text{AuPPh}_3)_8]^{2+}$ has been shown to exhibit amphoteric properties, undergoing both electrophilic addition reactions with AgNO_3 and $[\text{Hg}_2(\text{H}_2\text{O})_2](\text{NO}_3)_2$, as described previously, and nucleophilic addition reactions with small molecules such as CO and CNR (136, 241):



These reactions are rapid, with the additional ligand coordinating to the central platinum atom. This has the effect of increasing the total electron count of the cluster by two and results in a change in the skeletal geometry from toroidal to hemispherical as shown in Fig. 2. This reactivity is in contrast to that of the isoelectronic homonuclear gold cluster $[\text{Au}_9(\text{PPh}_3)_8]^{3+}$, which will undergo ligand substitution reactions with isocyanides but exhibits no reactivity toward carbon

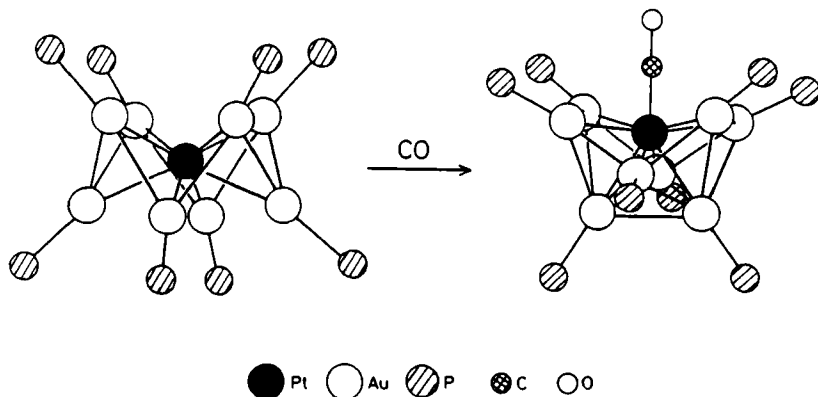
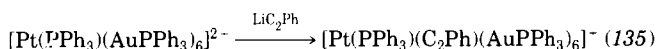
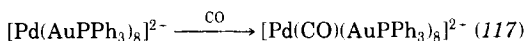
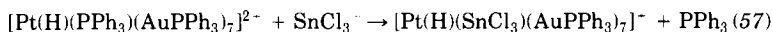
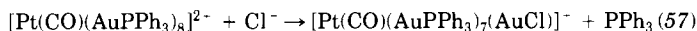


FIG. 2. Change in cluster geometry accompanying the reaction of $[\text{Pt}(\text{AuPPh}_3)_8]^{2+}$ with carbon monoxide.

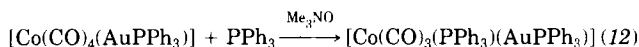
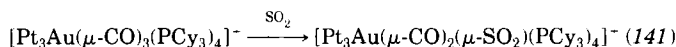
monoxide. Similar reactions have been observed for a number of transition metal-centered gold clusters in which the central metal is characterized by a 16-electron environment, as the following examples serve to illustrate:



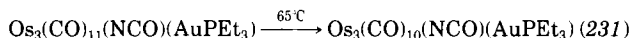
In contrast, those cluster compounds with an 18-electron environment at the central heterometal do not undergo nucleophilic addition reactions. Ligand substitution reactions at both the central heterometal and the peripheral gold atoms are observed to occur for both 16- and 18-electron cluster compounds, as in the reactions shown below:



Similar ligand substitution reactions, in which substitution occurs at the transition metal center, have been reported for smaller heteronuclear cluster compounds,



and elimination of CO is often observed on heating carbonyl-based heteronuclear clusters, as the following example illustrates:



Oxidative addition of SO_2 and Cl_2 to the complexes $[\text{Au}_2\text{Pt}\{\text{CH}_2\text{P}(\text{S})\text{Ph}_2\}_4]$ and $[\text{Ir}_2\text{AuCl}_2(\text{CO})_2(\mu\text{-dpma})_2]^+$ is accompanied by a marked increase in the Au–M interaction, which can be attributed to oxidation of the metal centers (138, 65).

4. Electrochemical Interconversions

Electrochemical interconversion of homo- and heteronuclear gold cluster compounds remains an area that has received scant attention, despite the potential for changing the electron count and hence the metal cage geometries of these clusters by electrochemical methods. The electrochemical redox reactions of $[\text{Pt}(\text{AuPPh}_3)_8]^{2+}$ have been studied, using pulse, differential pulse, and cyclic voltammetric techniques (124, 242) and two reversible, one-electron reduction steps have been

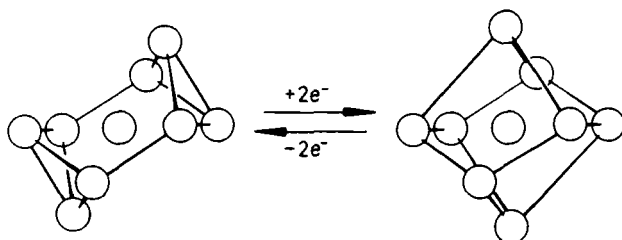


FIG. 3. Skeletal rearrangement accompanying the two-electron reduction of $[\text{Au}_9(\text{PR}_3)_8]^{3-}$ ($\text{R} = \text{Ph}$ or $p\text{-MeC}_6\text{H}_4$).

measured. The clusters $[\text{Au}_9(\text{PPh}_3)_8]^{3+}$ and $[\text{Au}_9\{\text{P}(p\text{-MeC}_6\text{H}_4)\}_8]^{3+}$ show the same behavior, but with one-electron reductions occurring at higher potentials. EHMO calculations indicate that this difference between the platinum- and gold-centered clusters is attributable to increased electron density at the platinum atom, which is also reflected in its increased reactivity toward carbon monoxide. In the case of the homonuclear gold cluster compounds, two-electron reduction results in the formation of $[\text{Au}_9(\text{PPh}_3)_8]^+$ as Fig. 3 illustrates. The structure of this gold cluster has been determined using X-ray techniques (243). Oxidation of $[\text{Pt}(\text{AuPPh}_3)_8]^{2+}$ is irreversible and complex and results in decomposition.

Electrochemical investigations of $[\text{Au}_2\text{Re}_2(\text{H})_6(\text{PPh}_3)_6](\text{PF}_6)$ have shown that this cluster displays a rich redox chemistry (244) and it has been concluded that the existence of this reversible electron transfer chemistry is due to the considerable amount of Re–Re multiple bond character that is retained in the cluster. A number of gold–osmium cluster compounds have been reported to show reversible redox chemistry (245).

III. Characterization of Heteronuclear Gold Cluster Compounds

Single-crystal X-ray crystallography remains the only definitive technique for the structural characterization of heteronuclear gold cluster compounds, although other techniques, in particular Mössbauer, NMR, IR, and fast atom bombardment mass spectroscopies (FABMS), have yielded valuable information, especially concerning the nature of these species in solution. Electron spectroscopy, which has proved to be of great value in the identification of homonuclear gold cluster compounds (210) has received little attention by workers in this area,

although the UV-vis absorption spectrum of the cluster $[\text{Pt}(\text{AuPPh}_3)_8]^{2+}$ has been reported (124). This was found to be remarkably similar to the solution spectra of isoelectronic $[\text{Au}_9(\text{PR}_3)_8]^{3+}$ clusters, indicating that they could possess a similar structure in solution.

The following sections summarize the applications of fast atom bombardment mass spectrometry, Mössbauer and NMR spectroscopies, and single-crystal X-ray diffraction studies in the characterization of heteronuclear gold cluster compounds.

A. FAST ATOM BOMBARDMENT MASS SPECTROMETRY

Conventional electron impact mass spectrometry, although a very useful technique in the characterization of low-molecular-weight organometallic and organic compounds, has proved to be of limited use in the analysis of high-molecular-weight cluster compounds. In particular, severe limitations on the range of compounds studied are imposed by the requirement that for ion formation samples be relatively volatile and thermally stable. The recent advent of fast atom bombardment mass spectrometry (246), in which ion generation is achieved by bombardment of the sample by a beam of fast rare gas atoms, overcomes these problems and a number of workers have applied the technique to the characterization of heteronuclear gold cluster compounds (96, 117, 124, 135, 149, 247).

The fast atom bombardment mass spectra of these species are found to consist of a number of peaks with well-resolved fine structure arising from the various possible isotopic combinations for a given molecular formula. A typical positive ion spectrum, that of the cationic cluster compound $[\text{Au}_6\text{Pt}(\text{PPh}_3)_7](\text{BPh}_4)_2$ (149), is illustrated in Fig. 4. An expanded view of the isotopic envelope due to the highest mass peak is shown in Fig. 5, together with a simulation based on the empirical formula $\text{C}_{150}\text{H}_{125}\text{Au}_6\text{BP}_7\text{Pt}$.

In general, the positive ion spectra of monocationic clusters have a highest mass intense peak due to the parent cluster ion $(\text{M})^+$, whereas dicationic clusters such as $[\text{Au}_6\text{Pt}(\text{PPh}_3)_7](\text{BPh}_4)_2$ often exhibit a peak due to the ion pair $(\text{M} + \text{X})^+$ (where X represents the anion). As ion fragmentation occurs in the spectrometer, characteristic patterns arising from the loss of anions, phosphine ligands, gold phosphine groups, etc., are also observed and often aid assignment of the highest mass peaks. The observed spectra are often complicated by the occurrence of additional peaks arising from the addition of oxygen atoms and fragments of the matrix in which the sample is suspended, although these are usually of low intensity.

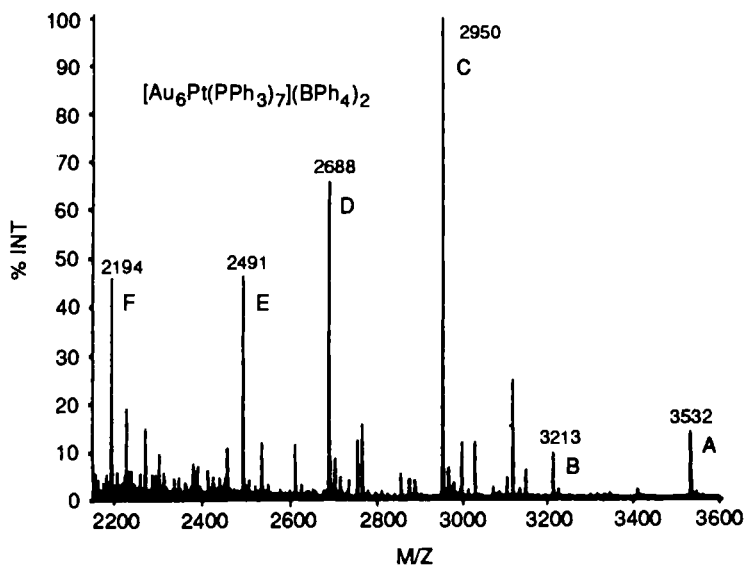


FIG. 4. Positive ion FABMS of $[\text{Au}_6\text{Pt}(\text{PPh}_3)_7](\text{BPh}_4)_2$. Peaks have been assigned as A = $(\text{M} + \text{BPh}_4)^+$; B = $(\text{M})^+$; C = $(\text{M} - \text{PPh}_3)^+$; D = $(\text{M} - 2\text{PPh}_3)^+$; E = $(\text{M} - \text{Au} - 2\text{PPh}_3)^+$; F = $(\text{M} - 3\text{PPh}_3 - 3\text{Ph})^+$, where M = $[\text{Au}_6\text{Pt}(\text{PPh}_3)_7]$ (149).

Fast atom bombardment mass spectroscopy has proved to be most useful when applied to the characterization of heteronuclear gold cluster compounds containing hydride ligands (137, 149, 155). Characterization is aided by the observation that peaks are invariably present in the spectrum corresponding to ions that contain all of the hydride

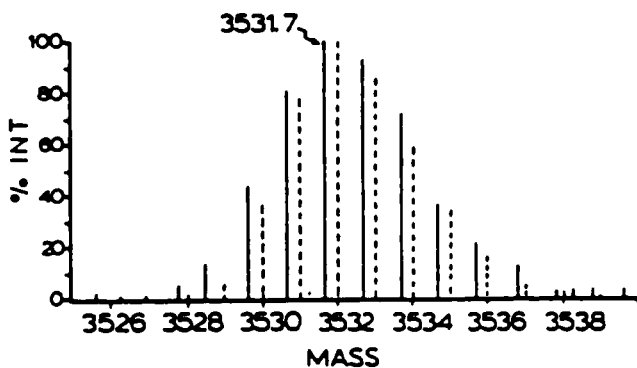


FIG. 5. Observed (solid line) and simulated (dashed line) isotopic ion distributions for the $(\text{M} + \text{BPh}_4)^+$ ion in the positive ion FABMS of $[\text{Au}_6\text{Pt}(\text{PPh}_3)_7](\text{BPh}_4)_2$ (149).

ligands, although hydride loss is an important fragmentation process and can give rise to overlapping isotopic distribution envelopes. Because of this, reliable formulations are achieved only by careful simulation of the observed isotopic distributions and when the results are used in conjunction with other spectroscopic and analytical techniques.

B. MÖSSBAUER SPECTROSCOPIC STUDIES

The only naturally occurring isotope of gold, ^{197}Au , is particularly amenable to Mössbauer investigation. The transition in ^{197}Au is from the 77.3 keV spin- $\frac{1}{2}$ excited state to the ground state of spin- $\frac{3}{2}$, and in the presence of an asymmetric field this transition is split into two lines of equal intensity (248). ^{197}Au Mössbauer spectroscopy has proved to be of great value in the characterization of simple complexes of gold and has been used effectively to elucidate oxidation states and coordination environments in these compounds (248, 249). Unfortunately, applications of this technique to homonuclear gold cluster compounds have yielded somewhat disappointing results. Although it has proved possible to distinguish signals for peripheral gold atoms bonded to different ligands, the resolution of the technique is insufficient to distinguish all of the different gold environments present in these cluster species, and deconvolution analyses are required to unravel the spectra (250, 251). A similar lack of resolution has been noted for the heteronuclear cluster compounds $[\text{Pt}(\text{AuPPh}_3)_8]^{2+}$ (124) and $[\text{Pt}(\text{H})(\text{PPh}_3)(\text{AuPPh}_3)_7]^{2+}$ (137), although the lack of a singlet in their ^{197}Au Mössbauer spectra are consistent with their formulation as platinum-centered clusters.

Parish and co-workers have recently reported the ^{197}Au Mössbauer spectra of a number of gold–ruthenium (252, 253), gold–iron (254), and gold–platinum (255) heteronuclear cluster compounds, and the relevant isomer shifts and quadrupole splittings are summarized in Table II. Their investigations of the gold–ruthenium cluster compounds have demonstrated that, although data fall into the range previously observed for homonuclear cluster compounds, the technique is sufficiently sensitive to resolve signals due to structurally inequivalent AuPPh_3 moieties within these clusters. Thus the ^{197}Au Mössbauer spectrum of $[\text{Ru}_4(\mu_3\text{-H})(\mu\text{-H})(\text{CO})_{12}(\text{AuPPh}_3)_2]$, shown in Fig. 6, although still requiring an analysis involving computer fitting, can be seen to contain two components, of which the inner doublet has been assigned to the gold atom of the AuRu_4 trigonal bipyramid.

Good correlations have been observed between the measured Mössbauer parameters and the gold–ruthenium bond lengths and the con-

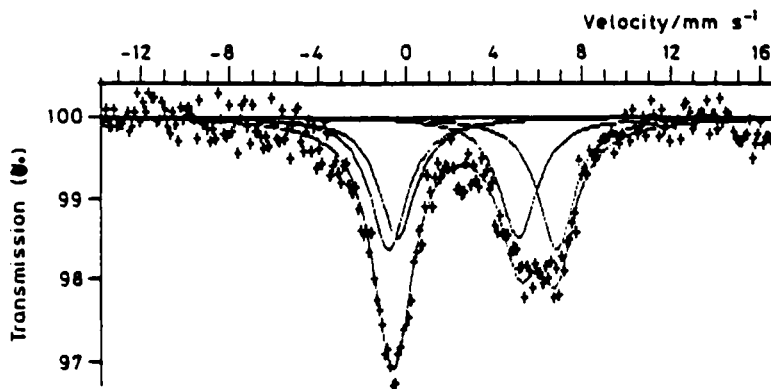
TABLE II

¹⁹⁷Au MÖSSBAUER DATA FOR HETERONUCLEAR GOLD CLUSTER COMPOUNDS

Compound	IS (mm s ⁻¹)	QS (mm s ⁻¹)	
[Fe(CO) ₄ (AuPCy ₃) ₂]	3.80	7.76	
[Fe(CO) ₄ (AuPCy ₃) ₃](PF ₆)	3.26	7.22	
[Pt ₃ Au(μ-CO) ₃ (PCy ₃) ₄](PF ₆)	3.83	6.58	
[Pt ₃ Au(μ-SO ₂) ₂ (μ-Cl)(PCy ₃) ₄]	3.69	6.67	
[Pt ₃ Au(μ-SO ₂) ₂ (μ-Cl)(PCy ₃) ₃ {P(C ₆ H ₄ F- <i>p</i>) ₃ }]	3.27	6.30	
[Pt ₃ Au ₂ (μ-SO ₂) ₂ (μ-Cl)(PCy ₃) ₃ {P(C ₆ H ₄ F- <i>p</i>) ₃ } ₂](PF ₆)	3.30	5.75	
[Pt ₂ Au ₂ (PPh ₃) ₄ (CNC ₈ H ₉) ₄](PF ₆) ₂	3.13	6.88	
[Ru ₃ (CO) ₉ (μ-H)(μ ₃ -COMe)(AuPPh ₃)]	3.38	7.38	
[Ru ₃ (CO) ₉ (C ₂ Bu ^t)(AuPPh ₃)]	3.51	7.33	
[Ru ₄ (CO) ₁₂ (μ-H) ₃ (AuPPh ₃)]	3.22	7.39	
[Ru ₃ (CO) ₉ (μ-H)(μ ₃ -COMe)(AuPPh ₃) ₂]	3.11	6.93	
[Ru ₃ (CO) ₉ (μ ₃ -S)(Au ₂ dppm)]	2.68	6.45	
[Ru ₄ (CO) ₁₂ (μ-H)(μ ₃ -H)(Au ₂ dppm)]	3.02	6.71	
[Ru ₄ (CO) ₁₂ (μ-H)(μ ₃ -H)(AuPPh ₃) ₂] ^a	Au _a	3.0	7.5
	Au _b	2.3	5.6
[Ru ₃ (CO) ₉ (μ ₃ -COMe)(AuPPh ₃) ₃] ^a	Au _a	2.8	7.4
	Au _b	2.5	5.2
[Ru ₄ (CO) ₁₂ (μ ₃ -H)(AuPPh ₃) ₂] ^a	Au _a	2.9	7.4
	Au _b	1.9	4.9

^a See Moore *et al.* (253) for atom labeling scheme.

nectivities of the gold atoms to other metal atoms in the clusters. Although the technique is not sufficiently sensitive to resolve the geometrically distinct gold atoms in [Ru₃(CO)₉(μ₃-S)Au₂(dppm)] and [Ru₄(μ₃-H)(μ-H)(CO)₁₂Au₂(dppm)], it should be noted that in each of

FIG. 6. ¹⁹⁷Au Mössbauer spectrum of [Ru₄(μ₃-H)(μ-H)(CO)₁₂(AuPPh₃)₂] (253).

these clusters the gold atom connectivities and mean Au–Ru bond lengths are the same.

The ^{197}Au Mössbauer spectroscopy studies reported for gold–iron and gold–platinum heteronuclear cluster compounds have yielded no useful structural information, but have been used as a probe of the bonding in these compounds. The IS and QS parameters measured are comparable to those reported for simple two-coordinate gold(I) complexes of the type $\text{Au}(\text{PR}_3)\text{X}$ (248). Mingos has shown that this is consistent with the bonding schemes proposed previously for these compounds (256), in which the gold fragment is considered to contribute a single sp hybrid orbital to the cluster bonding. A combination of ^{57}Fe and ^{197}Au Mössbauer data for $[\text{Fe}(\text{CO})_4(\text{AuPCy}_3)_2]$ and $[\text{Fe}(\text{CO})_4(\text{AuPCy}_3)_3](\text{PF}_6)$ has been shown to be consistent with the presence of two localized Au–Fe bonds in the former species and a delocalized four-center two-electron interaction in the latter.

C. NMR SPECTROSCOPY STUDIES

The characterization of gold heteronuclear cluster compounds using NMR spectroscopic techniques has been greatly facilitated by the presence in these compounds of NMR active nuclei such as ^{195}Pt , ^{183}W , and ^{103}Rh . $^{31}\text{P}\{^1\text{H}\}$ NMR spectroscopy studies have been used extensively, as the vast majority of these clusters are stabilized by phosphine ligands and a wealth of information concerning the number and types of phosphine ligands may be obtained from the solution spectra. Such studies have proved to be especially useful for differentiating between gold and platinum atoms, which are indistinguishable in single-crystal X-ray diffraction experiments.

An illustration of the potential of NMR spectroscopy for the characterization of heteronuclear gold cluster compounds is provided by reference to the series of gold–platinum clusters prepared in these laboratories. For example, $[\text{Pt}_2(\mu\text{-SO}_2)(\text{CNC}_8\text{H}_9)_2(\text{PCy}_3)_2(\mu\text{-AuPCy}_3)](\text{PF}_6)$, synthesized by addition of a mixture of $\text{Au}(\text{PCy}_3)\text{Cl}$ and TIPF_6 to $[\text{Pt}_2(\mu\text{-SO}_2)(\text{CNC}_8\text{H}_9)_2(\text{PCy}_3)_2]$, exhibits the $^{31}\text{P}\{^1\text{H}\}$ NMR spectrum illustrated in Fig. 7a (134). The spectrum consists of separate resonances due to the phosphorus atoms of the gold and platinum tricyclohexyl phosphine ligands, with satellites arising from coupling to the ^{195}Pt nuclei ($I = \frac{1}{2}$, 33.3% abundance). The spectrum may be considered a superposition of spectra due to the three isotopomers that arise due to the presence of the ^{195}Pt nuclei, namely A_2M (44.4%, no ^{195}Pt nuclei), $\text{AA}'\text{MX}$ (44.4%, one ^{195}Pt nucleus), and $\text{AA}'\text{MXX}'$ (11.1%, two ^{195}Pt nuclei). Characterization of this cluster has been based on a successful computer simula-

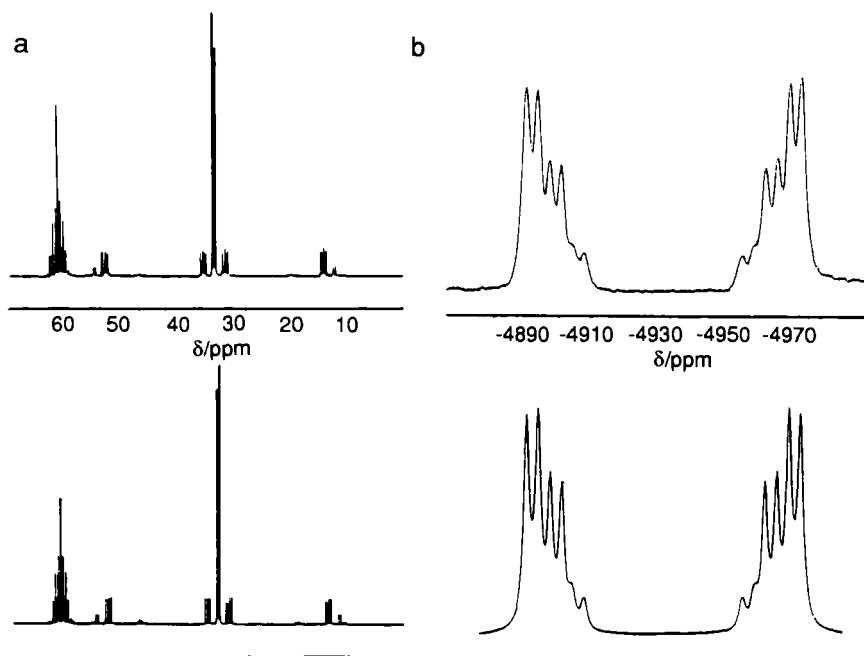


FIG. 7. (a) $^{31}\text{P}\{^1\text{H}\}$ NMR spectrum and (b) $^{195}\text{Pt}\{^1\text{H}\}$ NMR spectrum of $[\text{Pt}_2(\mu\text{-SO}_2)(\text{CNC}_8\text{H}_9)_2(\text{PCy}_3)_2(\mu\text{-AuPCy}_3)]^+$.

tion of the observed spectrum and is entirely consistent with the structure determined by X-ray diffraction methods (see Fig. 8). The $^{195}\text{Pt}\{^1\text{H}\}$ NMR spectrum has also been measured and satisfactorily simulated using the same parameters and is also illustrated in Fig. 7b.

The $^{31}\text{P}\{^1\text{H}\}$ NMR spectra of a number of heteronuclear gold cluster compounds are found to be deceptively simple and NMR studies have been used as a probe of the behavior of these species in solution. This is especially true of the higher nuclearity clusters, which often exhibit spectra that are much simpler than would be predicted on the basis of their solid-state structures. For example, $[\text{Pt}(\text{H})(\text{PPh}_3)(\text{AuPPh}_3)_7]^{2+}$, which adopts the solid-state structure illustrated in Fig. 9 (137) in which the phosphine ligands occupy several different chemical environments within the molecule, shows only two resonances in the $^{31}\text{P}\{^1\text{H}\}$ NMR spectrum. These are in a ratio of 7:1 and exhibit satellites due to coupling to the central platinum nucleus as Fig. 10 illustrates.

Similar observations have been made for the $^{31}\text{P}\{^1\text{H}\}$ NMR spectra of homonuclear gold clusters, which, with a few exceptions, are characterized by singlets in their $^{31}\text{P}\{^1\text{H}\}$ NMR spectra. This has been attributed

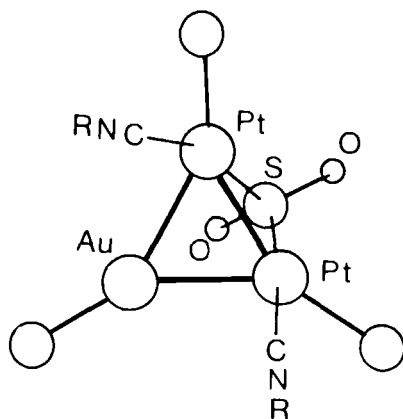


FIG. 8. Molecular structure of $[\text{Pt}_2(\mu\text{-SO}_2)(\text{CNC}_8\text{H}_9)_2(\text{PCy}_3)_2(\mu\text{-AuPCy}_3)]^+$.

to rapid intramolecular exchange processes occurring between different phosphorus sites, so averaging the phosphorus environments. Chemical exchange studies have shown that intermolecular exchange of phosphine or AuPR_3 groups occurs too slowly to account for the observed fluxional behavior (257). Furthermore, the structural characterization of two crystalline modifications of the $[\text{Au}_9\{\text{P}(p\text{-MeOC}_6\text{H}_4)_3\}_8]^{3+}$ cluster (258), which interconvert rapidly in solution, has provided excellent evidence for the existence of soft potential energy surfaces between the alternative polyhedral forms of gold cluster cations.

Similar fluxional processes are believed to operate in heteronuclear gold cluster compounds and these may be slowed down by lowering the

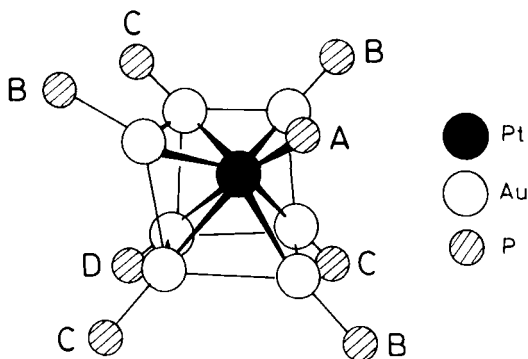


FIG. 9. Molecular structure of the $[\text{Pt}(\text{H})(\text{PPh}_3)(\text{AuPPh}_3)_7]^{2+}$ cation.

temperature. The following examples serve to illustrate the use of variable temperature NMR techniques in the study of these compounds.

Figure 10 shows the effect of lowering the temperature on the $^{31}\text{P}\{^1\text{H}\}$ NMR spectrum of $[\text{Pt}(\text{H})(\text{PPh}_3)(\text{AuPPH}_3)_7]^{2+}$ (259). The exchange of phosphorus sites in the cluster is slowed down sufficiently at 173 K to resolve signals due to the four distinct phosphorus sites in a ratio of 1:3:3:1. Low-temperature ^{31}P COSY experiments have been used to elucidate the relevant coupling constants and so assign the peaks as shown in the figure. The measured $^2J(\text{P-Pt})$ coupling constants have been shown to be consistent with the calculated trends in the radial Au-Pt overlap populations.

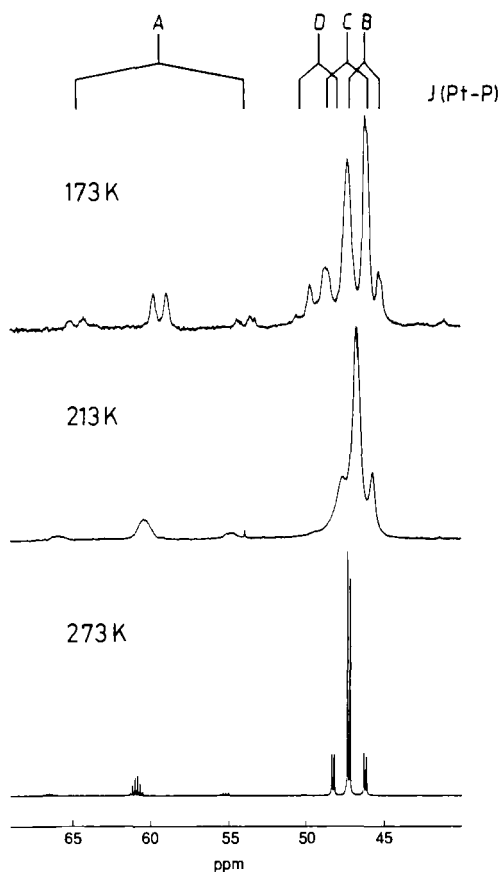


FIG. 10. $^{31}\text{P}\{^1\text{H}\}$ NMR spectra of $[\text{Pt}(\text{H})(\text{PPh}_3)(\text{AuPPH}_3)_7]^{2+}$ as a function of temperature.

Stone and co-workers have reported the $^{31}\text{P}\{^1\text{H}\}$ NMR spectra of the compounds $[\text{Ru}_3(\text{CO})_8(\mu_3\text{-S})(\text{L})(\text{AuPPh}_3)_2]$ (where $\text{L} = \text{CO}$ or PPh_3) (183), both of which show only one resonance due to the gold phosphine groups down to -90°C . This has been accounted for by a mechanism in which the metal atoms undergo a restricted Berry pseudo-rotation as shown in Fig. 11. Subsequent work has shown that this mechanism is consistent with the dynamic behavior observed in solution for a number of related gold-ruthenium cluster compounds, and cluster geometries mapping the full range of the reaction coordinate have since been characterized.

The $^{31}\text{P}\{^1\text{H}\}$ NMR spectrum of $[\text{Ru}_6\text{C}(\text{CO})_{16}(\text{AuPMePh}_2)_2]$ also consists of a sharp single resonance at room temperature, but on cooling this splits into two signals, the relative intensities of which vary with the solvent system used (177). The process is fully reversible and has been attributed to the presence of two isomers that rapidly interconvert at room temperature. Further evidence for the existence of a temperature dependent equilibrium between isomers has come from the determination of the crystal structure of the isoelectronic compound $[\text{Ru}_5\text{WC}(\text{CO})_{17}(\text{AuPEt}_3)_2]$ in which there is a different arrangement of gold atoms about the octahedral M_6C cluster core. The possibility of an intermolecular process interconverting the isomers has been ruled out.

Intermolecular dynamic processes are, in general, less common for gold heteronuclear cluster compounds. An example of such behavior in solution is provided by the compounds $[(\text{Ph}_3\text{PAu})(\mu\text{-H})\text{M}(\text{CO})_5]$ ($\text{M} = \text{Cr}, \text{Mo}, \text{W}$) and $[(\text{Ph}_3\text{PAu})(\mu\text{-H})\text{W}(\text{CO})_4\{\text{P}(\text{OMe}_3)\}]$ (32). The $^{31}\text{P}\{^1\text{H}\}$ NMR spectra of these species are sharp singlets that shift appreciably

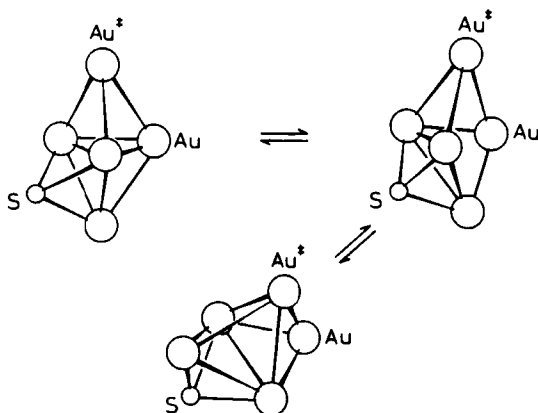


FIG. 11. Proposed fluxional behavior in solutions of $[\text{Ru}_3(\text{CO})_8(\mu_3\text{-S})(\text{L})(\text{AuPPh}_3)_2]$.

on cooling. Addition of PPh_3 to the solutions results in a single sharp resonance with a chemical shift intermediate between that of the cluster and free phosphine. This is consistent with a dynamic process in which the complexes exchange PPh_3 groups by a dissociative mechanism. Dynamic processes involving the hydride ligands are ruled out by the observation of $^1J(^{183}\text{W}-^1\text{H})$ coupling in the hydride signal of the compounds $[(\text{Ph}_3\text{PAu})(\mu\text{-H})\text{W}(\text{CO})_4(\text{L})]$ (where $\text{L} = \text{CO}$ or $\text{P}(\text{OMe})_3$).

^1H NMR spectroscopy has been used extensively in the characterization of gold heteronuclear cluster compounds that possess hydride ligands. For example, Fig. 12 illustrates the hydride region of the ^1H NMR spectrum of $[\text{Au}_4\text{Rh}(\text{H})_2\{\text{P}(\text{O-}i\text{-C}_3\text{H}_7)_3\}_2(\text{PPh}_3)_4]^+$ (155).

Although an X-ray diffraction analysis has revealed a trigonal bipyramidal arrangement of metal atoms in this cluster, with the rhodium atom occupying an equatorial position, the hydride ligands could not be located from the X-ray data. The ^1H NMR spectrum confirms the presence of two hydride ligands (based on an integration of peak areas) and consists of a pseudo-sextet in the hydride region of the spectrum. Selective decoupling experiments have allowed the coupling constants

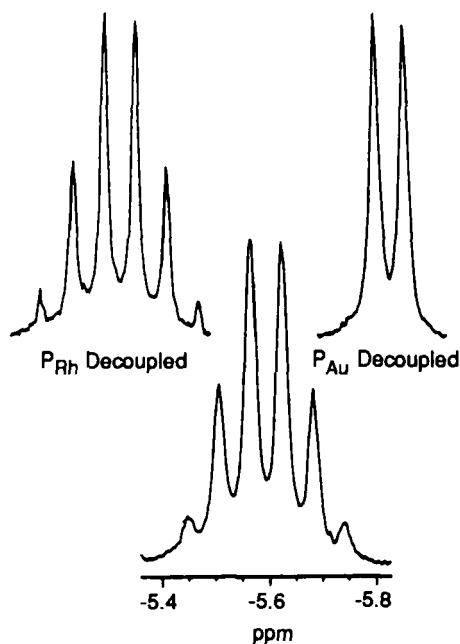


FIG. 12. Hydride region of the ^1H NMR spectrum of $[\text{Au}_4\text{Rh}(\text{H})_2\{\text{P}(\text{O-}i\text{-C}_3\text{H}_7)_3\}_2(\text{PPh}_3)_4]^+$.

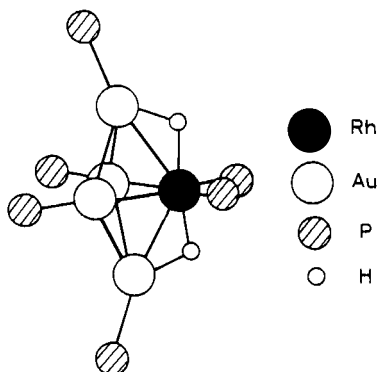


FIG. 13. Molecular structure of $[\text{Au}_4\text{Rh}(\text{H})_2\{\text{P}(\text{O}-i\text{-C}_3\text{H}_7)_3\}_2(\text{PPh}_3)_4]^+$.

between the ^{103}Rh , the ^{31}P , and the ^1H nuclei to be measured. The very small value of the $^{31}\text{P}_{\text{Rh}}-^1\text{H}$ coupling constant is consistent with a structure in which the hydride ligands bridge the axial $\text{Rh}-\text{Au}$ bonds, as shown in Fig. 13.

D. X-RAY CRYSTALLOGRAPHIC STUDIES

The discussion above has outlined the applications of conventional spectroscopic and analytical techniques to the problems of characterization of heterometallic gold cluster compounds. Although much useful information can be obtained from these methods, single-crystal X-ray diffraction still remains the most useful and most widely used single technique for the characterization of these compounds. Despite its obvious value in structure determination, problems can arise in X-ray diffraction studies due to the disorder of ligands and the location of light elements in heavy metal structures. This can be especially problematical with hydrido compounds, where it is not usually possible to locate the hydride ligands on the basis of the X-ray data and recourse to spectroscopic techniques and Orpen potential energy calculations is often necessary (260). Although neutron diffraction is the preferred technique for locating hydride ligands, crystals considerably larger than those used in X-ray studies are required and are rarely available.

The following sections summarize the crystallographic results that have been reported for compounds where gold-metal bonding interactions are considered to exist.

1. Monogold Heteronuclear Cluster Compounds

Numerous examples of heteronuclear cluster compounds containing only one gold moiety have been structurally characterized, the majority of which contain the AuPR₃ fragment. In the simplest compounds the gold phosphine group acts as a terminal ligand to a heterometal fragment to form a single gold-metal bond, examples of which are given in Table III. As will be discussed in more detail later, the AuPR₃ group is considered to be isolobal with the H and CH₃ ligands, its bonding being dominated by an outpointing *s/p_z* hybrid orbital, and a number of these compounds exhibit geometries similar to that of the corresponding hydrido complex. Thus [Co(CO)₄(AuPPh₃)] (20, 21) and [HCo(CO)₄] (261) both have geometries in which there is a distorted trigonal bipyramidal coordination around the cobalt atom, with the AuPPh₃ or H ligands occupying apical positions and with the equatorial ligands bent toward this coordination site. This is illustrated in Fig. 14.

TABLE III

SUMMARY OF METAL-METAL BOND LENGTHS FOR Au₁ HETERONUCLEAR CLUSTER COMPOUNDS CONTAINING TERMINAL AuPR₃ FRAGMENTS

Compound	Au-M (Å)	Reference
[Co(CO) ₃ (PPh ₃)(AuPPh ₃)]	Au-Co = 2.450(1)	12
[Co(CO) ₄ (AuPPh ₃)]	Au-Co = 2.50(1)	14, 20, 21
[(η^5 -C ₅ H ₄ CHO)Cr(CO) ₃ (AuPPh ₃)]	Au-Cr = 2.632(2)	30
[FeW(CO) ₉ (AuPPh ₃)] ⁻	Au-Fe = 2.520(3)	37
<i>mer</i> -[Fe(CO) ₃ (PPh ₃)(SiMePh ₂)(AuPPh ₃)]	Au-Fe = 2.551(1)	54
[(η^3 -C ₃ H ₅)Fe(CO) ₃ (AuPPh ₃)]	Au-Fe = 2.519(1)	55
[(<i>dppe</i>) ₂ Ir(AuPPh ₃)] ²⁻	Au-Ir = 2.625(1)	73
[IrH(CO)(PPh ₃) ₃ (AuPPh ₃)] ⁻	Au-Ir = 2.662(1)	76
[(η^5 -C ₅ H ₅)MoMn(μ -PPh ₂)(CH(Me)C ₂ H ₂ Au(PMe ₂ Ph))(CO) ₄]	Au-Mn = 2.716(2)	78
[Mn(CO) ₄ (P(OPh) ₃)(AuPPh ₃)]	Au-Mn = 2.57(1)	80
[Mn(CO) ₅ (AuPPh ₃)]	Au-Mn = 2.52(3)	81
[Mo(CO) ₃ (η^5 -C ₅ H ₄ CHO)(AuPPh ₃)]	Au-Mo = 2.7121(5)	85
[Pt ₃ (μ_3 -S)(AuPPh ₃)(μ_3 -AgCl)(μ - <i>dpmm</i>) ₃] ⁻	Au-Pt = 2.575(3)	132
[(η^5 -C ₅ H ₅)(CO)(<i>p</i> -N ₂ C ₆ H ₄ OMe)Re(AuPPh ₃)]	Au-Re = 2.615(1)	146
[(PhMe ₂ P) ₂ AuSnCl ₃]	Au-Sn = 2.881(1)	196
[V(CO) ₆ (AuPPh ₃)]	Au-V = 2.690(3)	198
[(η^5 -C ₅ H ₅)W(μ -CH(C ₆ H ₄ -Me-4))(CO) ₂ (PPh ₃)(AuPPh ₃)]	Au-W = 2.729(1)	130, 202
[(η -C ₂ B ₉ H ₉ Me ₂)W(μ -CC ₆ H ₄ -Me-4)(CO) ₂ (PPh ₃)(AuPPh ₃)]	Au-W = 2.780(8)	205, 206
[W{HB(pz) ₃ }(CO) ₂ (CS)(AuPPh ₃)]	Au-W = 2.8248(4)	207
[W{HB(pz) ₃ }(CO) ₂ (CS)(AuPMe ₃)]	Au-W = 2.8241(1)	207
[(η^5 -C ₅ H ₅)W(CO) ₃ (AuPPh ₃)]	Au-W = 2.698(3)	209

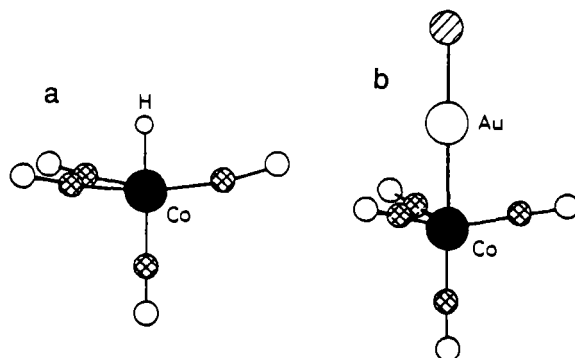


FIG. 14. A comparison of the molecular structures of (a) $[\text{HCo}(\text{CO})_4]$ and (b) $[\text{Co}(\text{CO})_4(\text{AuPPh}_3)]$.

The structures of $[\text{Mn}(\text{CO})_5(\text{AuPPh}_3)]$ (81), $[\text{Mn}(\text{CO})_4\{\text{P}(\text{OPh})_3\}(\text{AuPPh}_3)]$ (80), and $[\text{HMn}(\text{CO})_5]$ (261) are similarly closely related. Because of the similarities in the bonding of H and AuPR_3 and the problems associated with the location of hydride ligands in X-ray experiments, a number of workers have utilized the synthesis and characterization of gold heterometallic compounds to infer the position of the hydride ligand in the related hydrido complex. An interesting example is provided by the anions $[\text{HFeW}(\text{CO})_9]^-$ and $[(\text{Ph}_3\text{PAu})\text{FeW}(\text{CO})_9]^-$ (37, 262). An X-ray analysis of the former could not locate the hydride ligand, but it has been assumed to bond terminally to the iron atom and not to bridge the Fe–W bond by analogy with the molecular structure of the gold heteronuclear compound, which is illustrated in Fig. 15.

Examples of heteronuclear compounds containing terminally bonded

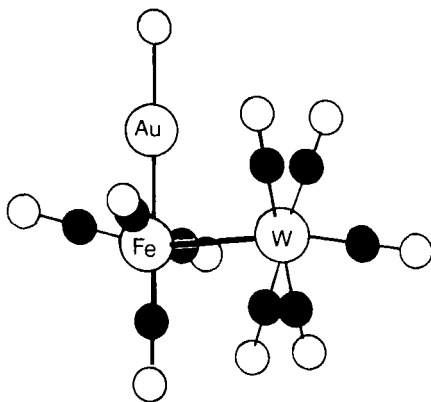


FIG. 15. Molecular structure of $[(\text{Ph}_3\text{PAu})\text{FeW}(\text{CO})_9]^-$.

TABLE IV

SUMMARY OF METAL–METAL BOND LENGTHS FOR Au_1 HETERONUCLEAR CLUSTER COMPOUNDS CONTAINING HYDRIDE BRIDGED TERMINAL AuPR_3 FRAGMENTS

Compound	Au–M (Å)	Reference
$[\text{Cr}(\text{CO})_5(\mu\text{-H})(\text{AuPPh}_3)]$	Au–Cr = 2.770(2)	31, 32
$[\text{Ir}(\text{PPh}_3)_3(\text{H})(\mu\text{-H})(\text{AuPPh}_3)]^+$	Au–Ir = 2.765(1)	62, 75
$[\text{Ir}(\text{bipy})(\text{PPh}_3)_2(\mu\text{-H})(\text{AuPPh}_3)]^{2+}$	Au–Ir = 2.699(0)	63
$[\text{Pt}(\text{C}_6\text{F}_5)(\text{PEt}_3)_2(\mu\text{-H})(\text{AuPPh}_3)]^+$	Au–Pt = 2.714(1)	118
$[\text{Pt}(\text{C}_6\text{Cl}_5)(\text{PPh}_3)_2(\mu\text{-H})(\text{AuPPh}_3)]^+$	Au–Pt = 2.792(1)	131
$[\text{Ru}(\text{PPh}_3)_3(\text{CO})(\mu\text{-H})(\text{AuPPh}_3)]^+$	Au–Ru = 2.786(1)	89
$[\text{Ru}(\text{dppm})_2(\mu\text{-H})(\text{AuPPh}_3)]^+$	Au–Ru = 2.694(1)	163

gold phosphine groups are given in Table III. The metal–gold bond lengths in these compounds approximate to those that would be anticipated on the basis of covalent radii, with bridged Au–M bonds in general being longer than unsupported bonds. An exception is provided by $[(\text{PMe}_2\text{Ph})_2\text{AuSnCl}_3]$ (196) in which the Au–Sn bond is considerably longer than would be predicted. This has been attributed to a Au–Sn bonding interaction that is considerably distorted toward a linear $[\text{Au}(\text{PMe}_2\text{Ph})_2]^+$ cation and an uncoordinated SnCl_3^- anion.

A number of examples of transition metal–gold bonds bridged by hydride ligands, as in the compound $[\text{Cr}(\text{CO})_5(\mu\text{-H})(\text{AuPPh}_3)]$ (31, 32), have been reported, and these are listed in Table IV. These complexes have all been prepared by addition of AuPPh_3^+ to transition metal hydrido complexes and may be considered examples of the gold phosphine fragment bridging a metal–hydride bond (Fig. 16).

The gold phosphine fragment has been used extensively as a cluster building unit and numerous examples of AuPR_3 groups bridging metal–metal bonds have been structurally characterized, in which the gold moieties exhibit μ_2 - and μ_3 -coordination modes. Tables V and VI

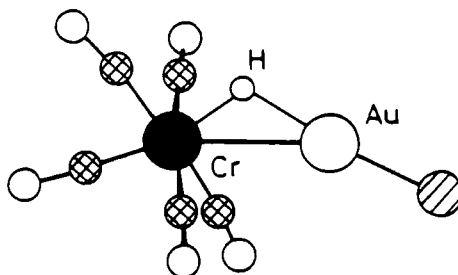


FIG. 16. Molecular structure of $[\text{Cr}(\text{CO})_5(\mu\text{-H})(\text{AuPPh}_3)]$.

TABLE V

SUMMARY OF BOND LENGTHS AND METAL CAGE GEOMETRIES FOR Au_1 HETERONUCLEAR CLUSTER COMPOUNDS CONTAINING μ_2 -AuPR₃ FRAGMENTS


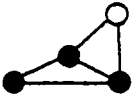
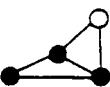
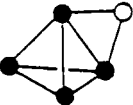

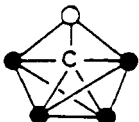
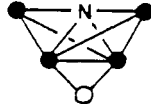
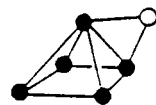
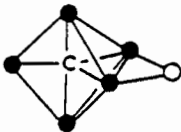
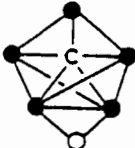
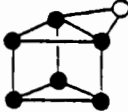
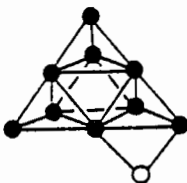
Metal cage geometry	Compound	Au-M (Å)	Reference
	[Fe ₂ (μ-CO) ₂ (CO) ₆ (μ-AuPPh ₃)]	Au-Fe = 2.622(1), 2.698(1)	53
	[Fe ₂ (CO) ₆ (C ₁₁ H ₁₉ S)(μ-AuPPh ₃)]	Au-Fe = 2.683(4), 2.700(3)	56
	[Mn ₂ (μ-PPh ₂)(CO) ₈ (μ-AuPMe ₂ Ph)]	Au-Mn = 2.681(6), 2.696(6)	79
	[Mn ₂ (μ-Br)(μ-tedip)(CO) ₆ (μ-AuPPh ₃)]	Au-Mn = 2.640(3), 2.679(3)	82
	[(C ₅ H ₅)W(μ-PCy ₂)(μ-AuPPh ₃)Pt(CO) ₃ (PCy ₂ H)] ⁺	Au-Pt = 2.860(2) Au-W = 2.763(2)	121
	[(C ₅ H ₅)(CO) ₂ W(μ ₃ -CR)(μ-AuPMe ₃)Pt(PMe ₃) ₂] ⁺	Au-Pt = 2.956(2) Au-W = 2.801(2)	130
	[Pt ₂ (μ-SO ₂)(CNC ₈ H ₉) ₂ (PCy ₃) ₂ (μ-AuPPh ₃)] ⁺	Au-Pt = 2.705(7) 2.717(7)	134
	[Re ₂ H ₇ (PPh ₃) ₄ (μ-AuPPh ₃)]	Au-Re = 2.7197(8) 2.9266(8)	151
	[Rh ₂ (μ-AuPPh ₃)(μ-L)(CO) ₂ (PPh ₃) ₂] ⁺	Au-Rh = 2.797(2) 2.690(2)	157
	[Rh ₂ (η ⁵ -C ₅ H ₅)(μ-CO)(μ-dppm)(μ-AuPPh ₃)] ⁺	Au-Rh = 2.718(1) 2.732(1)	161
	[Co ₂ Fe(μ ₃ -CPh)(CO) ₉ (μ-AuPPh ₃)]	Au-Co = 2.661(3) Au-Fe = 2.615(3)	11
	[Fe ₂ Co(η ⁵ -C ₅ H ₅)(μ ₃ -COCH ₃)(CO) ₇ (μ-AuPPh ₃)]	Au-Fe = 2.681(1) 2.698(1)	34
	[Fe ₃ (μ ₃ -HC≡NBu ^t)(CO) ₉ (μ-AuPPh ₃)]	Au-Fe = 2.659(2)- 2.717(3)	39
	[FeRuCo(CO) ₉ (μ ₃ -S)(μ-AuPPh ₃)]	No data	40
	[FeRuCo(CO) ₉ (μ ₃ -PMe)(μ-AuPPh ₃)]	Au-Fe = 2.677(2) Au-Ru = 2.729(2)	40
	[Os ₃ (μ-Cl)(CO) ₁₀ (μ-AuPPh ₃)]	Au-Os = 2.75 2.77	90
	[Os ₃ (μ-Br)(CO) ₁₀ (μ-AuPPh ₃)]	Au-Os = 2.73 2.76	90
	[Os ₃ (μ-CH=CHPh)(CO) ₁₀ (μ-AuPPh ₃)]	Au-Os = 2.738(1) 2.795(1)	92
	[Os ₃ (μ-CH=CHC ₆ F ₅)(CO) ₁₀ (μ-AuPPh ₃)]	Au-Os = 2.766(1) 2.777(1)	92
	[Os ₃ (2-NHC ₅ H ₄ N)(CO) ₈ (PPh ₃)(μ-AuPPh ₃)]	Au-Os = 2.738(2) 2.788(2)	94
	[Os ₃ (C ₂ Ph)(CO) ₁₀ (μ-AuPMe ₂ Ph)]	Au-Os = 2.770(1) 2.794(1)	97
	[Os ₃ (μ-COCH ₃)(CO) ₁₀ (μ-AuPPh ₃)]	Au-Os = 2.765(1) 2.790(1)	99
	[Os ₃ (μ-H)(CO) ₁₀ (μ-AuPPh ₃)]	Au-Os = 2.738(1) 2.771(2)	104
	[Os ₃ (μ-SCN)(CO) ₁₀ (μ-AuPPh ₃)]	Au-Os = 2.755(1) 2.768(1)	104
	[Ru ₃ (μ ₃ -COMe)(μ-H) ₂ (CO) ₉ (μ-AuPPh ₃)]	Au-Ru = 2.727(1) 2.763(1)	164, 165

TABLE V *Continued*

Metal cage geometry	Compound	Au-M (Å)	Reference
	[Ru ₃ (μ-COMe)(CO) ₉ (μ-AuPPh ₃)]	Au-Ru = 2.760(2) 2.762(2)	165, 185
	[Ru ₃ (C ₂ Bu ^t)(CO) ₉ (μ-AuPPh ₃)]	Au-Ru = 2.757(1)	168
	[Ru ₃ (μ ₃ -S)(μ-H)(CO) ₉ (μ-AuPPh ₃)]	Au-Ru = 2.763(1) 2.736(1)	174
	[Ru ₃ (μ ₃ -SBu ^t)(CO) ₉ (μ-AuPPh ₃)]	Au-Ru = 2.766(1) 2.773(1)	174
	[Ru ₃ (μ ₃ -PPhCH ₂ PPh ₂)(CO) ₉ (μ-AuPPh ₃)]	Au-Ru = 2.751(1) 2.786(1)	176
	[Ru ₃ H(CO) ₈ (PPh ₂) ₂ (μ-AuPPh ₃)]	Au-Ru = 2.7209(13) 2.9288(12)	190
	[Ru ₃ (μ ₃ -Cl)(CO) ₁₀ (μ-AuPPh ₃)]	Au-Ru = 2.7523(6) 2.7549(6)	191
	[Ru ₃ (μ ₃ -PPh)(μ-H)(CO) ₉ (μ-AuPMe ₂ Ph)]	Au-Ru = 2.749(4) 2.763(4)	192, 193
	[Ir ₃ (CO) ₁₀ (μ-PPh ₂)(μ-AuPPh ₃)]	No data	69
	[Os ₃ (μ-H) ₂ (CO) ₉ Ni(η-C ₅ H ₅)(μ-AuPPh ₃)]	Au-Os = 2.747(2) 2.775(2)	91
	[Os ₄ (μ-H)(CO) ₁₃ (μ-AuPEt ₃)]	Au-Os = 2.745(2) 2.799(2)	106
	[Os ₄ (μ-H) ₃ (CO) ₁₂ (μ-AuPEt ₃)]	Au-Os = 2.783(2) 2.803(2)	106
	[H ₃ Ru ₄ (CO) ₁₂ (μ-AuPPh ₃)]	Au-Ru = 2.723(1) 2.809(1)	182
	[Fe ₄ (COCH ₃)(CO) ₁₂ (μ-AuPEt ₃)]	Au-Fe = 2.666(2) 2.675(3)	42, 43
	[Fe ₄ (CO) ₁₃ (μ-AuPEt ₃)]	Au-Fe = 2.666(1)	43
	[Fe ₄ C(μ-H)(CO) ₁₂ (AuPPh ₃)]	Au-Fe = 2.854(1) 2.880(1)	49
	[Ru ₄ C(CO) ₁₂ (μ-I)(AuPEt ₃)]	Au-Ru _{av} = 2.92	181
	[Ru ₄ C(CO) ₁₂ (μ-H)(AuPPh ₃)]	Au-Ru _{av} = 2.95	181
	[FeRu ₃ N(CO) ₁₂ (μ-AuPPh ₃)]	Au-Ru = 2.755(1) 2.766(1)	167
	[Ru ₅ C(CO) ₁₃ (NO)(μ-AuPEt ₃)]	Au-Ru = 2.748(2) 2.792(2)	186

(continued)

TABLE V *Continued*

Metal cage geometry	Compound	Au-M (Å)	Reference
	$\{[\text{Ru}_5\text{C}(\text{CO})_{13}(\text{PPh}_3)(\mu\text{-I})(\mu\text{-AuPPh}_3)]$	Au-Ru = 2.661(1) 2.837(1)	179
	$[\text{Ru}_5\text{C}(\text{CO})_{15}\text{Cl}(\mu\text{-AuPPh}_3)]$	Au-Ru = 2.764(3)– 2.841(3)	188
	$[\text{Ru}_5\text{C}(\text{CO})_{14}(\mu\text{-Br})(\mu\text{-AuPPh}_3)]$	Au-Ru = 2.633(2) 2.850(2)	188
	$[\text{Ru}_5\text{C}(\text{CO})_{14}(\mu\text{-}\eta^2\text{-MeCO})(\mu\text{-AuPPh}_3)]$	Au-Ru = 2.721(3) 2.764(3)	180
	$[\text{Ru}_5\text{C}(\text{CO})_{13}(\eta^5\text{-C}_5\text{H}_5)(\mu\text{-AuPPh}_3)]$	Au-Ru = 2.750(1) 2.780(1)	180
	$[\text{Os}_6(\text{CO})_{18}\text{P}(\mu\text{-AuPPh}_3)]$	Au-Os = 2.775(1) 2.793(1)	95
	$[\text{Os}_{10}\text{C}(\text{CO})_{24}(\mu\text{-AuPPh}_3)]^-$	Au-Os = 2.781(2) 2.851(2)	109, 110

Note. L = 1,8-(NH)₂C₁₀H₆

TABLE VI

SUMMARY OF BOND LENGTHS AND METAL CAGE GEOMETRIES FOR Au₁ HETERONUCLEAR CLUSTER COMPOUNDS CONTAINING $\mu_3\text{-AuPR}_3$ FRAGMENTS

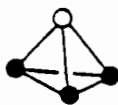
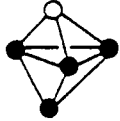

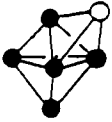
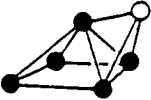
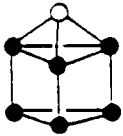
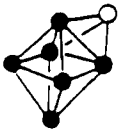
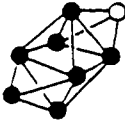
Metal cage geometry	Compound	Au-M (Å)	Reference
	$[\text{Pd}_3(\mu\text{-Cl})(\mu\text{-SO}_2)_2(\text{PCy}_3)_3(\mu_3\text{-AuPCy}_3)]$	Au-Pd = 2.72–2.79	116
	$[\text{Pt}_3(\mu\text{-CO})_3(\text{PPh}_3)_4(\mu_3\text{-AuPPh}_3)]^+$	Au-Pt = 2.700(1)– 2.910(1)	122
	$[\text{Pt}_3(\mu\text{-CO})_3(\text{PCy}_3)_3(\mu_3\text{-AuPCy}_3)]^+$	Au-Pt = 2.750(5)– 2.768(5)	127
	$[\text{Pt}_3(\mu\text{-CO})_2(\mu\text{-SO}_2)(\text{PCy}_3)_3(\mu_3\text{-AuPCy}_3)]^+$	Au-Pt = 2.755(1)– 2.759(5)	141
	$[\text{Pt}_3(\mu\text{-SO}_2)_2(\mu\text{-Cl})(\text{PCy}_3)_3(\mu_3\text{-AuP}\{p\text{-C}_6\text{H}_4\text{F}\}_3)]$	Au-Pt = 2.766(1)– 2.771(1)	141
	$[\text{Re}_3(\mu\text{-H})_3(\text{CO})_9(\mu_3\text{-AuPPh}_3)]^-$	Au-Re = 2.826(1)– 2.845(1)	147

TABLE VI *Continued*

Metal cage geometry	Compound	Au-M (Å)	Reference
	$[\text{Co}_3\text{Ru}(\text{CO})_{12}(\mu_3\text{-AuPPh}_3)]$	Au-Co = 2.679(4)– 2.745(4)	15, 16
	$[\text{CoRu}_3(\text{CO})_{13}(\mu_3\text{-AuPPh}_3)]$	Au-Co = 2.868(2) Au-Ru = 2.774(1), 2.776(1)	18
	$[\text{Co}_3\text{Fe}(\text{CO})_{12}(\mu_3\text{-AuPPh}_3)]$	Au-Co _{av} = 2.714(7)	22
	$[\text{Co}_3\text{Fe}(\text{CO})_{11}(\text{PMe}_2\text{Ph})(\mu_3\text{-AuPPh}_3)]$	Au-Co = 2.686(4)– 2.739(4)	23
	$[\text{Co}_3\text{Fe}(\text{CO})_{10}[\text{P}(\text{OMe})_3]_2(\mu_3\text{-AuPPh}_3)]$	Au-Co = 2.690(2)– 2.742(2)	23
	$[\text{Co}_{1.6}\text{Rh}_{1.4}\text{Ru}(\text{CO})_{12}(\mu_3\text{-AuPPh}_3)]$	Au-M = 2.749(1)– 2.810(1)	24
	$[\text{Fe}_2\text{Ir}_2(\text{CO})_{12}(\mu_3\text{-AuPPh}_3)]^-$	Au-Fe = 2.806(1) Au-Ir = 2.797(1), 2.829(1)	52
	$[\text{HOs}_4(\text{CO})_{12}(\mu_3\text{-N}(\text{CO})\text{Me})(\mu_3\text{-AuPPh}_3)]$	Au-Os = 2.762(1)– 2.940(1)	113, 114
	$[\text{Os}_5\text{H}(\text{CO})_{15}(\mu_3\text{-AuPPh}_3)]$	Au-Os = 2.831(1)– 2.926(1)	112
	$[\text{Ru}_5\text{C}(\text{CO})_{13}(\text{NO})(\mu_3\text{-AuPEt}_3)]$	Au-Ru = 2.783(2)– 3.033(2)	186
	$[\text{Rh}_6\text{C}(\text{CO})_{15}(\mu_3\text{-AuPPh}_3)]^-$	Au-Rh = 2.749(3)– 2.860(3)	158
	$[\text{Ru}_6\text{C}(\text{CO})_{15}(\text{NO})(\mu_3\text{-AuPPh}_3)]$	Au-Ru = 2.763(2)– 3.159(2)	189
	$[\text{Re}_7\text{C}(\text{CO})_{21}(\mu_3\text{-AuPPh}_3)]^{2-}$	Au-Re = 2.856(1)– 2.893(1)	150

summarize the structural data on these compounds and the range of metal core geometries that results from addition of the AuPR_3 group.

The flexibility of the AuPR_3 fragment to function as a face (μ_3^-) or edge (μ_2^-) bridging group is vividly demonstrated by the cluster compound $[\text{Ru}_5\text{C}(\text{CO})_{13}(\text{NO})(\text{AuPEt}_3)]$ (186). Two independent molecules, which are skeletal isomers, are found in the solid-state structure. Both are based on a square-pyramidal Ru_5 arrangement, with one molecule possessing a μ_2^- -coordinated AuPEt_3 group and the other a (μ_3^-) face capping gold fragment.

A number of examples of monogold heteronuclear complexes that do not contain the AuPR_3 moiety have been structurally characterized. These include a number of compounds in which the gold-metal distances lie toward the upper range of the sum of the metallic radii, as in the compounds $[\text{HgAu}\{\text{CH}_2\text{P}(\text{S})\text{Ph}_2\}_2](\text{PF}_6)$ (59) ($\text{Au-Hg} = 3.088(1)$ Å) and $[\text{AuTl}\{\text{CH}_2\text{P}(\text{S})\text{Ph}_2\}_2]_n$ (197) ($\text{Au-Tl} = 2.959(2)$ and $3.003(2)$ Å). The weak metal-metal interaction in these compounds is comparable to that found in binuclear $\text{Au}(\text{I})$ complexes such as $[\text{Au}_2(\text{Et}_2\text{PCH}_2\text{CH}_2\text{S})_2]$ (263) and $[\text{Au}_2(\text{S}_2\text{CNPr}_2)_2]_n$ (264), in which short $\text{Au}\cdots\text{Au}$ contacts perpendicular to the ligand-gold-ligand axis occur. In the latter complex the dimers are further linked to form infinite $\text{Au}\cdots\text{Au}$ chains, to give a solid-state structure similar to that of $[\text{AuTl}\{\text{CH}_2\text{P}(\text{S})\text{Ph}_2\}_2]_n$, which is illustrated in Fig. 17.

2. Digold Heteronuclear Cluster Compounds

Numerous examples of gold cluster compounds containing two gold phosphine fragments have been structurally characterized, and these are listed in Table VII. As the table illustrates, a wide range of metal cage geometries have been observed for these compounds. A noticeable feature of many of these cluster geometries is the tendency for the gold atoms to occupy adjacent sites in the metal cage. This has been attributed to the occurrence of supplementary $\text{Au}\cdots\text{Au}$ bonding interactions and gives rise to Au-Au bond lengths in these compounds that fall in the range $2.590(2)$ to $3.176(1)$ Å. Although many of these distances are longer than those found in metallic gold (2.884 Å) (265),

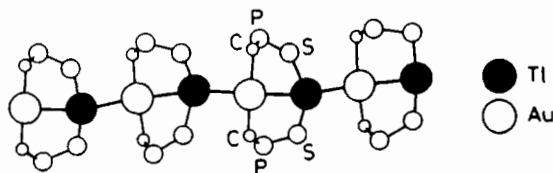

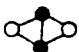
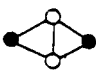
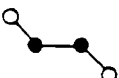



FIG. 17. The repeat structure of $[\text{AuTl}\{\text{CH}_2\text{P}(\text{S})\text{Ph}_2\}_2]_n$.

TABLE VII

SUMMARY OF BOND LENGTHS AND METAL CAGE GEOMETRIES FOR Au₂ HETERONUCLEAR CLUSTER COMPOUNDS CONTAINING AuPR₃ FRAGMENTS

Metal cage geometry	Compound	Au-M (Å)	Reference
	[Fe(CO) ₄ (AuPPh ₃) ₂]	Au-Au = 3.028(1)	51
	[Ru(H) ₂ (dppm) ₂ (AuPPh ₃) ₂] ²⁺	Au-Ru = 2.786(0), 2.776(0)	63
	[IrH(NO ₃)(PPh ₃) ₂ (AuPPh ₃) ₂]	Au-Au = 2.933(0) Au-Ir = 2.673(1), 2.697(1)	72
	[Nb(η ⁵ -C ₅ H ₄ SiMe ₃) ₂ (AuPPh ₃) ₂]	Au-Au = 2.728(1) Au-Nb = 2.9098(8), 2.9139(8)	88
	[Os(H) ₃ (PPh ₃) ₃ (AuPPh ₃) ₂] ⁺	Au-Au = 2.7359(5) Au-Os = 2.696(1), 2.709(1)	89
	[Os(CO) ₄ (AuPPh ₃) ₂]	Au-Os = 2.646(1), 2.667(1)	110
	[PtCl(PEt ₃) ₂ (AuPPh ₃) ₂] ⁺	Au-Au = 2.929(1) Au-Pt = 2.600(3), 2.601(4)	126
	[Re ₂ (PMe ₂ Ph) ₄ (μ-H) ₂ H ₄ (AuPPh ₃) ₂]	Au-Au = 2.737(3) Au-Re = 2.7625(9), 2.7725(10)	152
	[Au ₂ Pt ₂ (PPh ₃) ₄ (CNC ₈ H ₃) ₄] ²⁺	Au-Pt = 2.711(2)- 3.026(2) Au-Au = 2.590(2)	128, 129
	[Au ₂ Pt ₂ (μ-PPh ₂) ₂ (PPh ₃) ₄] ²⁺	Au-Pt = 2.634(1), 2.667(1)	120
	[W ₂ (CO) ₈ (μ-PPh ₂) ₂ (AuPPh ₃) ₂] ⁻	Au-W _{av} = 2.915 Au-Au = 2.749(2)	208
	[Fe ₃ (μ ₃ -S)(CO) ₉ (AuPPh ₃) ₂]	Au-Fe = 2.671(3)- 2.750(4)	25
	[Ru ₃ (μ ₃ -S)(CO) ₉ (AuPPh ₃) ₂]	Au-Au = 3.020(1) Au-Ru = 2.783(2)- 2.867(2)	174
	[Ru ₃ (μ ₃ -C≡CBu ^t)(CO) ₉ (AuPPh ₃) ₂]	Au-Au = 2.967(2) Au-Ru = 2.781(1)- 2.916(1)	175
	[Ru ₃ (μ ₃ -S)(CO) ₈ (AuPPh ₃) ₂]	Au-Au = 3.033(1) Au-Ru = 2.784(2)- 2.897(2)	183
		Au-Au = 2.915(2)	

(continued)

TABLE VII *Continued*

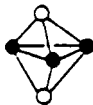
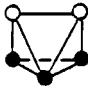




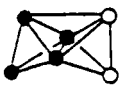

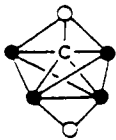
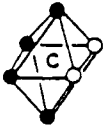
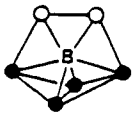
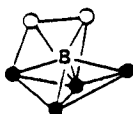
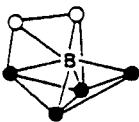
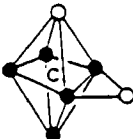

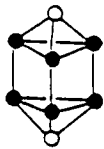
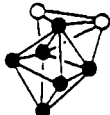

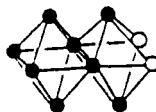
Metal cage geometry	Compound	Au-M (Å)	Reference
	$[\text{Pt}_3(\mu\text{-Cl})(\mu\text{-SO}_2)_2(\text{PCy}_3)_3\{\text{AuP}(p\text{-C}_6\text{H}_4\text{F})_3\}_2]^+$	Au-Pt = 2.772(2)– 2.803(2)	142
	{ [$\text{Ru}_3(\mu_3\text{-S})(\text{CO})_9(\text{Au}_2\text{dppm})$] [$\text{Ru}_3(\mu\text{-H})(\mu_3\text{-COMe})(\text{CO})_9(\text{AuPPh}_3)_2$] }	Au-Ru = 2.742(1)– 2.836(1)	169
		Au-Au = 2.802(1) Au-Ru = 2.702(1)– 2.796(1) Au-Au = 3.176(1)	183
	$[\text{Os}_3(\text{CO})_{10}(\text{AuPEt}_3)_2]$	Au-Os = 2.760(1), 2.762(1)	93
	{ [$\text{CoRu}_3(\text{H})(\text{CO})_{12}(\text{AuPPh}_3)_2$] [$\text{Ru}_4\text{H}_2(\text{CO})_{12}(\text{AuPPh}_3)_2$] }	Au-Co = 2.704(3) Au-Ru = 2.803(2)– 2.953(2) Au-Au = 2.787(1)	18
		Au-Ru = 2.840(1)– 3.091(1) Au-Au = 2.791(1)	184
	{ [$\text{Os}_4(\text{CO})_{13}(\text{AuPEt}_3)_2$] [$\text{Ru}_4(\mu\text{-H})(\mu_3\text{-H})(\text{CO})_{12}(\text{Au}_2\text{dppm})$] [$\text{Ru}_4(\mu\text{-H})(\mu_3\text{-H})(\text{CO})_{12}\{\text{Au}_2(\text{Ph}_2\text{AsCH}_2\text{PPh}_2)\}$] [$\text{Ru}_4(\mu\text{-H})(\mu_3\text{-H})(\text{CO})_{12}(\text{Au}_2\text{dppe})$] }	Au-Os = 2.739(1)– 2.963(1) Au-Au = 3.128(1) Au-Ru = 2.682(1)– 2.947(2) Au-Au = 2.823(1)	100
		Au-Ru = 2.689(4)– 2.846(4) Au-Au = 2.832(4)	166, 171
		Au-Ru = 2.682(1)– 2.947(2) Au-Au = 2.823(1), 2.833(2)	170
		Au-Ru = 2.839(4)– 3.004(5) Au-Au = 2.793(4)	105
	{ [$\text{Os}_4\text{H}_2(\text{CO})_{12}(\text{AuPPh}_3)_2$] [$\text{Ir}_4(\text{CO})_{11}(\text{PhPPPh})\text{Ir}_4(\text{CO})_9(\text{AuPEt}_3)_2$] }	Au-Ir = 2.713(3)– 3.007(3)	77
		Au-Au = 3.052(2) Au-Co = 2.613(3)– 2.866(3)	25
	$[\text{Co}_2\text{Ru}_2(\text{CO})_{12}(\text{AuPPh}_3)_2]$	Au-Ru = 2.872(2), 2.887(2) Au-Au = 2.890(1)	
	$[\text{Os}_4(\text{CO})_{12}(\text{AuPMePh}_2)_2]$	Au-Os = 2.739(1)– 2.863(1) Au-Au = 3.128(1)	100

TABLE VII *Continued*

Metal cage geometry	Compound	Au-M (Å)	Reference
	[Ru ₄ C(CO) ₁₂ (AuPMe ₂ Ph) ₂]	Au-Ru = 2.80–2.86	181
	[Fe ₄ C(CO) ₁₂ (AuPEt ₃) ₂]	Au-Fe = 2.770(1)– 2.999(2) Au-Au = 3.017(1)	49
	$\left\{ \begin{array}{l} [\text{HFe}_4(\text{CO})_{12}(\text{AuPEt}_3)_2\text{B}] \\ [\text{HRu}_4(\text{CO})_{12}(\text{AuPPh}_3)_2\text{B}] \end{array} \right.$	Au-Fe = 2.615(1) Au-Au = 2.880(1) Au-Ru = 2.728(1), 2.730(1) Au-Au = 2.849(1)	47, 48 178
	[Fe ₄ (CO) ₁₂ (AuPPh ₃) ₂ BH]	Au-Fe = 2.606(1)– 2.852(2) Au-Au = 2.943(1)	44, 45
	[Fe ₄ (CO) ₁₂ {AuP(<i>p</i> -MeC ₆ H ₄) ₃ } ₂ BH}]	Au-Fe = 2.635(2), 2.808(3) Au-Au = 2.975(1)	48
	[Fe ₅ C(μ-CO)(CO) ₁₁ (μ-AuPEt ₃)(μ ₄ -AuPEt ₃)]	Au-Fe = 2.696(2)– 3.036(3)	50
	[Os ₅ C(CO) ₁₄ (AuPPh ₃) ₂]	Au-Os = 2.662(1)– 2.873(1)	108
	[Rh ₆ C(CO) ₁₅ (AuPPh ₃) ₂]	Au-Rh = 2.781(1)– 2.863(1)	158

(continued)

TABLE VII *Continued*

Metal cage geometry	Compound	Au-M (Å)	Reference
	$\left\{ \begin{array}{l} [\text{Rh}_6\text{C}(\text{CO})_{13}(\text{AuPPh}_3)_2] \\ \\ [\text{Ru}_5\text{WC}(\text{CO})_{17}(\text{AuPEt}_3)_2] \end{array} \right.$	$\begin{array}{l} \text{Au-Rh} = 2.800(2)\text{--}3.147(2) \\ \text{Au-Au} = 2.929(2) \\ \text{Au-Ru} = 2.840(4)\text{--}2.935(4) \\ \text{Au-Au} = 2.808(3) \end{array}$	$\begin{array}{l} 159 \\ \\ 177 \end{array}$
	$[\text{Ru}_6\text{C}(\text{CO})_{16}(\text{AuPMePh}_2)_2]$	$\text{Au-Ru} = 2.758(1)\text{--}2.788(1)$	177
	$[\text{Os}_6(\text{CO})_{22}(\text{AuPPh}_3)_2]$	$\text{Au-Os} = 2.740(3)\text{--}3.003(3)$	107

they are not sufficiently long to be ignored as nonbonded contacts. The theoretical interpretation of this phenomenon will be discussed in Section IV.

This property of gold(I) moieties to form partially bonding contacts to other gold species has been described as “aurophilicity” by Schmidbaur and his co-workers (266) and represents an important limitation of the isolobal analogy. An example of this is provided by a comparison of the structures of $[\text{H}_2\text{Fe}(\text{CO})_4]$ (261) and $[\text{Fe}(\text{CO})_4(\text{AuPPh}_3)_2]$ (51), which are illustrated in Fig. 18.

In both compounds the iron atom geometries can be described as intermediate between octahedral and bicapped tetrahedral, but in the hydrido complex the H–Fe–H bond angle is 100° , whereas the Au–Fe–Au bond angle is only 73° . This smaller angle leads to an Au–Au distance of 3.028(1) Å, which is indicative of a weak interaction between the gold atoms.

3. Trigold Heteronuclear Cluster Compounds

The cluster compounds $[(\text{PhMe}_2\text{P})_3\text{ReH}_3(\text{AuPPh}_3)_3]^+$, $[\text{Rh}(\text{H})(\text{CO})(\text{PPh}_3)_2(\text{AuPPh}_3)_3]^+$, $[(\text{triphos})\text{RhH}_2(\text{AuPPh}_3)_3]^{2+}$, $[\text{V}(\text{CO})_5(\text{AuPPh}_3)_3]$, and $[\text{WH}_2(\mu\text{-H})_2(\text{PMe}_3)_3(\text{AuPPh}_3)_3]^+$ are all characterized by 54 valence electrons and adopt tetrahedral metal cage geometries. $[\text{Ir}(\text{NO}_3)(\text{PPh}_3)_2(\text{AuPPh}_3)_3]^+$ and $[(\text{PhMe}_2\text{P})_3\text{ReH}_2(\text{AuPPh}_3)_3]$ also possess 54 valence electrons but have planar arrangements of metal atoms. Inter-

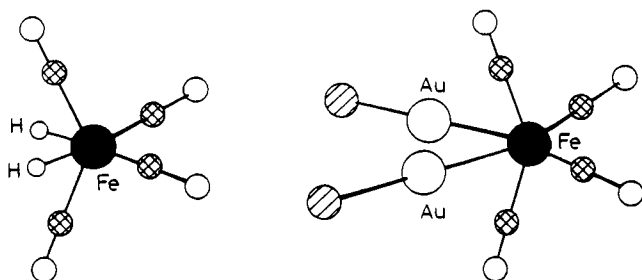


FIG. 18. A comparison of the molecular structures of $[\text{H}_2\text{Fe}(\text{CO})_4]$ and $[\text{Fe}(\text{CO})_4(\text{AuPPh}_3)_2]$.

estingly, protonation of $[(\text{PhMe}_2\text{P})_3\text{ReH}_2(\text{AuPPh}_3)_3]$ readily yields $[(\text{PhMe}_2\text{P})_3\text{ReH}_3(\text{AuPPh}_3)_3]^+$ and is accompanied by a skeletal rearrangement, as shown in Fig. 19.

A number of gold–ruthenium cluster compounds have been structurally characterized and exhibit a range of metal core geometries, which are illustrated in Fig. 20. Both $[\text{Ru}_3(\mu_3\text{-C}_{12}\text{H}_{15})(\text{CO})_8(\text{AuPPh}_3)_3]$ (173) and $[\text{Ru}_3(\mu_3\text{-COMe})(\text{CO})_9(\text{AuPPh}_3)_3]$ (164) contain gold capped Au_2Ru_3 cores, but with the AuPPh_3 group face-bridging Au_2Ru and AuRu_2 triangular faces, respectively. An open arrangement of gold atoms similar to that in $[\text{Ru}_3(\mu_3\text{-COMe})(\text{CO})_9(\text{AuPPh}_3)_3]$ is also observed in $[\text{HRu}_4(\text{CO})_{12}(\text{AuPPh}_3)_3]$ (164) and $[\text{CoRu}_3(\text{CO})_{12}(\text{AuPPh}_3)_3]$ (17), which adopt bicapped trigonal bipyramidal arrangements of metal atoms. Replacement of two PPh_3 groups in $[\text{HRu}_4(\text{CO})_{12}(\text{AuPPh}_3)_3]$ by a chelating dppm ligand to give $[\text{HRu}_4(\text{CO})_{12}(\text{Au}_2\text{dppm})(\text{AuPPh}_3)]$ (162) yields a capped square-pyramidal metal core. This metal core geometry can be

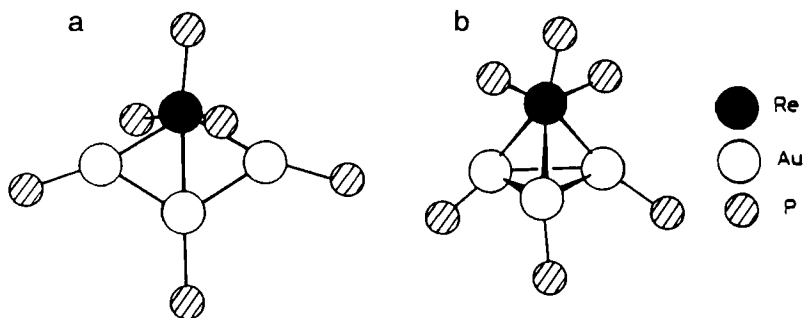


FIG. 19. The metal cage geometries of (a) $[(\text{PhMe}_2\text{P})_3\text{ReH}_2(\text{AuPPh}_3)_3]$ and (b) $[(\text{PhMe}_2\text{P})_3\text{ReH}_3(\text{AuPPh}_3)_3]^+$.

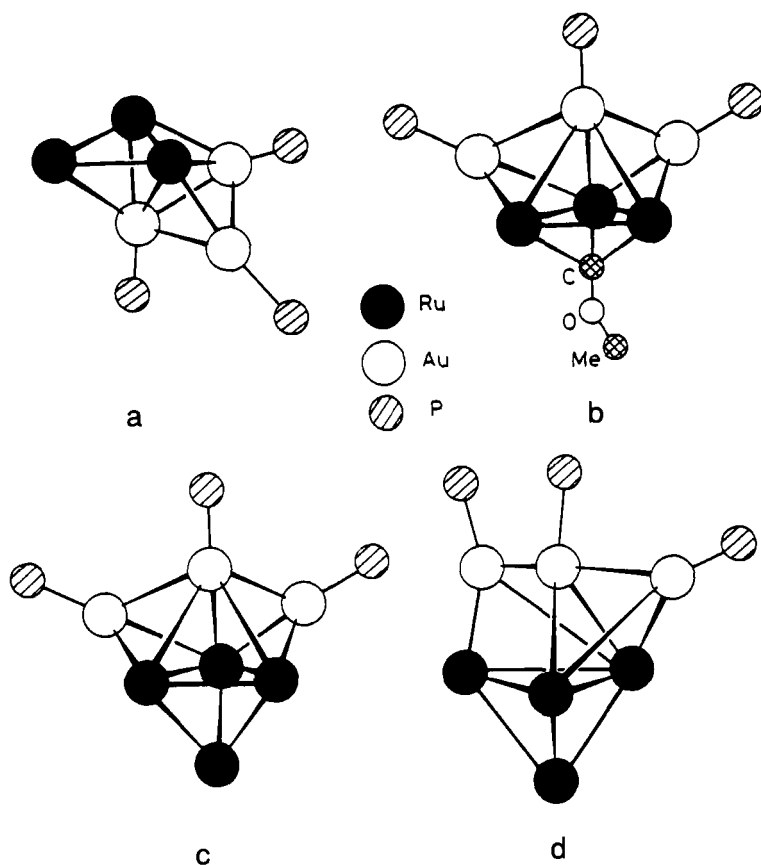


FIG. 20. Metal cage geometries of (a) $[\text{Ru}_3(\mu_3\text{-C}_{12}\text{H}_{15})(\text{CO})_8(\text{AuPPh}_3)_3]$; (b) $[\text{Ru}_3(\mu_3\text{-COMe})(\text{CO})_9(\text{AuPPh}_3)_3]$; (c) $[\text{HRu}_4(\text{CO})_{12}(\text{AuPPh}_3)_3]$; and (d) $[\text{HRu}_4(\text{CO})_{12}(\text{Au}_2\text{dppm})(\text{AuPPh}_3)]$.

considered to be derived from that of the hexanuclear cluster $[\text{Ru}_4(\mu\text{-H})(\mu_3\text{-H})(\text{CO})_{12}(\text{Au}_2\text{dppm})]$ (166, 171), with the additional AuPPh_3 group capping a triangular AuRu_2 face.

A particularly interesting example of a gold heteronuclear cluster compound is provided by $[\text{NbAuH}_2\{\text{C}_5\text{H}_4(\text{SiMe}_3)_2\}_2]_3$ (87), synthesized by reaction of $[(\text{C}_5\text{H}_4\text{SiMe}_3)_2\text{NbH}_3]$ with $\text{Au}[\text{N}(\text{SiMe}_3)_2]\text{PPh}_3$. The metal core consists of an almost equilateral triangle of gold atoms surrounded by a similarly equilateral niobium triangle (see Fig. 21). Although similar hexanuclear triangular raft clusters have been observed in silver cluster chemistry (267, 268), gold has a more pronounced tendency to adopt *closo* arrangements of metal atoms. As in the triatomic

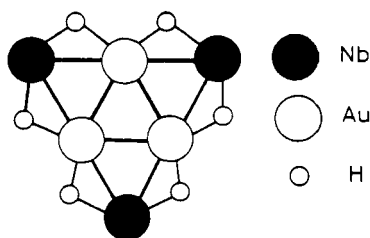


FIG. 21. Molecular structure of $[\text{NbAuH}_2\{\text{C}_5\text{H}_4(\text{SiMe}_3)_2\}_3]$. For reasons of clarity, only the metal and hydride ligands are shown.

cluster $[(\eta^5\text{-C}_5\text{H}_4\text{SiMe}_3)_2\text{Nb}(\text{AuPPh}_3)_2]^+$ (88), the Au–Au bond is considerably shorter than the Au–Nb bond, which has been attributed to the electron-poor character of the niobium center (see Table VIII).

4. Tetragold Heteronuclear Cluster Compounds

Two examples of heterometallic tetragold cluster compounds with a tetrahedral arrangement of gold atoms have been structurally characterized. Reaction of the giant tetrahedral dianion $[\text{Os}_{10}\text{C}(\text{CO})_{24}]^{2-}$ with the gold oxonium cation $[(\text{Cy}_3\text{PAu})_3\text{O}]^+$ over a period of 1 week has yielded the cluster compound $[\text{Os}_{10}\text{Au}_4\text{C}(\text{CO})_{24}(\text{PCy}_3)_3]$ (96), which has the structure illustrated in Fig. 22a. The product retains the geometry

TABLE VIII

SUMMARY OF METAL–METAL BOND LENGTHS FOR Au_3 HETERONUCLEAR CLUSTER COMPOUNDS

Compound	Au–M (Å)	Au–Au (Å)	Reference
$[\text{Ir}(\text{NO}_3)(\text{PPh}_3)_2(\text{AuPPh}_3)_3]^+$	2.593(1)–2.675(1)	2.727(1), 2.086(1)	71
$[\text{Mn}(\text{CO})_4(\text{AuPPh}_3)_3]$	2.601(3)–2.720(4)	2.695(1), 2.886(1)	83
$[(\text{PhMe}_2\text{P})_3\text{ReH}_2(\text{AuPPh}_3)_3]$	2.6881(19)–2.7295(16)	2.7868(19), 2.8123(20)	153
$[(\text{PhMe}_2\text{P})_3\text{ReH}_3(\text{AuPPh}_3)_3]^+$	2.7231(15)	2.9310(18)	153
$[\text{Rh}(\text{H})(\text{CO})(\text{PPh}_3)_2(\text{AuPPh}_3)_3]^-$	2.640(3)–2.722(3)	2.814(2)–2.914(2)	148
$[(\text{triphos})\text{RhH}_2(\text{AuPPh}_3)_3]^{2-}$	2.695(2)	2.887(1)	154
$[\text{V}(\text{CO})_5(\text{AuPPh}_3)_3]$	2.709(1)–2.756(1)	2.768(0)–2.855(0)	199
$[\text{WH}_2(\mu\text{-H})_2(\text{PMe}_3)_3(\text{AuPPh}_3)_3]^-$	2.793(1)–2.812(1)	2.796(1)–2.880(1)	201
$[\text{Ru}_3(\mu_3\text{-C}_{12}\text{H}_{15})(\text{CO})_6(\text{AuPPh}_3)_3]$	2.737(3)–2.943(4)	2.840(2)–2.911(3)	173
$[\text{Ru}_3(\mu_3\text{-COMe})(\text{CO})_9(\text{AuPPh}_3)_3]$	2.796(2)–2.987(2)	2.930(1), 3.010(1)	164, 165
$[\text{Ru}_4(\mu\text{-H})(\text{CO})_{12}(\text{AuPPh}_3)_3]$	2.822(2)–3.008(2)	2.835(2), 2.838(1)	164, 172, 187
$[\text{CoRu}_3(\text{CO})_{12}(\text{AuPPh}_3)_3]$	2.712(4)–3.054(3)	2.784(1), 2.836(1)	17, 18
$[\text{Ru}_4(\mu\text{-H})(\text{CO})_{12}(\text{AuPPh}_3)(\text{Au}_2\text{dppm})]$	2.762(3)–2.920(2)	2.749(2), 2.758(2)	162
$[\text{Fe}_4(\text{CO})_{12}\text{B}(\text{AuPPh}_3)_3]$	2.616(3)–2.711(3)	2.858(1), 2.877(1)	41
$[\text{Nb}_3\text{Au}_3\text{H}_6(\text{C}_5\text{H}_4\text{SiMe}_3)_6]$	2.985(2)–3.033(3)	2.757(2)–2.780(3)	87
$[\text{Au}_3\text{Cu}_2(\text{C}_2\text{Ph})_6]^-$	2.783(3)–3.016(3)	—	33

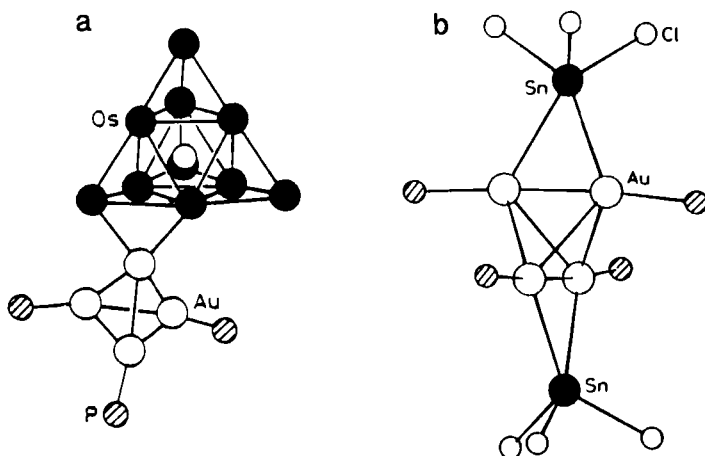


FIG. 22. The metal cage geometries of (a) $[\text{Os}_{10}\text{AuC}(\text{CO})_{24}(\text{PCy}_3)_3]$ and (b) $[\text{Au}_4(\text{PPh}_3)_4(\mu\text{-SnCl}_3)_2]$.

of the parent osmium cluster, with one gold atom of the Au_4 tetrahedron bridging an outer $\text{Os}-\text{Os}$ bond in an asymmetric fashion. This is accompanied by a lengthening of the $\text{Os}-\text{Os}$ bond to $3.025(2) \text{ \AA}$, compared to an average of $2.783(2) \text{ \AA}$ for the remaining outer $\text{Os}-\text{Os}$ bonds.

$[\text{Au}_4(\text{PPh}_3)_4(\mu\text{-SnCl}_3)_2]$, which has been prepared in these laboratories (195), is isoelectronic and isostructural with the homonuclear gold cluster compound $[\text{Au}_4(\text{PPh}_3)_4(\mu\text{-I})_2]$ (269) and has the structure illustrated in Fig. 22b. Both of these clusters exhibit longer $\text{Au}-\text{Au}$ bonds than are found in the gold-osmium cluster.

Three examples of cluster compounds of stoichiometry Au_4M have been structurally characterized. $[\text{Au}_4\text{Rh}(\text{H})_2\{\text{P}(\text{O}-i\text{-C}_3\text{H}_7)_3\}_2(\text{PPh}_3)_4](\text{PF}_6)$ has been synthesized by reaction of $\text{Au}(\text{PPh}_3)\text{NO}_3$ with the rhodium hydrido dimer $[\text{RhH}\{\text{P}(\text{O}-i\text{-C}_3\text{H}_7)_3\}_2]_2$ (155), and has been shown to have the same molecular structure as $[\text{Au}_4\text{Ir}(\text{H})_2(\text{PPh}_3)_6](\text{BF}_4)$, which was obtained on exposure of an acetone solution of $[\text{Au}_3\text{Ir}(\text{PPh}_3)_3\text{NO}_3](\text{BF}_4)$ to an atmosphere of H_2 (74). Both clusters are isoelectronic and have approximately trigonal bipyramidal cores in which the heterometal occupies an equatorial position, as shown previously in Fig. 13. A distortion from an idealized trigonal bipyramidal geometry occurs because the $\text{Au}-\text{M}$ bonds are shorter than the $\text{Au}-\text{Au}$ bonds (see Table IX).

Fast atom bombardment mass spectrometry and NMR spectroscopy have been used to confirm that both clusters possess two hydride ligands, but these could not be located in the X-ray analyses and are

TABLE IX

SUMMARY OF METAL–METAL BOND LENGTHS FOR Au₄ HETERONUCLEAR CLUSTER COMPOUNDS

Compound	Au–M (Å)	Au–Au (Å)	Reference
[Fe(CO) ₄ Au ₂ (dppm)] ₂	2.540(3), 2.608(3)	2.865(1)–3.163(1)	38
[Fe(CO) ₄ Au ₂ (dppe)] ₂	2.524(2), 2.535(2)	2.977(1)	38
[Os ₁₀ Au ₄ C(CO) ₂₄ (PCy ₃) ₃]	2.759(2)–2.808(2)	2.665(2)–2.758(2)	96
[Au ₄ (PPh ₃) ₄ (μ-SnCl ₃) ₂]	2.8150(7), 2.9725(8)	2.6341(5)–2.8128(5)	195
[Au ₄ Ir(H) ₂ (PPh ₃) ₆] [–]	2.637(2)–2.753(2)	2.794(2)–3.142(2)	74
[Au ₄ Rh(H) ₂ (P(<i>O</i> - <i>i</i> -C ₃ H ₇) ₃) ₂ (PPh ₃) ₄) [–]	2.651(1)–2.725(1)	2.813(1)–3.084(1)	155
[Au ₄ Re(H) ₄ (P(<i>p</i> -tol) ₃) ₂ (PPh ₃) ₄) [–]	2.709(1)–2.741(1)	2.802(2)–2.919(2)	145

considered to bridge the axial gold–metal bonds in μ_2 -fashion on the basis of potential energy calculations.

[Au₄Re(H)₄{P(*p*-tol)₃}₂(PPh₃)₄](BPh₄), which has been prepared by the reaction of [Au₅Re(H)₄{P(*p*-tol)₃}₂(PPh₃)₅]²⁺ with triphenylphosphine (145), is also characterized by 66 valence electrons, but has a metal cage geometry based on a Au₃Re tetrahedron edge-bridged by a gold triphenylphosphine group, with the rhenium atom at the most connected vertex (see Fig. 23). FABMS and NMR spectroscopic studies indicate the presence of four hydride ligands in the cluster, but a unique solution of their positions could not be achieved from the available data.

5. Pentagold Heteronuclear Cluster Compounds

Reaction of the rhenium hydride complex ReH₇(PR₃)₂ (where R = Ph or *p*-tol) with Au(PPh₃)NO₃ has yielded the heteronuclear cluster compounds [Au₅Re(H)₄(PR₃)₂(PPh₃)₅](PF₆)₂ (148) in which the metal cores are based on edge-shared bitetrahedra with the rhenium atom at one of the two most-connected vertices. This is illustrated in Fig. 24. A

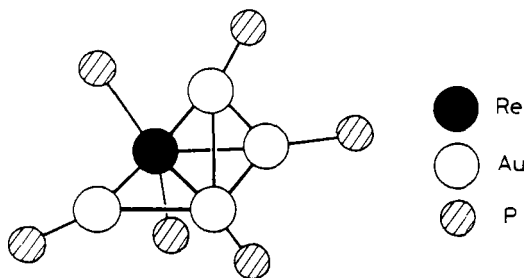


FIG. 23. Molecular structure of [Au₄Re(H)₄{P(*p*-tol)₃}₂(PPh₃)₄]⁺.

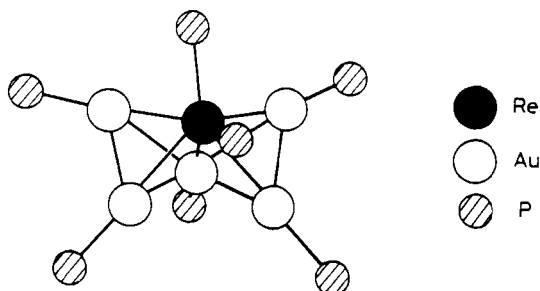


FIG. 24. Molecular structure of $[\text{Au}_5\text{Re}(\text{H})_4(\text{PR}_3)_2(\text{PPh}_3)_5]^{2+}$ ($\text{R} = \text{Ph}$ or $p\text{-tol}$).

similar metal cage geometry is observed in the gold cluster compounds $[\text{Au}_6(\text{PR}_3)_6]^{2+}$ (where $\text{PR}_3 = \text{PPh}_3$ and $\text{P}(o\text{-MeC}_6\text{H}_4)\text{Ph}_2$) (236), although these homonuclear clusters are characterized by two fewer valence electrons than the 78-electron gold-rhenium clusters.

Spectroscopic studies have again indicated the presence of four hydride ligands in both clusters and although these could not be positioned with certainty they most probably bridge between the rhenium and gold atoms. In both clusters, the Au-Re bond lengths are considerably shorter than the Au-Au bond lengths (see Table X).

This structure is related to that of $[\text{Au}_4\text{Re}\{\text{P}(p\text{-tol})_3\}_2(\text{PPh}_3)_2](\text{BF}_4)$ discussed previously by removal of one of the wing-tip AuPPh_3 groups, which has been accomplished by reaction with triphenylphosphine. This reaction is accompanied by a shortening of the Au-Re and Au-Au bond lengths, which has been attributed to a lessening of the steric crowding at the 11-coordinate rhenium atom in the pentagold cluster.

Ito *et al.* have described the structural characterization of two platinum-centered pentagold cluster compounds (58). $[\text{Pt}(\text{PPh}_3)(\text{AuPPh}_3)_5(\text{HgNO}_3)_2](\text{NO}_3)$ has a metal cage geometry similar to that of $[\text{Mo}(\text{CO})_3(\text{AuPPh}_3)_7](\text{OH})$ and will be discussed in more detail in a subsequent section. The metal cage of $[\text{Pt}(\text{PPh}_3)(\text{CO})(\text{AuPPh}_3)_5]\text{Cl}$ comprises

TABLE X

SUMMARY OF METAL-METAL BOND LENGTHS FOR Au_5 HETERONUCLEAR CLUSTER COMPOUNDS

Compound	Au-M (Å)	Au-Au (Å)	Reference
$[\text{Au}_5\text{Re}(\text{H})_4(\text{PPh}_3)_7]^{2-}$	2.758(1)–2.867(1)	2.841(1)–3.222(1)	148
$[\text{Pt}(\text{PPh}_3)(\text{CO})(\text{AuPPh}_3)_5]^-$	2.590(3)–2.676(3)	2.811(5)–3.028(3)	58
$[\text{Pt}(\text{PPh}_3)(\text{AuPPh}_3)_5(\text{HgNO}_3)_2]^+$	Au-Pt = 2.647(3)–2.705(3) Au-Hg = 2.775(4)–3.072(3)	2.811(3)–3.056(3)	58

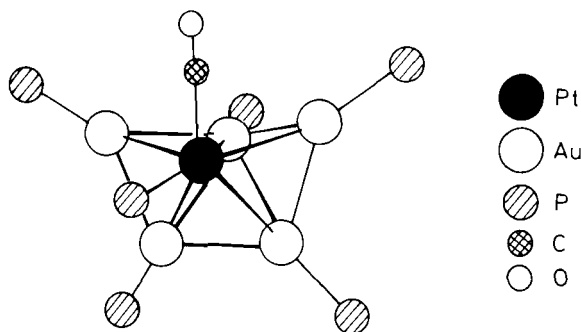


FIG. 25. Molecular structure of $[\text{Pt}(\text{PPh}_3)(\text{CO})(\text{AuPPh}_3)_5]^+$.

a PtAu_4 trigonal bipyramid capped by an AuPPh_3 group and is shown in Fig. 25. This metal cage geometry may also be considered to be derived from a centered icosahedron.

6. Hexagold Heteronuclear Cluster Compounds

$[\text{Pt}(\text{PPh}_3)(\text{AuPPh}_3)_6](\text{NO}_3)_2$ has been obtained in low yield from the carbon monoxide reduction of a mixture of $\text{Au}(\text{PPh}_3)\text{NO}_3$ and $\text{Pt}(\text{PPh}_3)_3$ (122), and in high yield from the reaction of H_2 with $[(\text{PPh}_3)_2(\text{NO}_3)\text{Pt}(\text{AuPPh}_3)_2]^+$ (135). The cluster has a metal cage geometry based on an edge-shared bitetrahedral Au_5Pt core, with a wing-tip Au_2Pt triangular face bridged by an additional AuPPh_3 group. This is shown in Fig. 26a.

Exposure of a solution of $[\text{Pt}(\text{PPh}_3)(\text{AuPPh}_3)_6](\text{NO}_3)_2$ to carbon monoxide results in an immediate reaction in which one molecule of carbon monoxide binds to the platinum atom, increasing the valence electron count of the cluster from 88 to 90 electrons. This is accompanied by a change in the geometry of the metal cage from the structure shown in Fig. 26a to one best described as two face-sharing trigonal bipyramids, with the platinum atom at the most-connected vertex. This structure is shown in Fig. 26b. As in $[\text{Pt}(\text{PPh}_3)(\text{AuPPh}_3)_6](\text{NO}_3)_2$, the Pt–Au bond lengths in $[\text{Pt}(\text{PPh}_3)(\text{CO})(\text{AuPPh}_3)_6](\text{NO}_3)_2$ are considerably shorter than the Au–Au bond lengths (see Table XI).

Puddephatt *et al.* have structurally characterized the platinum–gold cluster compound $[\text{Pt}(\text{PPh}_3)(\text{CC-}t\text{-Bu})(\text{AuPPh}_3)_6][\text{Au}(\text{CC-}t\text{-Bu})_2]$, obtained in 20% yield from the reaction of $[\text{Pt}(\text{PPh}_3)_3]$ with $[\text{AuCC-}t\text{-Bu}]$ (144). This also has 90 valence electrons, but a central core comprising two PtAu_4 square-based pyramids sharing a common triangular face and with the platinum atom in the apical position, as Fig. 27 illustrates.

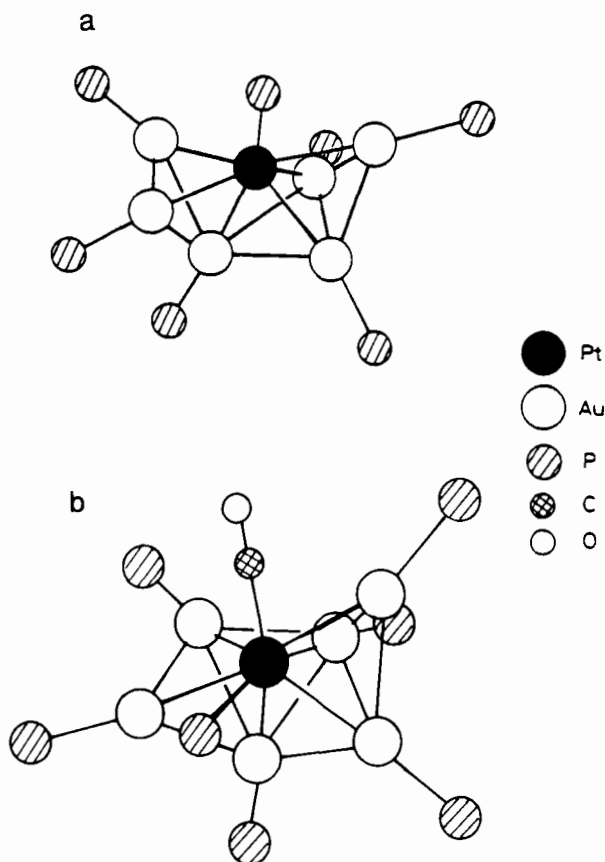


FIG. 26. Molecular structures of (a) $[\text{Pt}(\text{PPh}_3)(\text{AuPPh}_3)_6]^{2-}$ and (b) $[\text{Pt}(\text{PPh}_3)(\text{CO})(\text{AuPPh}_3)_6]^{2-}$.

TABLE XI

SUMMARY OF METAL-METAL BOND LENGTHS FOR Au₆ HETERONUCLEAR CLUSTER COMPOUNDS

Compound	Au-M (Å)	Au-Au (Å)	Reference
$[\text{Au}_6(\text{PPh}_3)_4\{\text{Co}(\text{CO})_4\}_2]$	2.460(16)	2.621(7)–2.823(9)	27, 28
$[\text{Pt}(\text{PPh}_3)(\text{AuPPh}_3)_6]^{2-}$	2.665(1)–2.699(1)	2.723(1)–2.938(1)	135
$[\text{Pt}(\text{CO})(\text{PPh}_3)(\text{AuPPh}_3)_6]^{2+}$	2.659(2)–2.714(2)	2.810(2)–2.976(2)	135
$[\text{Pt}(\text{PPh}_3)(\text{CC-}t\text{-Bu})(\text{AuPPh}_3)_6]^+$	2.625(2)–2.693(2)	2.832(2)–2.879(2)	144

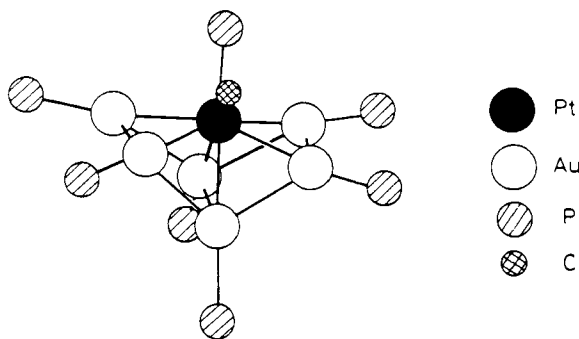


FIG. 27. Molecular structure of $[\text{Pt}(\text{PPh}_3)(\text{CC-}t\text{-Bu})(\text{AuPPh}_3)_6]^+$.

The adoption of two different geometries for these isoelectronic Au_6Pt clusters is probably due to electronic differences between the carbon monoxide and acetylide ligands, as neither ligand is sterically demanding in these compounds. However, both cluster compounds adopt metal cage geometries that are best described as hemispherical, as expected from their valence electron counts.

One other hexagold heteronuclear cluster compound, $[\text{Au}_6(\text{PPh}_3)_4\{\text{Co}(\text{CO})_4\}_2]$, has been structurally characterized (27, 28) and exhibits an edge-shared bitetrahedral arrangement of gold atoms, with the two $\text{Co}(\text{CO})_4$ groups acting as terminally bound ligands. These donate one electron each to the total valence electron count of the cluster; hence $[\text{Au}_6(\text{PPh}_3)_4\{\text{Co}(\text{CO})_4\}_2]$ is characterized by 76 electrons and is isostructural and isoelectronic with the gold cluster compounds $[\text{Au}_6(\text{PR}_3)_6]^{2+}$ discussed earlier.

7. Heptagold Heteronuclear Cluster Compounds

Two examples of heterometallic cluster compounds containing seven gold atoms have been structurally characterized by Beuter and Strähle. $[\text{Mo}(\text{CO})_3(\text{AuPPh}_3)_7](\text{OH})$, obtained in low yield from photolysis of a mixture of the gold azide complex $[\text{Au}(\text{PPh}_3)\text{N}_3]$ and $\text{Mo}(\text{CO})_6$, has been described as a half-sandwich compound of molybdenum, with the $\text{Au}_7(\text{PPh}_3)_7^+$ fragment acting as a pseudo- C_6H_6 ligand (84). More accurately, the structure is based on a molybdenum-centered icosahedron with five of the vertices removed, as shown in Fig. 28. A similar metal cage geometry has been noted for $[\text{Pt}(\text{PPh}_3)(\text{AuPPh}_3)_5(\text{HgNO}_3)_2](\text{NO}_3)$ (58).

$[(\text{PPh}_3\text{Au})_6\text{AuCo}_2(\text{CO})_6](\text{NO}_3)$ has also been prepared by photochemical means (13) and has the structure illustrated in Fig. 29. The cation

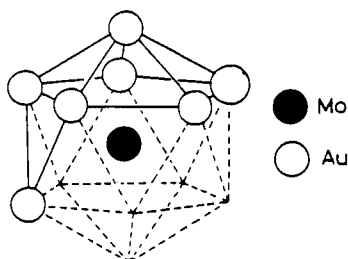


FIG. 28. View of the molecular structure of $[\text{Mo}(\text{CO})_3(\text{AuPPh}_3)_7]^+$ emphasizing its derivation from a centered icosahedron.

comprises two Au_4Co trigonal bipyramids sharing a common axial gold atom, each Au_4Co unit being distorted from an idealized geometry, as the Au–Co bonds are shorter than the Au–Au bonds

$[\text{Pt}(\text{H})(\text{PPh}_3)(\text{AuPPh}_3)_7](\text{PF}_6)_2$, synthesized by the hydrogen reduction of a mixture of $\text{Au}(\text{PPh}_3)\text{NO}_3$ and $\text{Pt}(\text{PPh}_3)_3$ and by reaction of $[\text{Pt}(\text{AuPPh}_3)_8]^{2+}$ with triphenylphosphine under acid conditions (137), has a molecular structure based on a distorted cube with a central platinum atom and has already been illustrated in Fig. 9. The metal cage geometry is very similar to that found for the isoelectronic homonuclear gold cluster compound $[\text{Au}_8(\text{PPh}_3)_8]^{2+}$ (207, 271), although Au–Au distances in the platinum complex are longer. The hydride ligand was not located in the X-ray analysis, but ^{31}P and ^{195}Pt NMR studies indicate that it is bonded directly to the platinum atom and Orpen potential energy calculations indicate a probable μ_3 -coordination mode, bridging the longer Au–Au bonds (see Table XII).

8. Octagold Heteronuclear Cluster Compounds

The heterometallic cluster compounds $[\text{Pt}(\text{AuPPh}_3)_8](\text{NO}_3)_2$ and $[\text{Pd}(\text{AuPPh}_3)_8](\text{NO}_3)_2$, synthesized by the coreduction of platinum or palladium complexes and $\text{Au}(\text{PPh}_3)\text{NO}_3$ (117, 123, 124), both adopt a

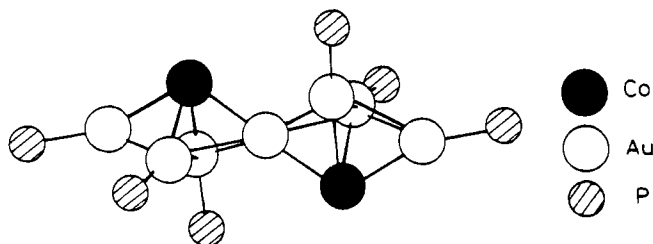


FIG. 29. Molecular structure of the $[(\text{Ph}_3\text{PAu})_6\text{AuCo}_2(\text{CO})_6]^+$ cation.

TABLE XII

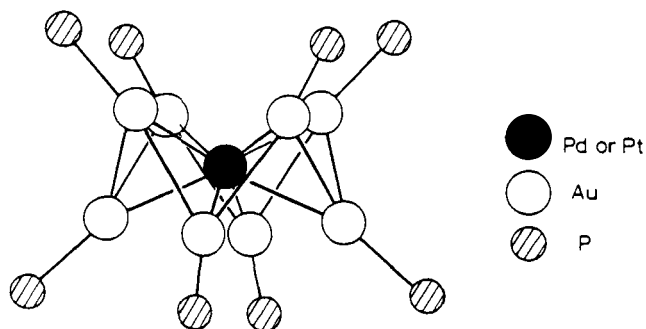
SUMMARY OF METAL-METAL BOND LENGTHS FOR Au_7 HETERONUCLEAR CLUSTER COMPOUNDS

Compound	Au-M (Å)	Au-Au (Å)	Reference
$[Mo(CO)_3(AuPPh_3)_7]^+$	2.7711(1)–2.8597(2)	2.8511(1)–3.0309(2)	13, 84
$[(AuPPh_3)_6AuCo_2(CO)_6]^+$	2.5757(6)–2.6557(6)	2.7824(3)–2.9190(3)	13
$[Pt(H)(PPh_3)(AuPPh_3)_7]^{2+}$	2.666(1)–2.737(1)	2.820(1)–3.326(2)	137

centered crown structure in the solid state with the palladium or platinum atom occupying the central position in the cluster. This molecular structure, illustrated in Fig. 30, is also exhibited by the isoelectronic gold cluster compound $[Au_9\{P(p-C_6H_4OMe)_3\}_8](BF_4)_3$ (272).

$[Pt(AuPPh_3)_8]^{2+}$ reacts rapidly with carbon monoxide to give $[Pt(CO)(AuPPh_3)_8]^{2+}$, in which the carbonyl ligand is bonded to the central platinum atom (136). The addition of two extra valence electrons to the cluster results in a change in the metal core geometry to give a hemispherical structure. This cluster rearrangement has been shown in Fig. 2.

As well as undergoing nucleophilic addition, $[Pt(AuPPh_3)_8]^{2+}$ will react with the electrophilic species $AgNO_3$ and $[Hg_2(H_2O)_2](NO_3)_2$ to generate the trimetallic cluster compounds $[Pt(AgNO_3)(AuPPh_3)_8](NO_3)_2$ and $[Pt(AuPPh_3)_8(HgNO_3)_2](NO_3)_2$ (3,238). The latter compound has not been structurally characterized by X-ray methods, but on recrystallization yielded red crystals of $[Pt(AuPPh_3)_8Hg_2](NO_3)_4$, the structure of which is given in Fig. 31a (57). $[Pt(CO)(AgNO_3)(AuPPh_3)_8](NO_3)_2$ has also been synthesized by addition of $AgNO_3$ to $[Pt(CO)(AuPPh_3)_8](NO_3)_2$ and by reaction of $[Pt(AgNO_3)(AuPPh_3)_8](NO_3)_2$ with carbon monoxide (3,238), and its molecular structure is shown in Fig. 31b.

FIG. 30. Molecular structure of $[Pt(AuPPh_3)_8]^{2+}$ and $[Pd(AuPPh_3)_8]^{2+}$.

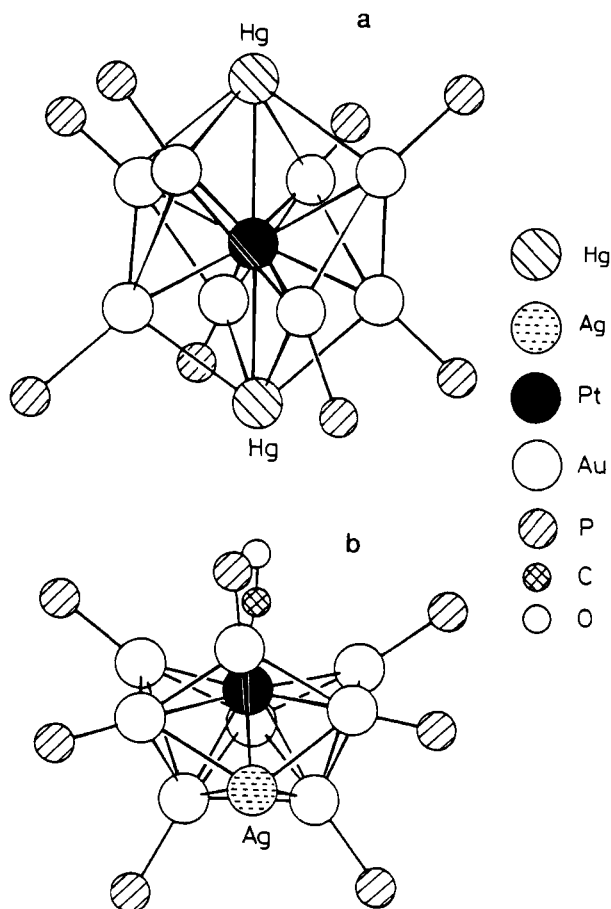


FIG. 31. Molecular structures of (a) $[\text{Pt}(\text{AuPPh}_3)_8\text{Hg}_2]^{4+}$ and (b) $[\text{Pt}(\text{CO})(\text{AgNO}_3)(\text{AuPPh}_3)_8]^{2+}$.

In both of the silver-containing products, an AgNO_3 group is bonded to the periphery of the platinum-centered cluster. $[\text{Pt}(\text{AgNO}_3)(\text{AuPPh}_3)_8](\text{NO}_3)_2$ is isoelectronic and isostructural with $[\text{Au}_{10}\text{Cl}_3(\text{PCy}_2\text{Ph})_6](\text{NO}_3)_2$ (273), adopting a toroidal geometry, whereas the metal cage of $[\text{Pt}(\text{CO})(\text{AgNO}_3)(\text{AuPPh}_3)_8](\text{NO}_3)_2$ can be considered to be derived from a platinum-centered icosahedron and describes a hemispherical topology. In $[\text{Pt}(\text{AuPPh}_3)_8\text{Hg}_2](\text{NO}_3)_4$, two mercury atoms have capped the square faces of the parent $[\text{Pt}(\text{AuPPh}_3)_8]^{2+}$ compound to give a metal cage of approximately D_{4d} symmetry, with Pt–Hg and Au–Hg bonds of average length 2.98 and 3.00 Å, respectively. No coordinated nitrate is observed (see Table XIII).

TABLE XIII

SUMMARY OF METAL–METAL BOND LENGTHS FOR Au₈ AND Au₉ HETERONUCLEAR CLUSTER COMPOUNDS

Compound	Au–M (Å)	Au–Au (Å)	Reference
[Pd(AuPPh ₃) ₈] ²⁻	2.611(2)–2.624(2)	2.765(2)–2.805(2)	117
[Pt(AuPPh ₃) ₈] ²⁺	2.631(3)–2.640(3)	2.800(4)–2.864(4)	123, 124
[Pt(CO)(AuPPh ₃) ₈] ²⁻	2.651(1)–2.703(1)	2.833(1)–3.079(1)	136
[Pt(AgNO ₃)(AuPPh ₃) ₈] ²⁺	Au–Pt = 2.607(3)–2.684(3) Au–Ag = 2.714(3)–2.786(5)	2.726(3)–3.042(4)	3
[Pt(CO)(AgNO ₃)(AuPPh ₃) ₈] ²⁺	Au–Pt = 2.7012(21)–2.7952(17) Au–Ag = 2.8149(24)–3.0738(28)	2.8579(23)–3.0299(20)	3
[Pt(AuPPh ₃) ₈ Hg ₂] ⁴⁺	Au–Pt = 2.6307(4)–2.6324(4) Au–Hg = 3.0011(5)–3.0070(5)	2.9036(4)–2.9298(4)	57
[Au ₈ (PPh ₃) ₇ (SnCl ₃)] ⁺	2.625(3)	2.633(2)–2.965(3)	194
[Pt(CN)(AuCN)(AuPPh ₃) ₈] ⁺	2.690(2)–2.734(2)	2.860(2)–3.060(2)	125

The octagold cluster compound [Au₈(PPh₃)₇(SnCl₃)]₂(SnCl₆) has also been prepared, by reaction of SnCl₂ and SnCl₃⁻ with preformed gold cluster compounds (194), and adopts a gold skeleton similar to that found in [Au₈(PPh₃)₇](NO₃)₂ (274), with a terminal SnCl₃ ligand coordinated exclusively to the central gold atom.

9. Enneagold Heteronuclear Cluster Compounds

[Pt(CN)(AuCN)(AuPPh₃)₈](NO₃) is a red crystalline compound that has been synthesized by the oxidative addition of Au(CN)₂⁻ to [Pt(AuPPh₃)₈](NO₃)₂ and in lower yield by reaction of the platinum–gold cluster with KCN (57). The structure of [Pt(CN)(AuCN)(AuPPh₃)₈](NO₃) is also based on a platinum-centered icosahedron, with the gold atoms occupying the vertices that remain after removal of a triangle of atoms. This metal cage geometry is to be contrasted with that of [Pt(CO)(AgNO₃)(AuPPh₃)₈](NO₃)₂, which is also derived from a platinum-centered icosahedron, but with a different triangle of vertices removed, as Fig. 32 illustrates.

10. Higher Nuclearity Heterometallic Gold Cluster Compounds

Teo and co-workers have characterized a series of gold–silver cluster compounds containing 25, 37, and 38 metal atoms (4–7), which represent the largest examples of structurally determined heteronuclear gold cluster compounds and are illustrated in Fig. 33. A preliminary account of the 46-metal atom cluster [Au₂₂Ag₂₄(PPh₃)₁₂Cl₁₀] has also appeared recently (275) and another group has characterized the 25-metal cluster cation [Au₁₃Ag₁₂(μ-Cl)₆(PPh₃)₁₀Cl₂]⁺ (2).

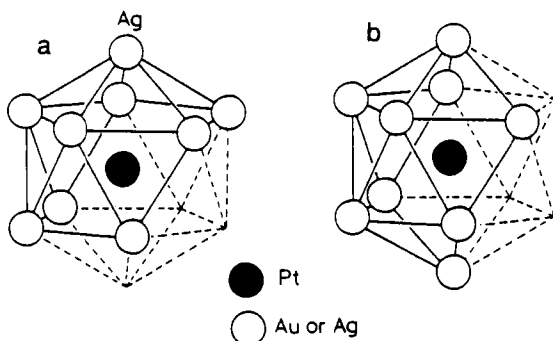


FIG. 32. Metal core geometries of (a) $[\text{Pt}(\text{CO})(\text{AgNO}_3)(\text{AuPPh}_3)_8]^{2+}$ and (b) $[\text{Pt}(\text{CN})(\text{AuCN})(\text{AuPPh}_3)_6]^+$ showing their derivation from centered icosahedra.

All of these species, which have been described as supracusters, are derived from vertex-sharing gold-centered Au_7Ag_6 icosahedral units in which the phosphine and halide ligands are bonded to the peripheral metal atoms. Thus $[\text{Au}_{13}\text{Ag}_{12}(\text{PPh}_3)_{12}(\mu\text{-Cl})_6]^{m+}$ can be considered two such icosahedra sharing a common vertex in an eclipsed conformation, in contrast to $[\text{Au}_{13}\text{Ag}_{12}(\text{PPh}_3)_{10}(\mu\text{-Cl})_6\text{Cl}_2]^+$ where there is a virtual staggered conformation of the icosahedra. Although the charge on $[\text{Au}_{13}\text{Ag}_{12}(\text{PPh}_3)_{12}(\mu\text{-Cl})_6]^{m+}$ has not been determined, conductivity measurements indicate a value for m between 3 and 5. Both $[\text{Au}_{18}\text{Ag}_{19}\{\text{P}(p\text{-tol})_3\}_{12}(\mu_3\text{-Br})_4(\mu\text{-Br})_6\text{Br}]^{2+}$ and $[\text{Au}_{18}\text{Ag}_{20}\{\text{P}(p\text{-tol})_3\}_{12}(\mu_3\text{-Cl})_6(\mu\text{-Cl})_6\text{Cl}_2]$ are built up from three Au_7Ag_6 icosahedra sharing three vertices in a cyclic manner, with one or two silver atoms, respectively, capping the resultant Au_3 triangle, and $[\text{Au}_{22}\text{Ag}_{24}(\text{PPh}_3)_{12}\text{Cl}_{10}]$ consists of four tetrahedrally arranged vertex-linked icosahedra. In all of these cluster compounds the metal-metal distances vary in the order $\text{Au-Au} \sim \text{Au-Ag} < \text{Ag-Ag}$ (see Table XIV).

TABLE XIV

SUMMARY OF METAL-METAL BOND LENGTHS FOR HIGH-NUCLEARITY GOLD-SILVER HETERONUCLEAR CLUSTER COMPOUNDS

Compound	Au-Au (Å)	Au-Ag (Å)	Ag-Ag (Å)	Reference
$[\text{Au}_{13}\text{Ag}_{12}(\text{PPh}_3)_{10}\text{Cl}_8]^+$	2.687-2.964(2)	2.719(4)-3.003(2)	2.822(5)-3.463(3)	2
$[\text{Au}_{13}\text{Ag}_{12}(\text{PPh}_3)_{12}\text{Cl}_6]^{m+}$	2.57(2)-3.04(2)	2.54(2)-3.26(2)	2.87(3)-3.54(3)	4
$[\text{Au}_{13}\text{Ag}_{12}\{\text{P}(p\text{-tol})_3\}_{10}\text{Br}_8]^+$	2.711(3)-3.014(2)	2.738(5)-3.107(4)	2.807(5)-3.290(8)	7
$[\text{Au}_{18}\text{Ag}_{19}\{\text{P}(p\text{-tol})_3\}_{12}\text{Br}_{11}]^{2+}$	2.66-3.20	2.73-3.01	2.79-3.34	5
$[\text{Au}_{18}\text{Ag}_{20}\{\text{P}(p\text{-tol})_3\}_{12}\text{Cl}_{14}]$	2.68-3.20	2.70-3.14	2.81-3.29	6

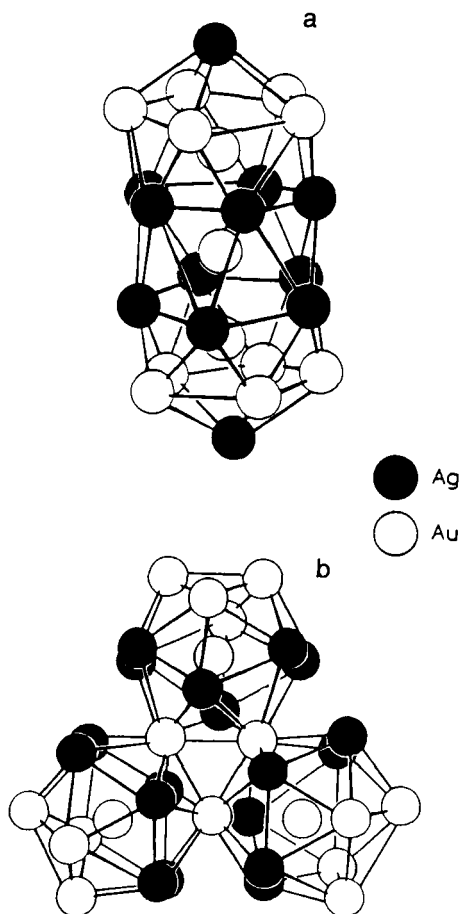


FIG. 33. Metal cage geometries of (a) $[\text{Au}_{13}\text{Ag}_{12}(\text{PPh}_3)_{12}\text{Cl}_6]^{n+}$ and (b) $[\text{Au}_{18}\text{Ag}_{19}\{\text{P}(p\text{-tol})_3\}_{12}\text{Br}_{11}]^{2+}$. In the latter structure, two additional silver atoms bridge above and below the central Au_3 triangle.

The characterization of these supraclusters has prompted a reexamination of the gold cluster compound synthesized by reduction of $\text{Au}(\text{PPh}_3)\text{Cl}$ in benzene at 50°C with B_2H_6 and formulated by Schmid as $\text{Au}_{55}(\text{PPh}_3)_{12}\text{Cl}_6$ (276, 277). Fackler and co-workers have recently reported ^{252}Cf plasma desorption mass spectrometric data on samples of this product (278) and concluded that the zones in the mass spectra are best interpreted in terms of the fragmentation of clusters with the stoichiometries $[\text{Au}_{67}\text{Cl}_8(\text{PPh}_3)_{14}]$, $[\text{Au}_{46}\text{Cl}_6(\text{PPh}_3)_{12}]$, and $[\text{Au}_{25}\text{Cl}_6(\text{PPh}_3)_{12}]$. These stoichiometries are consistent with the presence of gold clusters

based on vertex-sharing icosahedral Au_{13} units, analogous to Teo's gold-silver compounds.

IV. Structure and Bonding in Heteronuclear Gold Cluster Compounds

The nature of the bonding in heteronuclear gold cluster compounds has been investigated primarily by means of semiempirical molecular orbital calculations and the results of these studies have allowed a number of structural generalizations to be made. These theoretical developments have been discussed in detail in a series of papers by Mingos *et al.* (210, 256, 279–282) and only a brief description of the results of this work will be given in this section.

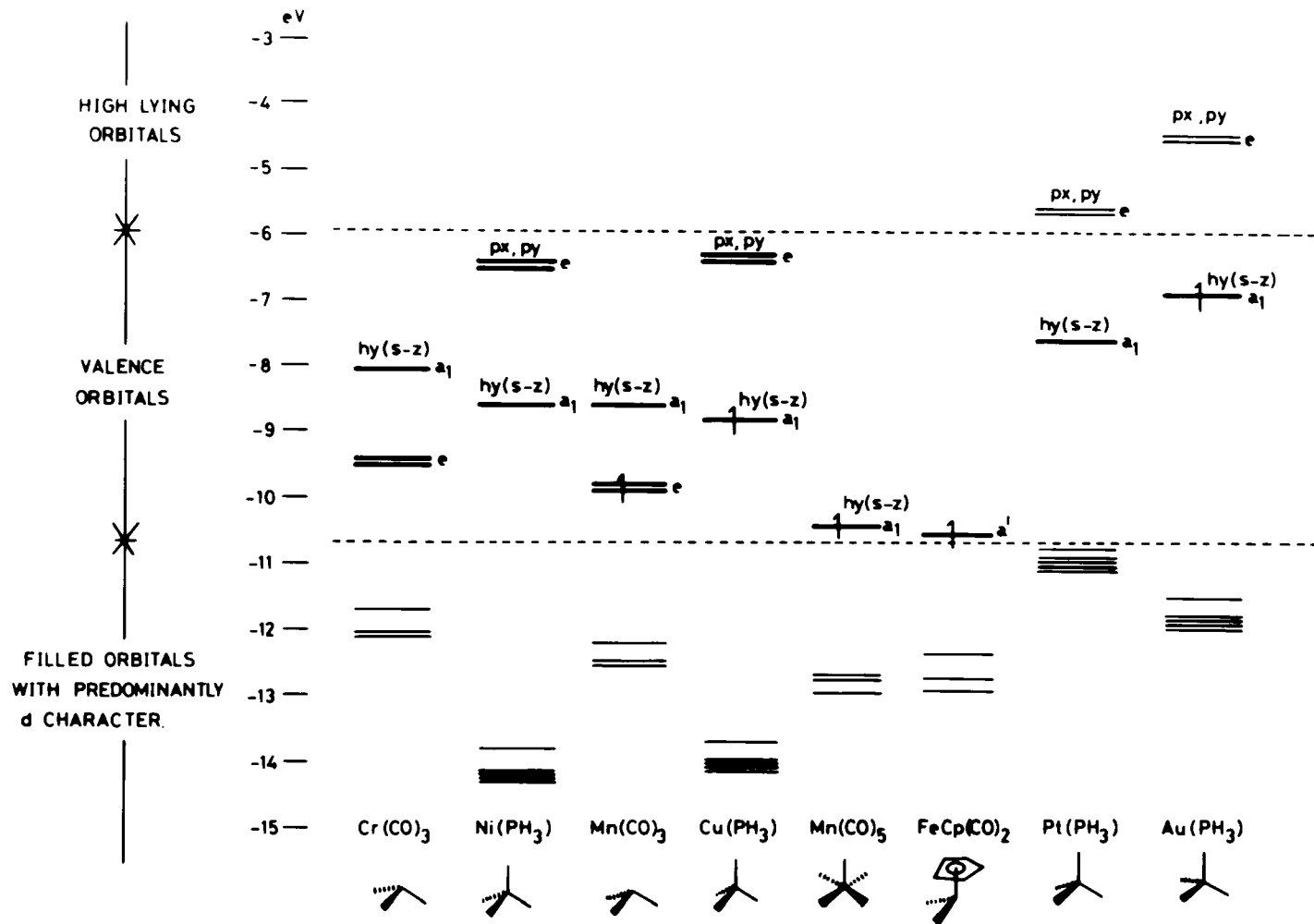
Isolobal relationships between the AuPR_3 fragment and hydride and alkyl ligands have been utilized to explain the bonding in clusters which contain a small number of gold(I) moieties. While such relationships have been shown to be valid for compounds which possess only one AuPR_3 group, the inclusion of additional gold(I) centers in the metal framework often leads to a breakdown in these isolobal analogies. Subsequently, this theoretical approach to the bonding in clusters which contain a high proportion of gold in the metal framework is inadequate and the structures of these compounds have been rationalized within a simple molecular orbital framework derived from Stone's Tensor Surface Harmonic Theory (283, 284).

A. ISOLOBAL ANALOGIES

The recognition that certain transition metal carbonyl fragments and main group fragments, for example $\text{Mn}(\text{CO})_5$ and BH , have frontier orbitals with similar bonding capabilities has proved to be an important ingredient for understanding the structural relationships between transition metal and main group cluster compounds (285). Previous sections of this chapter have illustrated the wide use of the AuPR_3 group in the synthesis of heteronuclear gold cluster compounds. The isolobal relationship between this fragment and the hydride ligand, first outlined by Lauher (22) and described in more detail below, has been used extensively to rationalize the structure and bonding in these compounds.

The frontier molecular orbitals of the AuPH_3 fragment are shown in Fig. 34 along with those of other common transition metal fragments.

FIG. 34. The relative energies of some transition metal phosphine and carbonyl fragments that are isolobal with CH or CH_3 .



For the AuPH_3 group, the orbitals with a predominance of d orbital character are filled and the bonding characteristics of the fragment are determined primarily by the a_1 $hy(s-z)$ orbital and the higher lying degenerate pair of metal p_x and p_y orbitals. On symmetry grounds alone, the AuPH_3 group would be anticipated to be isolobal with a conical $\text{M}(\text{CO})_3$ fragment. In the gold fragment, however, the e set of metal p orbitals are sufficiently high lying that they have only a secondary role in the bonding, which is determined primarily by the a_1 $hy(s-z)$ orbital (280). The AuPH_3 group has, therefore, been described as isolobal with the H , CH_3 , and $\text{Mn}(\text{CO})_5$ moieties, each of which possess only a single outpointing orbital. Numerous examples of this isolobal relationship between gold cluster complexes and metal hydride complexes exist in the literature and a number have been noted in previous sections.

Although the gold atom is considerably larger than the hydrogen atom, there are no steric problems associated with this analogy, as the metal–gold bond is larger than the metal–hydrogen bond. For example, the Co–Au distance in $[\text{Co}(\text{CO})_4(\text{AuPPh}_3)]$ has been determined to be 2.4897(7) Å (20), compared to the Co–H distance of 1.556(18) Å in the hydrido complex (261). Since the a_1 $hy(s-z)$ orbital of the AuPPh_3 fragment has a higher ionization potential than the $1s$ orbital of the hydrogen atom, the polarities of these M–Au and M–H bonds are not equivalent. Infrared studies have indicated that the gold–transition metal bonds are very polar, with an electron density on the transition metal intermediate between that of the free carbonyl anion and the hydrido complex (37).

The bonding in the above complexes may be described in terms of conventional two-center two-electron bonding schemes. As described previously, the gold phosphine fragment has been widely used in cluster aggregation reactions and commonly adopts μ_2 - and μ_3 -bridging modes. The bonding between the gold and the transition metal atoms in the resultant complexes may be described in terms of multicenter bonding schemes analogous to those used to describe bridging hydride ligands. Hence, $\mu_2\text{-AuPR}_3$ moieties are considered to form three-center two-electron bonds and $\mu_3\text{-AuPR}_3$ groups to form four-center two-electron bonds.

The addition of AuPR_3^+ to metal carbonyl clusters occurs readily and does not change the basic skeleton of the cluster. The capping principle of Mingos and Forsyth (286) predicts that addition of an AuPR_3 fragment will cause an increment in the polyhedral electron count of 12, regardless of whether the fragment is functioning as a face- or edge-bridging group. The successive addition of AuPR_3^+ fragments does not increase the number of electrons used in skeletal bonding and the

TABLE XV

EXAMPLES OF GOLD HETERONUCLEAR CLUSTER COMPOUNDS EXHIBITING CAPPED TETRAHEDRAL GEOMETRIES

Cluster	Geometry	Polyhedral electron count
$[\text{Os}_4\text{H}_4(\text{CO})_{12}]$	Tetrahedron	60
$[\text{FeCo}_3(\text{CO})_{12}(\text{AuPPh}_3)]$	Capped tetrahedron	72
$[\text{Ru}_4\text{H}_2(\text{CO})_{12}(\text{AuPPh}_3)_2]$	Bicapped tetrahedron	84
$[\text{Ru}_4\text{H}(\text{CO})_{12}(\text{AuPPh}_3)_3]$	Tricapped tetrahedron	96

number of bonding skeletal molecular orbitals of the capped polyhedron is identical to that of the parent uncapped polyhedron. It follows that these capped polyhedra are characterized by a total of $M + 12n$ valence electrons, where M is equal to the number of electrons that characterizes the parent polyhedron and n is equal to the number of gold capping groups. The examples in Table XV illustrate this point.

The fact that the AuPR_3 fragment can function as either a face- or an edge-bridging group and in each instance cause an increment in the polyhedral electron count of 12 also provides an explanation for the stereochemical nonrigidity observed for these compounds. The fragment may be considered to resemble the carbonyl ligand, which acts as a two-electron donor whether it is in a terminal, an edge-bridging, or a face-bridging location.

B. SUPPLEMENTARY $\text{Au}\cdots\text{Au}$ INTERACTIONS

The crystallographic studies summarized in Section III have demonstrated that in many compounds containing two or more gold(I) moieties there is a tendency for the gold atoms to have contacts that are partially bonding. This gives rise to $\text{Au}\cdots\text{Au}$ distances only slightly longer than those found in the metallic structure. Intermediate $\text{H}\cdots\text{H}$ contacts have not been observed in metal hydride complexes, although H_2 complexes are now well documented (287, 288).

This may be illustrated by a consideration of the molecular structures of the compounds $[\text{H}_2\text{Ru}_3(\text{CO})_9(\mu_3\text{-S})]$ (289), $[\text{HRu}_3(\text{CO})_9(\mu_3\text{-S})(\text{AuPPh}_3)]$ (174), and $[\text{Ru}_3(\text{CO})_9(\mu_3\text{-S})(\text{AuPPh}_3)_2]$ (174), which are illustrated in Fig. 35. The structure of the hydride complex has been determined by X-ray methods and the hydride ligands were found to bridge two of the Ru-Ru bonds in μ_2 -fashion on the side of the cluster opposite the sulfido ligand. Deprotonation of this cluster using $\text{K}[\text{HBBu}_3^s]$, followed by reaction with $[(\text{AuPPh}_3)_3\text{O}]^+$ or $\text{Au}(\text{PPh}_3)\text{Cl}/\text{TlPF}_6$, has yielded both

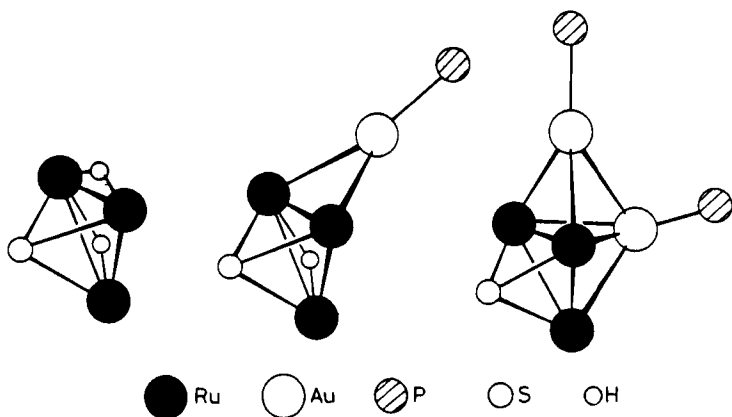


FIG. 35. Molecular structures of $[\text{H}_2\text{Ru}_3(\mu_3\text{-S})(\text{CO})_9]$, $[\text{HRu}_3(\mu_3\text{-S})(\text{CO})_9(\text{AuPPh}_3)]$, and $[\text{Ru}_3(\mu_3\text{-S})(\text{CO})_9(\text{AuPPh}_3)_2]$.

$[\text{HRu}_3(\text{CO})_9(\mu_3\text{-S})(\text{AuPPh}_3)]$ and $[\text{Ru}_3(\text{CO})_9(\mu_3\text{-S})(\text{AuPPh}_3)_2]$. An X-ray diffraction study of the former compound has revealed a butterfly cluster geometry, with the AuPPh_3 group bridging a single Ru–Ru edge and the hydride ligand located across an adjacent edge. The structure is, therefore, that expected on replacing one of the hydride ligands in $[\text{H}_2\text{Ru}_3(\text{CO})_9(\mu_3\text{-S})]$ by an isolobal AuPPh_3 fragment.

In contrast, $[\text{Ru}_3(\text{CO})_9(\mu_3\text{-S})(\text{AuPPh}_3)_2]$ adopts a distorted trigonal bipyramidal metal cage geometry, with an Au–Au separation of 2.967(2) Å. This geometry results from capping of the ruthenium triangular face by the first AuPPh_3 fragment, followed by a secondary capping process in which one of the resultant Ru_2Au triangular faces is capped by the additional AuPPh_3 group.

Similar metal–metal interactions have been observed for other polynuclear complexes containing d^{10} metal centers and have been interpreted on the basis of the results of semiempirical calculations (290, 291). These indicate that the repulsions between two d^{10} metal centers may be mitigated by the intervention of higher-lying, empty p orbitals. Thus, for two linearly coordinated gold(I) centers, a σ -type interaction between d_z^2 - s orbitals on adjacent gold atoms will lead to a partially bonding interaction if accompanied by electron donation to empty $6p_y$ orbitals on the gold atoms. This is illustrated in Fig. 36. Similarly, a π -interaction between filled d_{xy} orbitals on the gold fragments is mitigated by electron donation to the empty $6p_x$ orbitals.

The occurrence of weak $\text{Au}\cdots\text{Au}$ interactions of this type gives rise to the possibility of alternative descriptions of the bonding in clusters

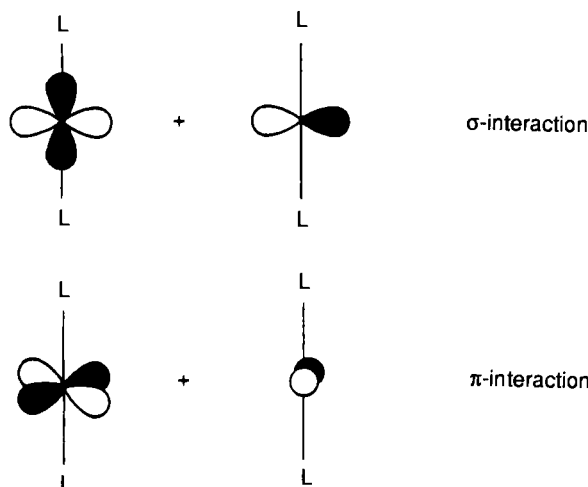


FIG. 36. Orbital interactions leading to supplementary Au...Au bonding between gold(I) moieties.

containing two or more gold atoms. For example, the compound $[\text{V}(\text{CO})_5(\text{AuPPh}_3)_3]$, synthesized by the reaction of $[\text{V}(\text{CO})_5]^{3-}$ with $\text{Au}(\text{PPh}_3)\text{Cl}$ (199), is based on a tetrahedral arrangement of metal atoms, with Au–Au bond lengths of 2.768(1) to 2.855(1) Å and V–Au bond lengths of 2.709(1) to 2.756(1) Å. This geometry may be described in terms of a four-center two-electron bonding interaction in the VAu_3 tetrahedron. The observation that the Au–P vectors do not point directly toward the centroid of the tetrahedron, but are approximately colinear with the V–Au vectors, suggests an alternative description of the bonding in terms of three two-center two-electron bonds between the vanadium and the gold atoms, with supplementary bonding interactions between the gold atoms similar to those described above.

In addition to these electronic effects, Housecroft *et al.* have demonstrated the importance of steric effects in determining the geometries of clusters containing AuPR_3 fragments. They have found that the tetra-iron and tetra-ruthenium butterfly clusters $[\text{HM}_4(\text{CO})_{12}\text{BH}_2]$ (where M = Fe or Ru), which have a boron atom midway between the wing-tip metal atoms, react, after deprotonation, with AuPR_3^+ fragments to form the complexes $[\text{Fe}_4(\text{CO})_{12}(\text{AuPR}_3)_2\text{BH}]$ and $[\text{HRu}_4(\text{CO})_{12}(\text{AuPPh}_3)_2\text{B}]$ (44, 45, 47, 48, 178). The AuPR_3^+ fragments bond to the boron atoms and either the wing-tip or hinge metal atoms leading to a cluster where the boron atom is coordinated to six metal atoms.

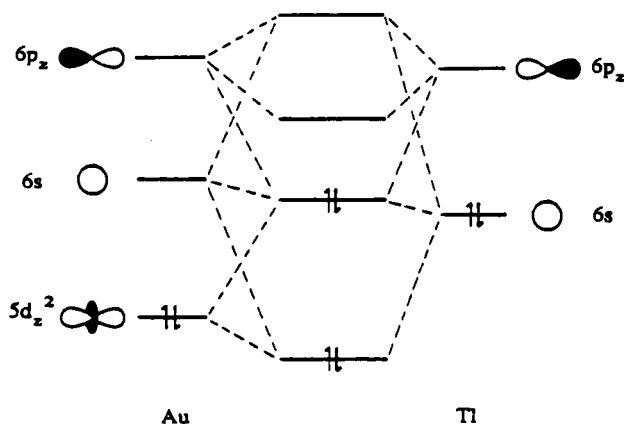


FIG. 37. Molecular orbital diagram for the Au-Tl unit in $[\text{AuTl}\{\text{CH}_2\text{P}(\text{S})\text{Ph}_2\}_2]_n$.

The precise geometric arrangement of metal atoms depends on both the steric and the electronic requirements of the AuPR_3^+ group.

Weak bonding interactions between gold(I) moieties have been observed in binuclear complexes such as $[\text{Au}_2(\text{Et}_2\text{PCH}_2\text{CH}_2\text{S}_2)]$ (263) and $[\text{Au}_2(\text{S}_2\text{CNPr}_2)_2]_n$ (264), which exhibit short $\text{Au}\cdots\text{Au}$ contacts perpendicular to the ligand-gold-ligand axis. In the case of $[\text{Au}_2(\text{S}_2\text{CNPr}_2)_2]_n$, these dimers are further linked to form infinite $\text{Au}\cdots\text{Au}$ chains, with gold-gold separations of 3.40 Å. Fackler has noted similar interactions in heterobimetallic compounds such as $[\text{Au}_2\text{Pb}\{\text{CH}_2\text{P}(\text{S})\text{Ph}_2\}_4]$ (115) and $[\text{AuTl}\{\text{CH}_2\text{P}(\text{S})\text{Ph}_2\}_2]$ (197), which form extended one-dimensional linear chain polymers with short metal-metal separations in the solid state. No interaction is anticipated between the d^{10} and s^2 metal centers in these compounds, but Fenske-Hall molecular orbital calculations indicate that the inclusion of vacant $6p_z$ and $6s$ orbitals on the gold and $6p_z$ orbitals on thallium in the bonding scheme results in net σ overlap. The relevant molecular orbital diagram is illustrated in Fig. 37. This bonding interaction has been described as a relativistic metal-metal bond, as relativistic effects in these heavy metals promote the mixing of orbitals (292).

C. TENSOR SURFACE HARMONIC THEORY

The bonding in heteronuclear gold clusters that contain a high proportion of gold in the metal framework may be understood by reference to the bonding schemes developed for high nuclearity homonuclear gold cluster compounds. Mingos *et al.* (281), using a delocalized molecular

orbital model derived from Stone's Tensor Surface Harmonic Theory, have demonstrated that these clusters may be classified into two broad topological classes according to the three-dimensional disposition of the peripheral gold atoms. If these lie approximately on a sphere, the cluster is characterized by $12n_s + 18$ valence electrons, where n_s equals the number of surface gold atoms. In contrast, toroidal clusters have a total electron count of $12n_s + 16$.

These generalizations have resulted from the recognition that the bonding in such clusters is dominated by the overlap of gold 6s orbitals and tangential bonding interactions between the p orbitals can be ignored. This can be attributed to the large 6s–6p promotion energy, which discourages the involvement of the 6p orbitals, and the small magnitudes of the 5d–5d overlap integrals, which preclude any significant interactions involving the 5d orbitals. Figure 38 illustrates the skeletal molecular orbitals for an icosahedral Au_{12} cluster derived from the overlap of gold 6s orbitals. The central gold atom possesses atomic 6s and 6p functions that can overlap effectively with the S^σ and P^σ skeletal molecular orbitals, to give four cluster bonding orbitals. When these are occupied and due account of the electrons in the 5d shells and the Au–P bonding molecular orbitals is made, the $12n_s + 18$ electron rule results. On lowering the symmetry of the cluster from spherical to toroidal, the degeneracy of the P^σ functions is removed and the P_z^σ orbital becomes either nonbonding or antibonding. Consequently, toroidal clusters are characterized by $12n_s + 16$ valence electrons.

The heteronuclear clusters described previously also conform to this generalization, as Tables XVI and XVII demonstrate. All of the clusters characterized by $12n_s + 16$ valence electrons adopt toroidal geometries and will readily add one molecule of carbon monoxide to give clusters with a valence electron count of $12n_s + 18$. The resultant metal cage geometries have been described as either spherical or hemispherical.

TABLE XVI
VALENCE ELECTRON COUNTS FOR SOME
HETERONUCLEAR GOLD CLUSTER COMPOUNDS
ADOPTING TOROIDAL GEOMETRIES

Cluster	Valence electron count
$[\text{Pt}(\text{PPh}_3)(\text{AuPPh}_3)_6]^{2+}$	88
$[\text{Pt}(\text{AuPPh}_3)_8]^{2+}$	112
$[\text{Pd}(\text{AuPPh}_3)_8]^{2+}$	112
$[\text{Pt}(\text{AgNO}_3)(\text{AuPPh}_3)_8]^{2+}$	124

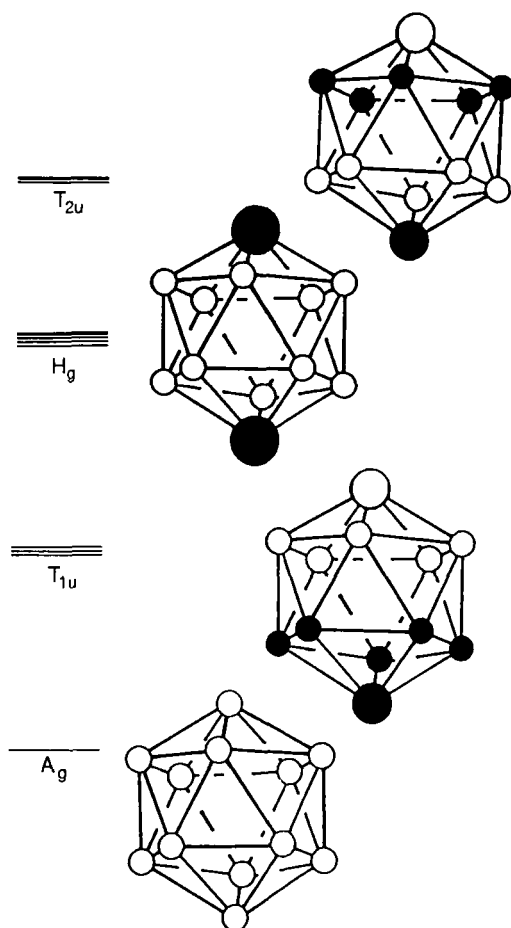


FIG. 38. The skeletal molecular orbitals for an icosahedral Au_{12} cluster derived from the overlap of gold 6s orbitals.

With the exception of the compounds $[\text{Pt}(\text{PPh}_3)(\text{CC-}t\text{-Bu})(\text{AuPPh}_3)_6]^+$ and $[\text{Pt}(\text{H})(\text{PPh}_3)(\text{AuPPh}_3)_7]^+$, which have distorted cubic geometries, all of the spherical cluster compounds adopt geometries that are fragments of a centered icosahedron (Fig. 39). Molecular orbital calculations have shown that for gold cluster cations with spherical topologies the preferred polyhedral geometry is that which maximizes the number of next-neighbor contacts. The icosahedral fragments maximize these interactions.

A general theoretical analysis of the site preferences in these clusters has appeared (293) that demonstrates that clusters with the transition

TABLE XVII

VALENCE ELECTRON COUNTS FOR SOME HETERONUCLEAR
GOLD CLUSTER COMPOUNDS ADOPTING
SPHERICAL GEOMETRIES

Cluster	Valence electron count
$[\text{Pt}(\text{PPh}_3)(\text{CO})(\text{AuPPh}_3)_5]^+$	78
$[\text{Pt}(\text{PPh}_3)(\text{CO})(\text{AuPPh}_3)_6]^{2+}$	90
$[\text{Pt}(\text{PPh}_3)(\text{CC-}t\text{-Bu})(\text{AuPPh}_3)_6]^-$	90
$[\text{Pt}(\text{H})(\text{PPh}_3)(\text{AuPPh}_3)_7]^{2+}$	102
$[\text{Mo}(\text{CO})_3(\text{AuPPh}_3)_7]^+$	102
$[\text{Pt}(\text{PPh}_3)(\text{AuPPh}_3)_5(\text{HgNO}_3)_2]^+$	102
$[\text{Pt}(\text{CO})(\text{AuPPh}_3)_8]^{2+}$	114
$[\text{Pt}(\text{CO})(\text{AgNO}_3)(\text{AuPPh}_3)_8]^{2+}$	126
$[\text{Pt}(\text{CN})(\text{AuCN})(\text{AuPPh}_3)_8]^+$	126

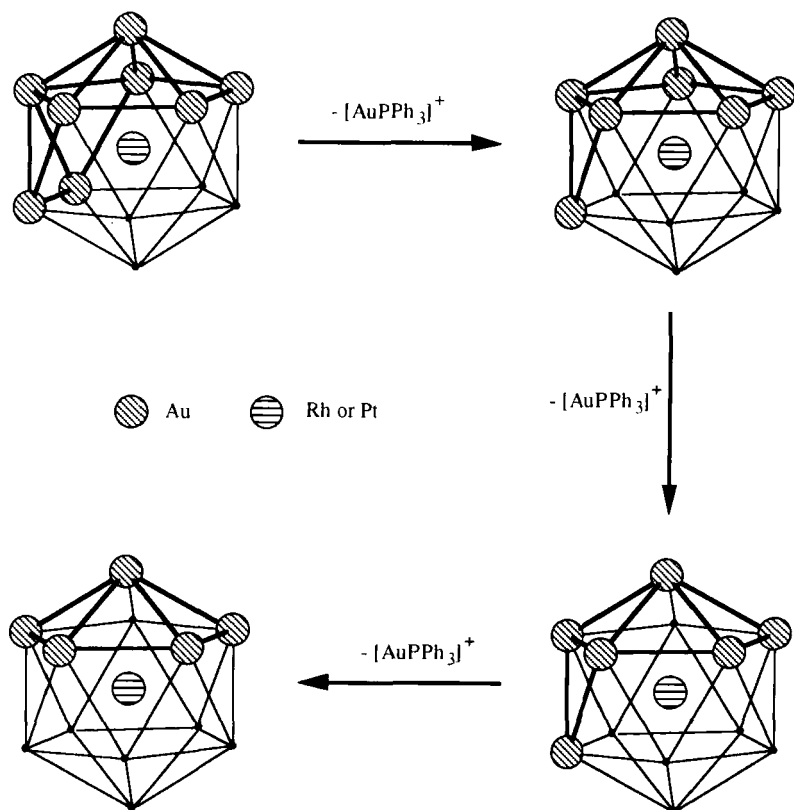


FIG. 39. Structural relationships for heterometallic clusters based on a centered icosahedron.

metal fragment in the interstitial site are the most stable. This has been attributed to the cumulative effect of increased Au–M versus Au–Au bond strengths.

V. Applications of Heteronuclear Gold Cluster Compounds

Gold metal has found a wide variety of applications, ranging from ornamental decoration and applications in the electronics industry, to the protection of heat-sensitive components from solar radiation in space vehicles (294). Whereas these applications make use of the unique properties of elemental gold, the controlled addition of other metals and metal complexes to the gold preparations is often used to enhance the properties of the metal. For example, the modification of the color of gold by the addition of other metals is important for applications in jewelry. The addition of platinum metals to dental gold alloys has also been used to inhibit tarnishing. Although there are no reports of the commercial use of heteronuclear gold cluster compounds in any of this technology, these compounds are of interest as potential precursors to such mixed-metal systems.

Much interest has been directed toward the potential catalytic applications of heteronuclear gold cluster compounds. The catalytic chemistry of gold is much less extensive than that of the other noble metals (295), and not surprisingly there have been no reports of homonuclear gold cluster compounds acting in a catalytic fashion. It has been established, however, that alloy formation modifies the catalytic ability of the substrate and there are examples where the addition of gold to transition metal catalysts leads to an enhancement of their selectivities (296). Heteronuclear gold cluster compounds have, therefore, been proposed as potential precursors for the synthesis of selective catalysts and also as models of the modifications to the substrate that arise at a molecular level. Braunstein has reviewed in more detail the catalytic applications of gold-containing polymetallic systems (212).

Few cluster compounds have been studied in detail. Evans and Jing-xing have discussed the activity of some gold–ruthenium clusters as homogeneous catalysts toward pent-1-ene isomerization (297). Substitution of AuPPh_3 for H in $[\text{Ru}_4\text{H}_4(\text{CO})_{12}]$ increases the catalytic activity over that of the parent ruthenium cluster, but this activity is inhibited by the presence of carbon monoxide. These observations are consistent with an initial step in the catalytic cycle involving dissociation of CO from the cluster. Such dissociation reactions in heteronuclear cluster compounds have been discussed previously.

Reports on the preparation of supported gold-containing bimetallic clusters have also appeared (298, 299). $[\text{Os}_3(\mu\text{-H})(\text{CO})_{10}(\mu\text{-AuPPh}_3)]$ and $[\text{Os}_3(\mu\text{-Cl})(\text{CO})_{10}(\mu\text{-AuPPh}_3)]$ have been attached to functionalized poly(styrene-divinylbenzene) and silica supports by ligand exchange reactions and infrared spectroscopic studies have confirmed that both clusters were anchored intact. Although the hydrido cluster was inactive for alkene hydrogenation and isomerization, the chloride cluster was found to be active for alkene hydrogenation.

REFERENCES

1. O. M. Abu-Salah, and C. B. Knobler, *J. Organomet. Chem.* **302**, C10 (1986).
2. M. Hong, Z. Huang, B. Kang, X. Lei, and H. Liu, *Inorg. Chim. Acta* **168**, 163 (1990).
3. R. P. F. Kanters, P. P. J. Schlebos, J. J. Bour, W. P. Bosman, J. M. M. Smits, P. T. Beurskens, and J. J. Steggerda, *Inorg. Chem.* **29**, 324 (1990).
4. B. K. Teo, and K. Keating, *J. Am. Chem. Soc.* **106**, 2221 (1984).
5. B. K. Teo, M. C. Hong, H. Zhang, and D. B. Huang, *Angew. Chem., Int. Ed. Engl.* **26**, 897 (1987).
6. B. K. Teo, M. Hong, H. Zhang, D. Huang, and X. Shi, *J. Chem. Soc., Chem. Commun.* p. 204 (1988).
7. B. K. Teo, H. Zhang, and X. Shi, *Inorg. Chem.* **29**, 2083 (1990).
8. R. Usón, A. Laguna, M. Laguna, A. Usón, P. G. Jones, and C. F. Erdbrügger, *Organometallics* **6**, 1778 (1987).
9. R. Usón, A. Laguna, M. Laguna, P. G. Jones, and G. M. Sheldrick, *J. Chem. Soc., Chem. Commun.* p. 1097 (1981).
10. R. Usón, A. Laguna, M. Laguna, B. R. Manzano, P. G. Jones, and G. M. Sheldrick, *J. Chem. Soc., Dalton Trans.* p. 285 (1984).
11. M. Åhlgrén, T. T. Pakkanen, and I. Tahvanainen, *J. Organomet. Chem.* **323**, 91 (1987).
12. J. Bashkin, C. E. Briant, D. M. P. Mingos, and R. W. M. Wardle, *Transition Met. Chem.* **10**, 113 (1985).
13. G. Beuter and J. Strähle, *J. Organomet. Chem.* **372**, 67 (1989).
14. T. L. Blundell and H. M. Powell, *J. Chem. Soc. A* p. 1685 (1971).
15. P. Braunstein, J. Rosé, Y. Dusauso, and J.-P. Mangeot, *C. R. Hebd. Seances Acad. Sci., Ser. 2* **294**, 967 (1982).
16. P. Braunstein, J. Rosé, A. Dedieu, Y. Dusauso, J.-P. Mangeot, A. Tiripicchio, and M. Tiripicchio Camellini, *J. Chem. Soc., Dalton Trans.* p. 225 (1986).
17. M. I. Bruce, and B. K. Nicholson, *J. Chem. Soc., Chem. Commun.*, p. 1141 (1982).
18. M. I. Bruce, and B. K. Nicholson, *Organometallics* **3**, 101 (1984).
19. N. Carr, M. C. Gimeno, and F. G. A. Stone, *J. Chem. Soc., Dalton Trans.* p. 2247 (1990).
20. J. M. Forward, unpublished results.
21. B. T. Kilbourn, T. L. Blundell, and H. M. Powell, *J. Chem. Soc., Chem. Commun.* p. 444 (1965).
22. J. W. Lauher, and K. Wald, *J. Am. Chem. Soc.* **103**, 7648 (1981).
23. A. A. Low and J. W. Lauher, *Inorg. Chem.* **26**, 3863 (1987).
24. J. Pursiainen, M. Åhlgrén, and T. A. Pakkanen, *J. Organomet. Chem.* **297**, 391 (1985).

25. E. Roland, K. Fischer, and H. Vahrenkamp, *Angew. Chem., Int. Ed. Engl.* **22**, 326 (1983).
26. R. Usón, A. Laguna, M. Laguna, P. G. Jones, and G. M. Sheldrick, *J. Chem. Soc., Dalton Trans.* p. 366 (1981).
27. J. W. A. van der Velden, J. J. Bour, B. F. Otterloo, W. P. Bosman, and J. H. Noordik, *J. Chem. Soc., Chem. Commun.* p. 583 (1981).
28. J. W. A. van der Velden, J. J. Bour, W. P. Bosman, and J. H. Noordik, *Inorg. Chem.* **22**, 1913 (1983).
29. P. Braunstein, U. Schubert, and M. Burgard, *Inorg. Chem.* **23**, 4057 (1984).
30. F. Edelmann, S. Töfke, and U. Behrens, *J. Organomet. Chem.* **309**, 87 (1986).
31. M. Green, A. G. Orpen, I. D. Salter, and F. G. A. Stone, *J. Chem. Soc., Chem. Commun.* p. 813 (1982).
32. M. Green, A. G. Orpen, I. D. Salter, and F. G. A. Stone, *J. Chem. Soc., Dalton Trans.* p. 2497 (1984).
33. O. M. Abu-Salah, A-R. A. Al-Ohaly, and C. B. Knobler, *J. Chem. Soc., Chem. Commun.* p. 1502 (1985).
34. A. A. Aitchison and L. J. Farrugia, *Organometallics* **5**, 1103 (1986).
35. V. G. Andrianov, Y. T. Struchkov, and E. R. Rossinskaja, *J. Chem. Soc., Chem. Commun.* p. 338 (1973).
36. V. G. Andrianov, Y. T. Struchkov, and E. R. Rossinskaja, *Zh. Strukt. Khim.* **15**, 74 (1974).
37. L. W. Arndt, M. Y. Darensbourg, J. P. Fackler, Jr., R. J. Lusk, D. O. Marler, and K. A. Youngdahl, *J. Am. Chem. Soc.* **107**, 7218 (1985).
38. C. E. Briant, K. P. Hall, and D. M. P. Mingos, *J. Chem. Soc., Chem. Commun.* p. 843 (1983).
39. M. I. Bruce, and B. K. Nicholson, *J. Organomet. Chem.* **250**, 627 (1983).
40. K. Fischer, M. Müller, and H. Vahrenkamp, *Angew. Chem., Int. Ed. Engl.* **23**, 140 (1984).
41. K. S. Harpp, C. E. Housecroft, A. L. Rheingold, and M. S. Shongwe, *J. Chem. Soc., Chem. Commun.* p. 965 (1988).
42. C. P. Horwitz, E. M. Holt, and D. F. Shriver, *J. Am. Chem. Soc.* **107**, 281 (1985).
43. C. P. Horwitz, E. M. Holt, C. P. Brock, and D. F. Shriver, *J. Am. Chem. Soc.* **107**, 8136 (1985).
44. C. E. Housecroft, and A. L. Rheingold, *J. Am. Chem. Soc.* **108**, 6420 (1986).
45. C. E. Housecroft and A. L. Rheingold, *Organometallics*, **6**, 1332 (1987).
46. C. E. Housecroft, A. L. Rheingold, and M. S. Shongwe, *J. Chem. Soc., Chem. Commun.* p. 1630 (1988).
47. C. E. Housecroft, M. S. Shongwe, and A. L. Rheingold, *Organometallics* **7**, 1885 (1988).
48. C. E. Housecroft, M. S. Shongwe, and A. L. Rheingold, *Organometallics* **8**, 2651 (1989).
49. B. F. G. Johnson, D. A. Kaner, J. Lewis, P. R. Raithby, and M. J. Rosales, *J. Organomet. Chem.* **231**, C59 (1982).
50. B. F. G. Johnson, D. A. Kaner, J. Lewis, and M. J. Rosales, *J. Organomet. Chem.* **238**, C73 (1982).
51. J. W. Lauher, unpublished results.
52. R. D. Pergola, L. Garlaschelli, F. Demartin, M. Manassero, N. Masciocchi, and M. Santoni, *J. Chem. Soc., Dalton Trans.* p. 127 (1990).
53. O. Rossell, M. Seco, and P. G. Jones, *Inorg. Chem.* **29**, 348 (1990).
54. U. Schubert, E. Kunz, M. Knorr, and J. Müller, *Chem. Ber.* **120**, 1079 (1987).

55. F. E. Simon and J. W. Lauher, *Inorg. Chem.* **19**, 2338 (1980).
56. H. Umland and U. Behrens, *J. Organomet. Chem.* **287**, 109 (1985).
57. J. J. Bour, Ph.D. Thesis, University of Nijmegen, 1990.
58. L. N. Ito, A. M. P. Felicissimo, and L. H. Pignolet, unpublished results.
59. S. Wang and J. P. Fackler, Jr., *Organometallics* **7**, 2415 (1988).
60. S. Wang and J. P. Fackler, Jr., *Organometallics* **8**, 1578 (1989).
61. S. Wang and J. P. Fackler, Jr., *Organometallics* **9**, 111 (1990).
62. A. Albinati, C. Anklin, P. Janser, H. Lehner, D. Matt, P. S. Pregosin, and L. M. Venanzi, *Inorg. Chem.* **28**, 1105 (1989).
63. B. D. Alexander, B. J. Johnson, S. M. Johnson, A. L. Casalnuovo, and L. H. Pignolet, *J. Am. Chem. Soc.* **108**, 4409 (1986).
64. A. L. Balch, D. E. Oram, and P. E. Reedy, Jr., *Inorg. Chem.* **26**, 1836 (1987).
65. A. L. Balch, J. K. Nagle, D. E. Oram, and P. E. Reedy, Jr., *J. Am. Chem. Soc.* **110**, 454 (1988).
66. A. L. Balch, B. J. Davis, and M. M. Olmstead, *Inorg. Chem.* **28**, 3148 (1989).
67. A. L. Balch, V. J. Catalano, and M. M. Olmstead, *Inorg. Chem.* **29**, 585 (1990).
68. A. L. Balch, V. J. Catalano, and M. M. Olmstead, *J. Am. Chem. Soc.* **112**, 2010 (1990).
69. D. Braga, F. Grepioni, F. S. Livotto, and M. D. Vargas, *Proc. R. Soc. Chem., Conf. Chem. Platinum Met., 4th*, 1990.
70. M. I. Bruce, P. E. Corbin, P. A. Humphrey, G. A. Koutsantonis, M. J. Liddell, and E. R. T. Tienkink, *J. Chem. Soc., Chem. Commun.* p. 674 (1990).
71. A. L. Casalnuovo, L. H. Pignolet, J. W. A. van der Velden, J. J. Bour, and J. J. Steggerda, *J. Am. Chem. Soc.* **105**, 5957 (1983).
72. A. L. Casalnuovo, T. Laska, P. V. Nilsson, J. Olofson, L. H. Pignolet, W. Bos, J. J. Bour, and J. J. Steggerda, *Inorg. Chem.* **24**, 182 (1985).
73. A. L. Casalnuovo, T. Laska, P. V. Nilsson, J. Olofson, and L. H. Pignolet, *Inorg. Chem.* **24**, 233 (1985).
74. A. L. Casalnuovo, J. A. Casalnuovo, P. V. Nilsson, and L. H. Pignolet, *Inorg. Chem.* **24**, 2554 (1985).
75. H. Lehner, D. Matt, P. S. Pregosin, and L. M. Venanzi, *J. Am. Chem. Soc.* **104**, 6825 (1982).
76. M. A. Luke, D. M. P. Mingos, D. J. Sherman, and R. W. M. Wardle, *Transition Met. Chem.* **12**, 37 (1987).
77. J. N. Nicholls, P. R. Raithby, and M. D. Vargas, *J. Chem. Soc., Chem. Commun.* p. 1617 (1986).
78. A. D. Horton, M. J. Mays, and M. McPartlin, *J. Chem. Soc., Chem. Commun.* p. 424 (1987).
79. J. A. Iggo, M. J. Mays, P. R. Raithby, and K. Henrick, *J. Chem. Soc., Dalton Trans.* p. 633 (1984).
80. Kh. A. I. F. M. Mannan, *Acta Crystallogr.* **23**, 649 (1967).
81. H. M. Powell, K. Mannan, B. T. Kilbourn, and P. Porta, *Proc. Int. Conf. Coord. Chem. 8th*, 1964 p. 155 (1964).
82. V. Riera, M. A. Ruiz, A. Tiripicchio, and M. Tiripicchio Camellini, *J. Chem. Soc., Dalton Trans.* p. 1551 (1987).
83. G. F. Warnock, and J. E. Ellis, unpublished results; see also reference 50 in A. M. Mueting *et al.*, *New J. Chem.* **12**, 505 (1988).
84. G. Beuter and J. Strähle, *Angew. Chem., Int. Ed. Engl.* **27**, 1094 (1988).
85. B. N. Strunin, K. I. Grandberg, V. G. Andrianov, V. N. Setkina, E. G. Perevalova, Yu. T. Struchkov, and D. N. Kursanov, *Dokl. Akad. Nauk SSSR* **281**, 599 (1985).

86. H. P. Kim, P. E. Fanwick, and C. P. Kubrak, *J. Organomet. Chem.* **346**, C39 (1988).
87. A. Antinolo, J. K. Burdett, B. Chaudret, O. Eisenstein, M. Fajardo, F. Jalon, F. Lahoz, J. A. Lopez, and A. Otero, *J. Chem. Soc., Chem. Commun.* p. 17 (1990).
88. M. Fajardo, M. P. Gómez-Sal, P. Royo, S. M. Carrera, and S. G. Blanco, *J. Organomet. Chem.* **312**, C44 (1986).
89. B. D. Alexander, M. P. Gómez-Sal, P. R. Gannon, C. A. Blaine, P. D. Boyle, A. M. Mueting, and L. H. Pignolet, *Inorg. Chem.* **27**, 3301 (1988).
90. C. W. Bradford, W. van Bronswijk, R. J. H. Clark, and R. S. Nyholm, *J. Chem. Soc. A* p. 2889 (1970).
91. P. Braunstein, J. Rosé, A. M. M. Landfredi, and A. Tiripicchio, *J. Chem. Soc., Dalton Trans.* p. 1843 (1984).
92. M. I. Bruce, E. Horn, J. G. Matisons, and M. R. Snow, *J. Organomet. Chem.* **286**, 271 (1985).
93. K. Burgess, B. F. G. Johnson, D. A. Kaner, J. Lewis, P. R. Raithby, and S. N. A. B. Syed-Mustaffa, *J. Chem. Soc., Chem. Commun.* p. 455 (1983).
94. K. Burgess, B. F. G. Johnson, J. Lewis, and P. R. Raithby, *J. Chem. Soc., Dalton Trans.* p. 1661 (1983).
95. S. B. Colbran, C. M. Hay, B. F. G. Johnson, F. J. Lahoz, J. Lewis, and P. R. Raithby, *J. Chem. Soc., Chem. Commun.* p. 1766 (1986).
96. V. Dearing, S. R. Drake, B. F. G. Johnson, J. Lewis, M. McPartlin, and H. R. Powell, *J. Chem. Soc., Chem. Commun.* p. 1331 (1988).
97. A. J. Deeming, S. Donovan-Mtunzi, and K. Hardcastle, *J. Chem. Soc., Dalton Trans.* p. 543 (1986).
98. S. R. Drake, K. Henrick, B. F. G. Johnson, J. Lewis, M. McPartlin, and J. Morris, *J. Chem. Soc., Chem. Commun.* p. 928 (1986).
99. L. J. Farrugia, *Acta Crystallogr., Sect. C* **C42**, 680 (1986).
100. C. M. Hay, B. F. G. Johnson, J. Lewis, R. C. S. McQueen, P. R. Raithby, R. M. Sorrell, and M. J. Taylor, *Organometallics* **4**, 202 (1985).
101. A. F. Hill, W. R. Roper, J. M. Waters, and A. H. Wright, *J. Am. Chem. Soc.* **105**, 5939 (1983).
102. J. A. K. Howard, L. Farrugia, C. Foster, F. G. A. Stone, and P. Woodward, *Eur. Cryst. Meet.* **6**, 73 (1980).
103. B. F. G. Johnson, D. A. Kaner, J. Lewis, and P. R. Raithby, *J. Chem. Soc., Chem. Commun.* p. 753 (1981).
104. B. F. G. Johnson, D. A. Kaner, J. Lewis, and P. R. Raithby, *J. Organomet. Chem.* **215**, C33 (1981).
105. B. F. G. Johnson, D. A. Kaner, J. Lewis, P. R. Raithby, and M. J. Taylor, *Polyhedron* **1**, 105 (1982).
106. B. F. G. Johnson, D. A. Kaner, J. Lewis, P. R. Raithby, and M. J. Taylor, *J. Chem. Soc., Chem. Commun.* p. 314 (1982).
107. B. F. G. Johnson, J. Lewis, W. J. H. Nelson, P. R. Raithby, and M. D. Vargas, *J. Chem. Soc., Chem. Commun.* p. 608 (1983).
108. B. F. G. Johnson, J. Lewis, W. J. H. Nelson, J. N. Nicholls, J. Puga, P. R. Raithby, M. J. Rosales, M. Schröder, and M. D. Vargas, *J. Chem. Soc., Dalton Trans.* p. 2447 (1983).
109. B. F. G. Johnson, J. Lewis, W. J. H. Nelson, M. D. Vargas, D. Braga, and M. McPartlin, *J. Organomet. Chem.* **246**, C69 (1983).
110. B. F. G. Jonnson, J. Lewis, P. R. Raithby, and A. Sanders, *J. Organomet. Chem.* **260**, C29 (1984).

111. B. F. G. Johnson, J. Lewis, W. J. H. Nelson, M. D. Vargas, D. Braga, K. Henrick, and M. McPartlin, *J. Chem. Soc., Dalton Trans.* p. 975 (1986).
112. B. F. G. Johnson, R. Khattar, J. Lewis, and P. R. Raithby, *J. Chem. Soc., Dalton Trans.* p. 1421 (1989).
113. J. Puga, R. A. Sánchez-Delgado, J. Ascanio, and D. Braga, *J. Chem. Soc., Chem. Commun.* p. 1631 (1986).
114. J. Puga, A. Arce, R. A. Sánchez-Delgado, J. Ascanio, A. Andriollo, D. Braga, and F. Grepioni, *J. Chem. Soc., Dalton Trans.* p. 913 (1988).
115. S. Wang, G. Garzón, C. King, J.-C. Wang, and J. P. Fackler, Jr., *Inorg. Chem.* **28**, 4623 (1989).
116. O. J. Ezomo, D. Phil. Thesis, University of Oxford, 1988.
117. L. N. Ito, B. J. Johnson, A. M. Mueting, and L. H. Pignolet, *Inorg. Chem.* **28**, 2026 (1989).
118. A. Albinati, H. Lehner, L. M. Venzani, and M. Wolfer, *Inorg. Chem.* **26**, 3933 (1987).
119. G. J. Arsenault, L. Manojlović-Muir, K. W. Muir, I. Treurnicht, and R. J. Puddephatt, *Angew. Chem., Int. Ed. Engl.* **26**, 86 (1987).
120. R. Bender, P. Braunstein, A. Dedieu, and Y. Dusauroy, *Angew. Chem., Int. Ed. Engl.* **28**, 923 (1989).
121. T. Blum, P. Braunstein, A. Tiripicchio, and M. Tiripicchio Camellini, *New J. Chem.* **12**, 539 (1988).
122. J. J. Bour, R. P. F. Kanthers, P. P. J. Schlebos, W. Bos, W. P. Bosman, H. Behm, P. T. Beurskens, and J. J. Steggerda, *J. Organomet. Chem.* **329**, 405 (1987).
123. J. J. Bour, R. P. F. Kanthers, P. P. J. Schlebos, W. P. Bosman, H. Behm, P. T. Beurskens, and J. J. Steggerda, *Recl. Trav. Chim. Pays-Bas* **106**, 157 (1987).
124. J. J. Bour, R. P. F. Kanthers, P. P. J. Schlebos, and J. J. Steggerda, *Recl. Trav. Chim. Pays-Bas* **107**, 211 (1988).
125. J. J. Bour, P. P. J. Schlebos, R. P. F. Kanthers, W. P. Bosman, J. M. M. Smits, P. T. Beurskens, and J. J. Steggerda, *Inorg. Chim. Acta* **171**, 177 (1990).
126. P. Braunstein, H. Lehner, D. Matt, A. Tiripicchio, and M. Tiripicchio Camellini, *Angew. Chem., Int. Ed. Engl.* **23**, 304 (1984).
127. C. E. Briant, R. W. M. Wardle, and D. M. P. Mingos, *J. Organomet. Chem.* **267**, C49 (1984).
128. C. E. Briant, D. I. Gilmour, and D. M. P. Mingos, *J. Organomet. Chem.* **267**, C52 (1984).
129. C. E. Briant, D. I. Gilmour, and D. M. P. Mingos, *J. Chem. Soc., Dalton Trans.* p. 835 (1986).
130. G. A. Carriedo, J. A. K. Howard, F. G. A. Stone, and M. J. Went, *J. Chem. Soc., Dalton Trans.* p. 2545 (1984).
131. M. Crespo, J. Sales, and X. Solans, *J. Chem. Soc., Dalton Trans.* p. 1089 (1989).
132. G. Douglas, M. C. Jennings, L. Manojlović-Muir, and R. J. Puddephatt, *Inorg. Chem.* **27**, 4516 (1988).
133. M. F. Hallam, D. M. P. Mingos, T. Adatia, and M. McPartlin, *J. Chem. Soc., Dalton Trans.* p. 335 (1988).
134. C. M. Hill, D. M. P. Mingos, H. R. Powell, and M. J. Watson, unpublished results.
135. L. N. Ito, J. D. Sweet, A. M. Mueting, L. H. Pignolet, M. F. J. Schoondergang, and J. J. Steggerda, *Inorg. Chem.* **28**, 3696 (1989).
136. R. P. F. Kanthers, P. P. J. Schlebos, J. J. Bour, W. P. Bosman, H. J. Behm, and J. J. Steggerda, *Inorg. Chem.* **27**, 4034 (1988).
137. R. P. F. Kanthers, J. J. Bour, P. P. J. Schlebos, W. P. Bosman, H. Behm, J. J. Steggerda, L. N. Ito, and L. H. Pignolet, *Inorg. Chem.* **28**, 2591 (1989).

138. C. King, D. D. Heinrich, G. Garzón, J.-C. Wang, and J. P. Fackler, Jr., *J. Am. Chem. Soc.* **111**, 2300 (1989).
139. L. Manojlović-Muir, K. W. Muir, I. Treurnicht, and R. J. Puddephatt, *Inorg. Chem.* **26**, 2418 (1987).
140. L. Manojlović-Muir, A. N. Henderson, I. Treurnicht, and R. J. Puddephatt, *Organometallics* **8**, 2055 (1989).
141. D. M. P. Mingos and R. W. M. Wardle, *J. Chem. Soc., Dalton Trans.* p. 73 (1986).
142. D. M. P. Mingos, P. Oster, and D. J. Sherman, *J. Organomet. Chem.* **320**, 257 (1987).
143. H. H. Murray, D. A. Briggs, G. Garzón, R. G. Raptis, L. C. Porter, and J. P. Fackler, Jr., *Organometallics* **6**, 1992 (1987).
144. D. E. Smith, A. J. Welch, I. Treurnicht, and R. J. Puddephatt, *Inorg. Chem.* **25**, 4616 (1986).
145. B. D. Alexander, P. D. Boyle, B. J. Johnson, J. A. Casalnuovo, S. M. Johnson, A. M. Mueting, and L. H. Pignolet, *Inorg. Chem.* **26**, 2547 (1987).
146. C. F. Barrientos-Penna, F. W. B. Einstein, T. Jones, and D. Sutton, *Inorg. Chem.* **24**, 632 (1985).
147. T. Beringhelli, G. Ciani, G. D'Alfonso, V. De Maldé, and M. Freni, *J. Chem. Soc., Chem. Commun.* p. 735 (1986).
148. P. D. Boyle, B. J. Johnson, A. Buehler, and L. H. Pignolet, *Inorg. Chem.* **25**, 5 (1986).
149. P. D. Boyle, B. J. Johnson, B. D. Alexander, J. A. Casalnuovo, P. R. Gannon, S. M. Johnson, E. A. Larka, A. M. Mueting, and L. H. Pignolet, *Inorg. Chem.* **26**, 1346 (1987).
150. T. J. Henly, J. R. Shapley, and A. L. Rheingold, *J. Organomet. Chem.* **310**, 55 (1986).
151. G. A. Moehring, P. E. Fanwick, and R. A. Walton, *Inorg. Chem.* **26**, 1861 (1987).
152. B. R. Sutherland, D. M. Ho, J. C. Huffman, and K. G. Caulton, *Angew. Chem., Int. Ed. Engl.* **26**, 135 (1987).
153. B. R. Sutherland, K. Folting, W. E. Streib, D. M. Ho, J. C. Huffman, and K. G. Caulton, *J. Am. Chem. Soc.* **109**, 3489 (1987).
154. A. Albinati, F. Demartin, P. Janser, L. F. Rhodes, and L. M. Venanzi, *J. Am. Chem. Soc.* **111**, 2115 (1989).
155. B. D. Alexander, A. M. Mueting, and L. H. Pignolet, *Inorg. Chem.* **29**, 1313 (1990).
156. N. Carr, M. C. Gimeno, J. E. Goldberg, M. U. Pilotti, F. G. A. Stone, and I. Topaloglu, *J. Chem. Soc., Dalton Trans.* p. 2253 (1990).
157. M. J. Fernández, J. Modrego, L. A. Oro, M.-C. Apreda, F. H. Cano, and C. Foces-Foces, *J. Chem. Soc., Dalton Trans.* p. 1249 (1989).
158. A. Fumagalli, S. Martinengo, V. G. Albano, and D. Braga, *J. Chem. Soc., Dalton Trans.* p. 1237 (1988).
159. A. Fumagalli, S. Martinengo, V. G. Albano, D. Braga, and F. Grepioni, *J. Chem. Soc., Dalton Trans.* p. 2343 (1989).
160. R. J. McNair, P. V. Nilsson, and L. H. Pignolet, *Inorg. Chem.* **24**, 1935 (1985).
161. S. L. Schiavo, G. Bruno, F. Nicolò, P. Piraino, and F. Faraono, *Organometallics* **4**, 2091 (1985).
162. T. Adatia, M. McPartlin, and I. D. Salter, *J. Chem. Soc., Dalton Trans.* p. 751 (1988).
163. B. D. Alexander, B. J. Johnson, S. M. Johnson, P. D. Boyle, N. C. Kann, A. M. Mueting, and L. H. Pignolet, *Inorg. Chem.* **26**, 3507 (1987).
164. L. W. Bateman, M. Green, J. A. K. Howard, K. A. Mead, R. M. Mills, I. D. Salter, F. G. A. Stone, and P. Woodward, *J. Chem. Soc., Chem. Commun.* p. 773 (1982).
165. L. W. Bateman, M. Green, J. A. K. Howard, K. A. Mead, R. M. Mills, I. D. Salter, F. G. A. Stone, and P. Woodward, *J. Chem. Soc., Dalton Trans.* p. 2599 (1983).

166. P. A. Bates, S. S. D. Brown, A. J. Dent, M. B. Hursthouse, G. F. M. Kitchen, A. G. Orpen, I. D. Salter, and V. Šik, *J. Chem. Soc., Chem. Commun.* p. 600 (1986).
167. M. L. Blohm and W. L. Gladfelter, *Inorg. Chem.* **26**, 459 (1987).
168. P. Braunstein, G. Predieri, A. Tiripicchio, and E. Sappa, *Inorg. Chim. Acta* **63**, 113 (1982).
169. S. S. D. Brown, S. Hudson, I. D. Salter, and M. McPartlin, *J. Chem. Soc., Dalton Trans.* p. 1967 (1987).
170. S. S. D. Brown, I. D. Salter, D. B. Dyson, R. V. Parish, P. A. Bates, and M. B. Hursthouse, *J. Chem. Soc., Dalton Trans.* p. 1795 (1988).
171. S. S. D. Brown, I. D. Salter, A. J. Dent, G. F. M. Kitchen, A. G. Orpen, P. A. Bates, and M. B. Hursthouse, *J. Chem. Soc., Dalton Trans.* p. 1227 (1989).
172. M. I. Bruce and B. K. Nicholson, *J. Organomet. Chem.* **252**, 243 (1983).
173. M. I. Bruce, O. B. Shawkataly, and B. K. Nicholson, *J. Organomet. Chem.* **275**, 223 (1984).
174. M. I. Bruce, O. B. Shawkataly, and B. K. Nicholson, *J. Organomet. Chem.* **286**, 427 (1985).
175. M. I. Bruce, E. Horn, O. B. Shawkataly, and M. R. Snow, *J. Organomet. Chem.* **280**, 289 (1985).
176. M. I. Bruce, M. L. Williams, J. M. Patrick, B. W. Skelton, and A. H. White, *J. Chem. Soc., Dalton Trans.* p. 2557 (1986).
177. S. R. Bunkhall, H. D. Holden, B. F. G. Johnson, J. Lewis, G. N. Pain, P. R. Raithby, and M. J. Taylor, *J. Chem. Soc., Chem. Commun.* p. 25 (1984).
178. A. K. Chipperfield, C. E. Housecroft, and A. L. Rheingold, *Organometallics* **9**, 681 (1990).
179. A. G. Cowie, B. F. G. Johnson, J. Lewis, J. N. Nicholls, P. R. Raithby, and M. J. Rosales, *J. Chem. Soc., Dalton Trans.* p. 2311 (1983).
180. A. G. Cowie, B. F. G. Johnson, J. Lewis, J. N. Nicholls, P. R. Raithby, and A. G. Swanson, *J. Chem. Soc., Chem. Commun.* p. 637 (1984).
181. A. G. Cowie, B. F. G. Johnson, J. Lewis, and P. R. Raithby, *J. Chem. Soc., Chem. Commun.* p. 1710 (1984).
182. J. Evans, A. C. Street, and M. Webster, *Organometallics* **6**, 794 (1987).
183. L. J. Farrugia, M. J. Freeman, M. Green, A. G. Orpen, F. G. A. Stone, and I. D. Salter, *J. Organomet. Chem.* **249**, 273 (1983).
184. M. J. Freeman, A. G. Orpen, and I. D. Salter, *J. Chem. Soc., Dalton Trans.* p. 379 (1987).
185. M. Green, K. A. Mead, R. M. Mills, I. D. Salter, F. G. A. Stone, and P. Woodward, *J. Chem. Soc., Chem. Commun.* p. 51 (1982).
186. K. Henrick, B. F. G. Johnson, J. Lewis, J. Mace, M. McPartlin, and J. Morris, *J. Chem. Soc., Chem. Commun.* p. 1617 (1985).
187. J. A. K. Howard, I. D. Salter, and F. G. A. Stone, *Polyhedron* **3**, 567 (1984).
188. B. F. G. Johnson, J. Lewis, J. N. Nicholls, J. Puga, and K. H. Whitmire, *J. Chem. Soc., Dalton Trans.* p. 787 (1983).
189. B. F. G. Johnson, J. Lewis, W. J. H. Nelson, J. Puga, P. R. Raithby, D. Braga, M. McPartlin, and W. Clegg, *J. Organomet. Chem.* **243**, C13 (1983).
190. H. Jungbluth, H. Stoeckli-Evans, and G. Süss-Fink, *J. Organomet. Chem.* **391**, 109 (1990).
191. G. Lavigne, F. Papageorgiou, and J.-J. Bonnet, *Inorg. Chem.* **23**, 609 (1984).
192. M. J. Mays, P. R. Raithby, P. L. Taylor, and K. Henrick, *J. Organomet. Chem.* **224**, C45 (1982).

193. M. J. Mays, P. R. Raithby, P. L. Taylor, and K. Henrick, *J. Chem. Soc., Dalton Trans.* p. 959 (1984).
194. Z. Demidowicz, R. L. Johnston, J. C. Machell, D. M. P. Mingos, and I. D. Williams, *J. Chem. Soc., Dalton Trans.* p. 1751 (1988).
195. D. M. P. Mingos, H. R. Powell, and T. L. Stolberg, unpublished results.
196. W. Clegg, *Acta Crystallogr., Sect. B* **B34**, 278 (1978).
197. S. Wang, J. P. Fackler, Jr., C. King, and J. C. Wang, *J. Am. Chem. Soc.* **110**, 3308 (1988).
198. M. G. B. Drew, *Acta Crystallogr., Sect. B* **B38**, 254 (1982).
199. J. E. Ellis, *J. Am. Chem. Soc.* **103**, 6106 (1981).
200. M. R. Awang, G. A. Carriedo, J. A. K. Howard, K. A. Mead, I. Moore, C. M. Nunn, and F. G. A. Stone, *J. Chem. Soc., Chem. Commun.* p. 964 (1983).
201. A. Berry, J. E. Bandy, and M. L. H. Green, unpublished results.
202. G. A. Carriedo, D. Hodgson, J. A. K. Howard, K. Marsden, F. G. A. Stone, M. J. Went, and P. Woodward, *J. Chem. Soc., Chem. Commun.* p. 1006 (1982).
203. G. A. Carriedo, J. A. K. Howard, K. Marsden, F. G. A. Stone, and P. Woodward, *J. Chem. Soc., Dalton Trans.* p. 1589 (1984).
204. G. A. Carriedo, V. Riera, G. Sánchez, and X. Solans, *J. Chem. Soc., Dalton Trans.* p. 1957 (1988).
205. M. Green, J. A. K. Howard, A. P. James, C. M. Nunn, and F. G. A. Stone, *J. Chem. Soc., Chem. Commun.* p. 1113 (1984).
206. M. Green, J. A. K. Howard, A. P. James, C. M. Nunn, and F. G. A. Stone, *J. Chem. Soc., Dalton Trans.* p. 61 (1987).
207. H. P. Kim, S. Kim, R. A. Jacobson, and R. J. Angelici, *J. Am. Chem. Soc.* **108**, 5154 (1986).
208. J. T. Lin, Y.-M. Hsiao, L.-K. Liu, and S.K. Yeh, *Organometallics* **7**, 2065 (1988).
209. J. B. Wilford and H. M. Powell, *J. Chem. Soc. A* p. 8 (1969).
210. K. P. Hall, and D. M. P. Mingos, *Prog. Inorg. Chem.* **32**, 237 (1984).
211. M. F. Hallam, M. A. Luke, D. M. P. Mingos, and I. D. Williams, *J. Organomet. Chem.* **325**, 271 (1987).
212. P. Braunstein, and J. Rose, *Gold Bull.* **18**, 17 (1985).
213. A. M. Mueting, W. Bos, B. D. Alexander, P. D. Boyle, J. A. Casalnuovo, S. Balaban, L. N. Ito, S. M. Johnson, and L. H. Pignolet, *New J. Chem.* **12**, 505 (1988).
214. I. D. Salter, *Adv. Organomet. Chem.* **29**, 249 (1989).
215. P. G. Jones, *Gold Bull.* **14**, 159 (1981).
216. P. G. Jones, *Gold Bull.* **16**, 114 (1983).
217. P. G. Jones, *Gold Bull.* **19**, 46 (1986).
218. C. E. Coffey, J. Lewis, and R. S. Nyholm, *J. Chem. Soc.* p. 1741 (1964).
219. A. S. Kasenally, R. S. Nyholm, R. J. O'Brien, and M. H. B. Stiddard, *Nature (London)* **204**, 871 (1964).
220. A. S. Kasenally, J. Lewis, A. R. Manning, J. R. Miller, R. S. Nyholm, and M. H. B. Stiddard, *J. Chem. Soc.* p. 3407 (1965).
221. J. Lewis and R. S. Nyholm, *Sci. Prog.* **52**, 557 (1964).
222. R. J. Haines, R. S. Nyholm, and M. H. B. Stiddard, *J. Chem. Soc. A* p. 46 (1968).
223. J. P. Collman, F. D. Vastine, and W. R. Roper, *J. Am. Chem. Soc.* **90**, 2282 (1968).
224. M. A. Bennett and D. J. Patmore, *Inorg. Chem.* **10**, 2387 (1971).
225. M. Casey, and A. R. Manning, *J. Chem. Soc. A* p. 2989 (1971).
226. J. Lewis and B. F. G. Johnson, *Pure Appl. Chem.* **54**, 97 (1982).
227. B. Chiswell, and L. M. Venanzi, *J. Chem. Soc. A* p. 901 (1966).

228. S. S. D. Brown, I. D. Salter, T. Adatia, and M. McPartlin, *J. Organomet. Chem.* **332**, C6 (1987).
229. S. S. D. Brown, I. D. Salter, T. Adatia, and M. McPartlin, *J. Chem. Soc., Dalton Trans.* p. 799 (1990).
230. L. J. Farrugia, J. A. K. Howard, P. Mitrprachachon, J. L. Spencer, F. G. A. Stone, and P. Woodward, *J. Chem. Soc., Chem. Commun.* p. 260 (1978).
231. K. Burgess, B. F. G. Johnson, and J. Lewis, *J. Organomet. Chem.* **247**, C42 (1983).
232. A. J. Layton, R. S. Nyholm, G. A. Pneumaticakis, and M. L. Tobe, *Chem. Ind. (London)* p. 465 (1967).
233. A. Davison and J. E. Ellis, *J. Organomet. Chem.* **36**, 113 (1972).
234. P. Braunstein and J. Dehand, *J. Organomet. Chem.* **88**, C24 (1975).
235. F. Cariati and L. Naldini, *J. Chem. Soc., Dalton Trans.* p. 2286 (1972).
236. C. E. Briant, K. P. Hall, D. M. P. Mingos, and A. C. Wheeler, *J. Chem. Soc., Dalton Trans.* p. 687 (1986).
237. C. E. Briant, B. R. C. Theobald, J. W. White, L. K. Bell, and D. M. P. Mingos, *J. Chem. Soc., Chem. Commun.* p. 201 (1981).
238. R. P. F. Kanters, J. J. Bour, P. P. J. Schlebos, and J. J. Steggerda, *J. Chem. Soc., Chem. Commun.* p. 1634 (1988).
239. G. A. Moehring and R. A. Walton, *J. Chem. Soc., Dalton Trans.* p. 1701 (1988).
240. A. G. Cowie, B. F. G. Johnson, and J. Lewis, *J. Chem. Soc., Dalton Trans.* p. 2839 (1987).
241. R. P. F. Kanters, P. P. J. Schlebos, J. J. Bour, W. Winjnhoven, E. van der Berg, and J. J. Steggerda, *J. Organomet. Chem.* **388**, 233 (1990).
242. J. G. M. van der Linden, A. M. Roelofson, and G. H. W. Ipskamp, *Inorg. Chem.* **28**, 967 (1989).
243. J. G. M. van der Linden, M. L. H. Paulissen, and J. E. J. Schmitz, *J. Am. Chem. Soc.* **105**, 1903 (1983).
244. P. D. Boyle, D. C. Boyd, A. M. Mueting, and L. H. Pignolet, *Inorg. Chem.* **27**, 4424 (1988).
245. S. R. Drake, *Polyhedron* **9**, 455 (1990).
246. M. S. Barber, R. S. Bordoli, R. D. Sedgwick, and A. N. Tyler, *J. Chem. Soc., Chem. Commun.* p. 325 (1981).
247. T. Blumenthal, M. I. Bruce, O. B. Shawkataly, B. N. Green, and I. Lewis, *J. Organomet. Chem.* **269**, C10 (1984).
248. R. V. Parish, *Gold Bull.* **15**, 51 (1982).
249. M. O. Faltens and D. A. Shirley, *Chem. Phys.* **53**, 4249 (1970).
250. F. A. Vollenbroek, P. C. P. Bouten, J. M. Trooster, J. P. van den Berg, and J. J. Bour, *Inorg. Chem.* **17**, 1345 (1978).
251. F. A. Vollenbroek, J. W. A. van der Velden, J. J. Bour, and J. M. Trooster, *Recl. Trav. Chim. Pays-Bas* **100**, 375 (1981).
252. S. S. D. Brown, L. S. Moore, R. V. Parish, and I. D. Salter, *J. Chem. Soc., Chem. Commun.* p. 1453 (1986).
253. L. S. Moore, R. V. Parish, S. S. D. Brown, and I. D. Salter, *J. Chem. Soc., Dalton Trans.* p. 2333 (1987).
254. R. V. Parish, L. S. Moore, A. J. J. Dens, D. M. P. Mingos, and D. J. Sherman, *J. Chem. Soc., Dalton Trans.* p. 781 (1988).
255. R. V. Parish, L. S. Moore, A. J. J. Dens, D. M. P. Mingos, and D. J. Sherman, *J. Chem. Soc., Dalton Trans.* p. 539 (1989).
256. D. I. Gilmour and D. M. P. Mingos, *J. Organomet. Chem.* **302**, 127 (1986).

257. F. A. Vollenbroek, J. P. van den Berg, J. W. A. van der Velden, and J. J. Bour, *Inorg. Chem.* **19**, 2685 (1980).
258. C. E. Briant, K. P. Hall, and D. M. P. Mingos, *J. Chem. Soc., Chem. Commun.* p. 290 (1984).
259. R. P. F. Kanters, P. P. J. Schlebos, J. Bour, J. J. Steggerda, W. E. J. R. Maas, and R. Janssen, unpublished results.
260. A. G. Orpen, *J. Chem. Soc., Dalton Trans.* p. 2509 (1980).
261. E. A. McNeill and F. R. Scholer, *J. Am. Chem. Soc.* **99**, 6243 (1977).
262. L. W. Arndt, T. Delord, and M. Y. Darensbourg, *J. Am. Chem. Soc.* **106**, 456 (1984).
263. W. S. Crane and H. Beall, *Inorg. Chim. Acta* **31**, L469 (1978).
264. R. Hesse and P. Jennische, *Acta Chem. Scand.* **26**, 3855 (1972).
265. W. B. Pearson, "Lattice Spacings and Structures of Metals and Alloys." Pergamon, Oxford, 1957.
266. H. Schmidbaur, *Gold Bull.* **23**, 11 (1990).
267. F. Bachechi, J. Ott, and M. Venanzi, *J. Am. Chem. Soc.* **107**, 1760 (1985).
268. F. Calderazzo, G. Pampaloni, U. Englert, and J. Strähle, *Angew. Chem., Int. Ed. Engl.* **28**, 471 (1989).
269. F. Demartin, M. Manassero, L. Naldini, R. Ruggeri, and M. Sansoni, *J. Chem. Soc., Chem. Commun.* p. 22 (1981).
270. M. Manassero, L. Naldini, and M. Sansoni, *J. Chem. Soc., Chem. Commun.* p. 385 (1979).
271. F. A. Vollenbroek, W. P. Bosman, J. J. Bour, J. H. Noordik, and P. T. Beurskens, *J. Chem. Soc., Chem. Commun.* p. 387 (1979).
272. K. P. Hall, B. R. C. Theobald, D. I. Gilmour, D. M. P. Mingos, and A. J. Welch, *J. Chem. Soc., Chem. Commun.* p. 528 (1982).
273. C. E. Briant, K. P. Hall, A. C. Wheeler, and D. M. P. Mingos, *J. Chem. Soc., Chem. Commun.* p. 248 (1984).
274. J. W. A. van der Velden, J. J. Bour, W. P. Bosman, and J. H. Noordik, *J. Chem. Soc., Chem. Commun.* p. 1218 (1981).
275. For a brief account, see *Chem. Eng. News* **67**, 6 (1989).
276. G. Schmid, R. Pfeil, R. Boese, F. Bandermann, S. Meyer, G. H. M. Calis, and J. W. A. van der Velden, *Chem. Ber.* **114**, 3634 (1981).
277. G. Schmid, *Struct. Bonding (Berlin)* **62**, 51 (1985).
278. J. P. Fackler, Jr., C. J. McNeil, R. E. P. Winpenny, and L. H. Pignolet, *J. Am. Chem. Soc.* **111**, 6434 (1989).
279. D. M. P. Mingos, *J. Chem. Soc., Dalton Trans.* p. 1163 (1976).
280. D. G. Evans and D. M. P. Mingos, *J. Organomet. Chem.* **232**, 171 (1982).
281. K. P. Hall, D. I. Gilmour, and D. M. P. Mingos, *J. Organomet. Chem.* **268**, 275 (1984).
282. D. G. Evans and D. M. P. Mingos, *J. Organomet. Chem.* **295**, 389 (1985).
283. A. J. Stone, *Mol. Phys.* **41**, 1339 (1980).
284. D. M. P. Mingos, *Polyhedron* **3**, 1289 (1984).
285. R. Hoffmann, *Angew. Chem., Int. Ed. Engl.* **21**, 71 (1982).
286. D. M. P. Mingos and M. I. Forsyth, *J. Chem. Soc., Dalton Trans.* p. 610 (1977).
287. G. J. Kubas, *Acc. Chem. Res.* **21**, 120 (1988).
288. G. J. Kubas, *Comments Inorg. Chem.* **7**, 17 (1988).
289. R. D. Adams and D. A. Katahira, *Organometallics* **1**, 53 (1982).
290. P. K. Mehrotra and R. Hoffmann, *Inorg. Chem.* **17**, 2187 (1978).
291. K. M. Merz, Jr. and R. Hoffmann, *Inorg. Chem.* **27**, 2120 (1988).
292. P. Pykkö, *Chem. Rev.* **88**, 563 (1988).

- 293. D. M. P. Mingos and Z. Lin, *Comments Inorg. Chem.* **9**, 95 (1989).
- 294. A. N. Papazian, *Gold Bull.* **15**, 81 (1982).
- 295. J. Schwank, *Gold Bull.* **16**, 103 (1983).
- 296. E. G. Allison, and G. C. Bond, *Catal. Rev.* **7**, 233 (1972).
- 297. J. Evans and G. Jingxing, *J. Chem. Soc., Chem. Commun.* p. 39 (1985).
- 298. R. Pierantozzi, K. J. McQuade, B. C. Gates, M. Wolf, H. Knözinger, and W. Ruhmann, *J. Am. Chem. Soc.* **101**, 5436 (1979).
- 299. M. Wolf, H. Knözinger, and B. Tesche, *J. Mol. Catal.* **25**, 273 (1984).